

**Role of Aromatic L-Amino Acid Decarboxylase (AADC)
after Spinal Cord Injury**

by

Yaqing Li

A thesis submitted in partial fulfilment of the requirements for the degree of

Doctor of Philosophy

Centre for Neuroscience

University of Alberta

© Yaqing Li, 2015

ABSTRACT

Spinal cord transection leads to elimination of brainstem-derived monoamine fibers that normally synthesize most of the monoamines in the spinal cord, including serotonin (5-HT) and noradrenaline (NA). Such spinal cord injury (SCI) thus leads to the loss of monoamines, as well as monoamine-synthesizing enzymes, including tryptophan hydroxylase (TPH) and aromatic L-amino acid decarboxylase (AADC). However, several studies suggest that after SCI the spinal cord spontaneously recovers AADC, but not other monoamine synthesizing enzymes. Thus, we explore here the mechanisms and outcomes of this plasticity in AADC. AADC alone cannot produce 5-HT, but it can produce 5-HT when its precursor, 5-HTP, is made available. As well, AADC can produce trace amines (like tryptamine) directly from dietary amino acids (like tryptophan). In the first chapter of this thesis, we used an immunolabelling method to determine locations of recovered AADC after SCI. We found that AADC is ectopically upregulated in microvasculature, especially in pericytes on capillaries, and in certain AADC-containing interneurons in the spinal cord caudal to lesion. We then tested the action of AADC on motoneurons and muscle spasms (long-lasting reflexes, LLRs) by both in vivo and in vitro methods, and we found that the upregulated spinal AADC in both vessels and interneurons produced functional amounts of 5-HT from exogenously applied 5-HTP, which increased both motoneuron and LLR activity. However, we found that this AADC was not capable of *endogenously* producing functional classic monoamines, like 5-HT, leaving the endogenous function of spinal AADC uncertain. Thus in chapter 3 we examined whether spinal AADC was able to *endogenously* produce functional trace amines. Initially, we found no direct effect of physiological trace amine on motoneurons and spasms, and thus we turned to investigating blood vessel function, because vessel AADC was highly upregulated. Blood vessels in the central

nervous system (CNS) are controlled by neuronal activity, including widespread vessel constrictions induced by brainstem-derived monoamines (5-HT and NA), and local vessel dilation mediated by glutamatergic neuron activity. SCI eliminates this monoamine innervation of vessels, and thus we examined whether trace amines could replace this lost innervation. Using infrared differential interference contrast (IR-DIC) microscopy, we found that AADC produced trace amines (TAs, like tryptamine) from dietary amino acids (tryptophan) and this in turn led to constrictions of capillaries adjacent to pericytes. These TA-induced constrictions were mediated by 5-HT_{1B} and alpha₂ adrenergic receptors. These receptors play a critical role in compensating for the loss of classic monoamines, and restoring microvessel tone. However, we also found that this vessel tone was excessive, with spinal cord oxygenation and blood flow about half of normal after SCI (in vivo). This led to the cord below the injury being in a chronic state of hypoxia. Blocking monoamine receptors or AADC, or briefly inhaling pure oxygen, produced long-term relief from hypoxia and improved motor functions, including locomotion.

PREFACE

I would like to acknowledge the generous support of my supervisor (Dr. David J. Bennett), my supervisory committee (Drs. David J. Bennett, Karim Fouad and Glen B. Baker), defense committee (Drs. Shawn Hochman, Richard B. Stein) and members of the Bennett lab (Leo Sanelli, Marilee J. Stephens, Katie C. Murry, Sophie Black, Dwight Zenner, and Ana M. Luca Osma). Portions of this thesis were carried out in collaboration with the laboratories of Dr. Fouad (immunohistology and rat locomotion testing), Dr. Baker (HPLC analysis) and Dr. Ian R. Winship (confocal imaging and 2-photon microscopy in vivo blood flow measurement), and I would like to thank them for their kind support.

Chapter 2 of this thesis has been published as Y. Li, L. Li, M.J. Stephens, D. Zenner, K.C. Murray, I.R. Winship, R. Vavrek, G.B. Baker, K. Fouad, and D.J. Bennett, “Synthesis, transport, and metabolism of serotonin formed from exogenously applied 5-HTP after spinal cord injury in rats.” *Journal of Neurophysiology*, vol. 111, 145-163, 2014. I designed and participated in all research projects, interpreted results and wrote the paper, under the supervision of David Bennett. I performed most of *in vitro* rat experiments. Katie Murray contributed to some of the initial *in vitro* rat experiments. Leo Sanelli performed all sacral spinal transections in rats. David Bennett, Leo Sanelli, Dwight Zenner and I conducted all *in vivo* EMG tests. Marilee Stephens contributed to electrophysiology data analysis. Karim Fouad, Lisa Li, Romana Vavrek and Ian Winship contributed to immunolabelling experiments. Glen Baker and Gail Rauw performed the HPLC analysis.

Chapter 3 of this thesis will be submitted to *Nature Medicine*, with the authors: Yaqing Li, Ana M. Lucas Osma, Mischa V. Bandet, Marilee J. Stephens, Romana Vavrek, Leo Sanelli, Keith K. Fenrich, Ian R. Winship, Karim Fouad and David J. Bennett. I designed and participated in all research projects, interpreted results and wrote the paper, under the supervision of David Bennett. I performed all *in vitro* rat experiments, *in vivo* pO₂ measurements and *in vivo* EMG tests, and contributed to all other rat studies. Romana Vavrek and Karim Fouad contributed to the *in vivo* rat locomotor experiments. Ana Lucas Osma, Romana Vavrek, Leo Sanelli, Ian Winship and Karim Fouad contributed to immunolabeling experiments. Ian Winship, Mischa Bandet contributed to blood flow measurements. Leo Sanelli performed all sacral spinal cord transections. Marilee Stephens contributed to analysis. Keith Fenrich contributed to paper editing.

The research projects in this thesis received ethics approval from the University of Alberta's Animal Care and Use Committee (ACUC), in compliance with the Canadian Council on Animal Care (CCAC), under the project name "Neuronal plasticity after spinal cord injury" (AUP00000224), May 27, 2016 (annual expiry date). Funding for this research was provided by CIHR and NIH.

Other than thesis projects, I also contributed to the following published work:

M. Manuel, Y. Li, S.M. ElBasiouny, K.C. Murray, A. Griener, C.J. Heckman and D.J. Bennett, NMDA induces persistent inward and outward currents that cause rhythmic bursting in adult rodent motoneurons. *Journal of Neurophysiology*, vol. 108, 2991-2998, 2012

J.M. D'Amico, K.C. Murray, Y. Li, K.M. Chan, M.G. Finlay, D.J. Bennett and M.A. Gorassini, Constitutively active 5-HT₂/α₁ receptors facilitate muscle spasms after human spinal cord injury.

Journal of Neurophysiology, vol. 109, 1473-1484, 2013

J.M. D'Amico, Y. Li, D.J. Bennett and M.A. Gorassini, Reduction of spinal sensory transmission by facilitation of 5-HT_{1B/D} receptors in noninjured and spinal cord-injured humans. *Journal of*

Neurophysiology, vol. 109, 1485-1493, 2013

A.F.D. Narzo, A. Kozlenkov, Y. Ge, B. Zhang, L. Sanelli, Z. May, Y. Li, K. Fouad, C. Cardozo,

E.V. Koonin, D.J. Bennett and S. Dracheva, Decrease of mRNA edition after spinal cord injury is caused by down-regulation of ADAR₂ that is triggered by inflammatory response. *Scientific*

Reports, vol. 10, 1038/srep12615, 2015

TABLE OF CONTENT

1. Chapter 1: Introduction.....	1
1-1 Monoamines in the spinal cord.....	2
1-2 Trace amines (TAs) and trace amine-associated receptors (TAARs).....	3
1-3 Aromatic L-amino Acid Decarboxylase (AADC).....	5
1-4 Spinal cord injury (SCI) and monoamines after spinal cord injury.....	7
1-5 AADC after Parkinson's Disease (PD) and spinal cord injury.....	8
1-6 Blood flow control in the central nervous system.....	9
1-7 Basal vessel tone after spinal cord injury.....	12
1-8 Pericytes.....	13
1-9 Outline of the thesis.....	15
1-10 References.....	17
2. Chapter 2: Synthesis, transport and metabolism of serotonin from exogenously applied 5-HTP after spinal cord injury in rats.....	26
2-1 Introduction.....	27
2-2 Methods.....	33
2-2-1 In vitro preparation.....	33
2-2-2 Ventral root reflex recording and averaging.....	34
2-2-3 Intracellular recording.....	35
2-2-4 Drugs and solutions.....	36
2-2-5 Spasms in awake chronic spinal rat.....	37
2-2-6 Immunolabelling.....	37
2-2-7 HPLC analysis.....	40
2-2-8 Data analysis.....	40
2-3 Results.....	42
2-3-1 AADC is upregulated in microvasculature after SCI.....	42
2-3-2 After injury AADC is upregulated in dorsolateral neurons associated with blood vessels.....	43
2-3-3 Upregulated AADC synthesizes 5-HT from exogenous 5-HTP after SCI.....	46
2-3-4 Diffusely distributed uptake of 5-HT in spinal cord, separate from AADC cells.....	47
2-3-5 Diffusely distributed uptake of 5-HT in the spinal cord, verified with HPLC.....	48

2-3-6 Exogenous 5-HT derived in periphery is not accumulated in AADC-containing cells	49
2-3-7 Detailed morphology of AADC neurons, seen with in vitro 5-HTP incubation	50
2-3-8 5-HT is not endogenously produced by spinal cord AADC after spinal cord injury ..	52
2-3-9 Variability of 5-HT synthesis in AADC-containing neurons, vessels and pericytes...	54
2-3-10 Carbidopa blocks vessel but not neuronal AADC activity	54
2-3-11 Leucine blocks neuronal but not vessel AADC synthesis of 5-HT from 5-HTP.....	55
2-3-12 New class of AADC neurons are NeuN positive and GFAP negative	56
2-3-13 D-cells in the central canal disappear with spinal cord injury	58
2-3-14 AADC-neurons and microvessels both increase spasms in 5-HTP treated rats	61
2-3-15 Mechanisms of action of 5-HTP, including roles of AADC, 5-HT ₂ receptors and MAO.....	64
2-3-16 5-HT produced by AADC activates receptors on motoneurons	68
2-4 Discussion.....	70
2-4-1 AADC plasticity.....	74
2-4-2 Novel emergence of AADC in neurons with spinal cord injury.....	74
2-4-3 Vessels contribute to 5-HT synthesis from exogenous 5-HTP after spinal cord injury	75
2-4-4 5-HT is not endogenously synthesized in the spinal cord after injury.....	77
2-4-5 MAO plays a major role in metabolizing 5-HT after injury.....	79
2-4-6 Diffuse amine transport after spinal cord injury	80
2-4-7 Summary and possible roles of AADC.....	82
2-5 References.....	83
3. Chapter 3: Chronic hypoxia mediated by trace amines after spinal cord injury	88
3-1 Introduction.....	89
3-2 Results.....	93
3-2-1 Endogenously produced trace amines constrict capillaries at pericytes	93
3-2-2 Trace amines activate 5-HT _{1B} and alpha ₂ adrenergic receptors to constrict capillaries	94
3-2-3 AADC, trace amines and 5-HT _{1B} receptors are co-localized in capillary pericytes	98
3-2-4 Endogenous trace amines reduce blood flow and induce hypoxia after SCI.....	101
3-2-5 Motoneuron function is enhanced by blocking trace amine action and preventing hypoxia	105

3-2-6 Locomotor function after SCI is improved by treatments that improve capillary blood flow.....	108
3-3 Discussion.....	111
3-4 Methods.....	117
3-4-1 In vitro preparation	118
3-4-2 In vitro ventral root reflex recording and averaging.....	118
3-4-3 IR-DIC microscopy of vessels, in vitro	119
3-4-4 Spasms in awake chronic spinal rat	120
3-4-5 Spinal vascular imaging and blood flow, in vivo	121
3-4-6 Oxygen concentration measurement, in vivo.....	122
3-4-7 Locomotion analysis and i.t. drug injections	123
3-4-8 Drugs and solutions.....	124
3-4-9 Immunolabeling.....	125
3-5 References.....	128
3-6 Supplementary information	134
3-7 Supplementary information references	140
4. Chapter 4: Thesis discussion and future directions	141
4-1 Discussion.....	142
4-2 Future direction.....	145
5. Reference.....	147

LIST OF FIGURES

Figure 2-1. L-Amino acid decarboxylase (AADC) is upregulated in microvasculature and neurons after spinal cord injury.	45
Figure 2-2. Serotonin (5-hydroxytryptamine, 5-HT) synthesis from exogenous 5-hydroxytryptophan (5-HTP) in chronic spinal rats.	51
Figure 2-3. 5-HT is not endogenously synthesized by AADC after injury.	53
Figure 2-4. Characterization of AADC neurons that appear after spinal cord injury.	57
Figure 2-5. Characterization of AADC containing D-cells that line the central canal.	60
Figure 2-6. AADC-neurons and vessels both increase spasms in 5-HTP treated rats.	63
Figure 2-7. 5-HTP increases spasms in the isolated spinal cord of chronic spinal rats, via synthesis of 5-HT with AADC and activation of 5-HT ₂ receptors, although much of this 5-HT is metabolized by MAO.	67
Figure 2-8. 5-HTP directly increases motoneuron excitability in chronic spinal rats.	69
Figure 2-9. Schematic of the action of AADC and MAO after spinal cord injury.	72
Figure 3-1. Trace amines produced in spinal microvasculature of chronic spinal rats constrict capillaries at pericytes.	96
Figure 3-2. AADC, trace amines and 5-H _{1B} receptors are co-expressed in pericytes after SCI. .	99
Figure 3-3. Poor spinal cord blood flow and hypoxia after chronic SCI, due to trace amines. .	103
Figure 3-4. Increased motoneuron activity after SCI induced by treatments that improve perfusion and oxygenation.	107
Figure 3-5. Thoracic SCI induces chronic hypoxia that impairs locomotion.	109
Supplementary Figure 3-1. Tryptophan induces both tonic and rhythmic contractions of capillaries.	134
Supplementary Figure 3-2. Bimodal modal action of 5-HTP on capillary diameter.	135
Supplementary Figure 3-3. 5-HT _{1b} receptors on capillary pericytes and dorsal fibres.	136
Supplementary Figure 3-4. Hypoxia is followed by a rebound increased oxygenation in the spinal cord in rats with SCI.	137
Supplementary Figure 3-5. Endogenously produced trace amines do not affect motoneuron activity after SCI, even though exogenously applied trace amines do.	138

LIST OF ABBREVIATIONS

5-Hydroxyindole-3-acetic acid	5-HIAA
Serotonin (5-hydroxytryptamine)	5-HT
5-Hydroxytryptophan	5-HTP
Aromatic L-amino acid decarboxylase	AADC
Artificial cerebrospinal fluid	ACSF
Anterior spinal artery	ASA
Amine precursor uptake and decarboxylase system	APUD
Blood-brain barrier	BBB
Central nervous system	CNS
p-Chlorophenylalanine	pCPA
Cerebral perfusion pressure	CPP
Cerebro-spinal fluid	CSF
Dopamine	DA
Dopamine transporter	DAT
Electromyogram	EMG
Functional magnetic resonance imaging	fMRI
L-3, 4-Dihydroxyphenylalanine	L-DOPA

Dopamine β -hydroxylase	DBH
Glial fibrillary acidic protein	GFAP
High pressure liquid chromatography	HPLC
Infrared differential interference contrast	IR-DIC
Intermittent hypoxia	IH
Large neutral amino acid transporter	LAT
Monoamine oxidase	MAO
Noradrenaline	NA
Nitric oxide	NO
Organic cation transporter	OCT
Parkinson's disease	PD
Persistent inward current	PIC
β -Phenylethylamine	PEA
Plasma membrane monoamines transporter	PMAT
Posterior spinal artery	PSA
Spinal cord injury	SCI
Standard deviation	SD

Serotonin transporter	SERT
Smooth muscle actin	SMA
Smooth muscle cell	SMC
Trace amines	TAs
Tryptophan hydroxylase	TPH
Tyrosine hydroxylase	TH
Vesicular monoamine transporter	VMAT
Ventral tegmental area	VTA

Chapter 1: Introduction

Monoamines in the spinal cord

Classical monoamines, such as serotonin (5-hydroxytryptamine, 5-HT), noradrenaline (NA) and dopamine (3,4-dihydroxyphenethylamine, DA), play a powerful role in modulating spinal motor and sensory function via influencing the excitability of neurons in the spinal cord (Harvey et al. 2006; Heckmann et al. 2005; Hochman et al. 2001; Jacobs et al. 1992; Murray et al. 2010; Perrier et al. 2005; Schmidt et al. 2000). Serotonin, in particular, increases motoneurons' resting membrane potential and facilitates low-voltage-gated persistent inward currents composed of sodium (Na PIC) and calcium (Ca PIC), allowing motoneurons to depolarize more easily and therefore generate appropriate muscle contractions (Harvey et al. 2006; Heckmann et al. 2005). Spinal monoamines are primarily produced in the terminals of descending monoaminergic fibers from supraspinal nuclei, including the raphe nucleus for 5-HT, the locus coeruleus for NA, and the substantia nigra or ventral tegmental area (VTA) for DA (Bjorklund et al. 2007; Carlsson et al. 1964; Dahlstroem et al. 1964; Fritschy et al. 1990; Jacobs et al. 1992; Rajaofetra et al. 1989). These monoaminergic fibers contain all the necessary monoamine biosynthesis enzymes, such as tryptophan hydroxylase (TPH), tyrosine hydroxylase (TH), and aromatic L-amino acid decarboxylase (AADC). First, TPH converts the dietary amino acid tryptophan to 5-hydroxytryptophan (5-HTP) and TH converts dietary tyrosine to L-dihydroxyphenylalanine (L-DOPA). Then AADC converts 5-HTP to 5-HT and L-DOPA to DA (vesicle dopamine β -hydroxylase (DBH) further converts DA to NA) (Best et al. 2010; Hardebo et al. 1980b; Ikemoto 2004). Once these classical monoamines are produced they are packed into vesicles through vesicular monoamine transporters (VMAT), and therefore their release is precisely modulated by neuronal activities. Vesicle packaging also protects classical monoamines from being metabolized into non-active compounds by monoamine oxidase (MAO), which is on the outer membrane of mitochondria in monoamine axon terminals. 5-HT and NA are preferentially

metabolized by MAO type A, while DA is metabolized by both MAO A and B (Bortolato et al. 2008).

Trace amines (TAs) and trace amine-associated receptors (TAARs)

Trace amines (TAs), such as tryptamine, tyramine, β -phenylethylamine (PEA) and octopamine, are included in a class of monoamines named for their low endogenous concentration in mammals (Saavedra 1989). More and more studies demonstrate the involvement of TAs in many neuropsychiatric disorders, including depression, schizophrenia and attention deficit disorder (Berry 2007; Boulton 1980; Branchek et al. 2003; Davis et al. 1994; Heller et al. 1976; Narang et al. 2011; Potkin et al. 1980). They originate from the same amino acids as classical monoamines, but are directly converted via AADC: tryptophan is converted to tryptamine, tyrosine is converted to tyramine and phenylalanine is converted to PEA respectively (octopamine requires DBH to further hydroxylate tyramine). Even though TAs can be synthesized at the same rate as or a greater rate than classical monoamines in monoamine axon terminals, they are not packed into vesicles but diffuse freely in the synapse and through the cell membrane, rendering them ready to be metabolized by both MAO A and B, and thus the concentration of TAs is kept low at a nanomolar range (Berry 2004; Burden et al. 1980; Paterson et al. 1990; Shimazu et al. 2004). Sharing close biosynthesis and metabolic pathways results in their structural and pharmacological similarity to classical monoamines.

Trace amines are traditionally known as “false transmitters” because they activate classical monoamine receptors as well, and interfere with the classical monoamine actions, including 5-HT_{1/2/7} and α_2 adrenergic receptors (Battaglia et al. 1983; Gozlan et al. 1983; Knight et al.

2004; Kopin 1968; Kopin et al. 1964; Shen et al. 1993; U'Prichard et al. 1977). However, the binding affinity of monoamine receptors to TAs is much lower than for classical monoamines. Micromolar concentrations of TAs are required to produce the same potency on neurons as nanomolar concentrations of classical monoamines. As a consequence, TAs used to be thought of as by-products of classical monoamines, even though they clearly activate neuronal activities when they are exogenously applied at a considerably higher concentration (Berry 2004; Boulton 1976; Boulton et al. 2012; Saavedra 1989). In 1976, Boulton's group reported a phenomenon that had tyramine and PEA significantly enhancing DA's and NA's action on a single cortex neuron, while tyramine and PEA themselves had very weak effects (Boulton 1976). Even though they didn't pursue the mechanism further at that time, they hypothesized that the continuously released TAs exerted a tonic modulation of synaptic transmission via some unknown pathways.

In 2001, two independent groups identified a family of mammalian G protein-coupled receptors that have high affinity to TAs (Borowsky et al. 2001; Bunzow et al. 2001). These so called trace amine-associated receptors (TAARs) provide TAs an opportunity to have their own modulatory effects in CNS. Although a lot of subtypes of TAARs have been determined in different species, only TAAR₁ and TAAR₄ are capable of being activated by biogenic amines and have been found to be expressed in both human and rodent (Lindemann et al. 2005; Miller 2011). Therefore, most studies are focusing on these two receptors. TAAR_{1/4}s are extensively expressed in the brain and the neonatal spinal cord, but there is still lack of evidence of TAAR₄'s expression in the adult spinal cord (Borowsky et al. 2001; Bunzow et al. 2001; Gozal et al. 2014; Lindemann et al. 2005). TAAR₁ is localized mainly in the cytoplasm rather than on extracellular membranes,

so TAs are capable of carrying out their function right near the places where they are synthesized (Xie et al. 2008; 2009). PEA is the most potent TA to activate TAAR_{1/4}, while tyramine and tryptamine are less potent. Octopamine has the lowest binding affinity to TAARs (Borowsky et al. 2001; Bunzow et al. 2001). Activation of TAAR₁ in cerebral monoaminergic neurons inhibits the function of the high affinity monoamine transporters, thereby enhancing monoamine actions (Miller 2011; Xie et al. 2008; 2009; 2007). Very recently, Hochman's group has suggested that TAs are an independent modulatory system that enhances motor output and promotes recruitment of locomotor circuits in the neonatal spinal cord (Gozal et al. 2014). These TAs' actions are independent of high affinity monoamine transporters, but interfere with low affinity Na⁺-independent membrane transporters, such as organic cation transporters (OCTs), plasma membrane monoamine transporters (PMAT) and large neutral amino acid transporters (LATs). Interference with these transporters modulates amino acid transportation into a cell, causing a change of intracellular TAs' production, which further regulates TAARs' action.

Aromatic L-amino Acid Decarboxylase (AADC)

AADC is the only enzyme involved in biosynthetic pathways producing 5-HT, NA and DA, as well as producing TAs. Though AADC is not the rate-limiting enzyme in producing classical monoamines under normal conditions, it is the rate-limiting enzyme for the synthesis of TAs (Berry et al. 1996; Dyck et al. 1983). Other than existing in monoamine fibers, AADC is also abundant in the liver, kidney, pancreas, gastrointestinal tract and blood vessels (Berry et al. 1996; Hardebo et al. 1979a). In the liver and kidney, AADC is thought to play a role in disposing of excess monoamine precursors and amino acids: here, cells take up precursors, and AADC

catalyzes them to form 5-HT, catecholamines, and trace amines, which are then either directly discarded into the urine (kidney) or further broken down by MAO (liver) (Berry et al. 1996). Peripheral AADC like this consumes a large fraction of precursors 5-HTP or L-DOPA (Warsh et al. 1976), and thus concentrations of circulating classical monoamine precursors are as low as in the nanomolar range.

Central nervous system (CNS) blood vessels also contain some AADC as well as abundant MAO, which together are thought to perform a similar trapping and disposal system, regulating excess monoamine precursors (Hardebo et al. 1980a; Hardebo et al. 1979a; Hardebo et al. 1980b; Kalaria et al. 1987; Spatz et al. 1998). Specifically, exogenously injected circulating monoamine precursors are normally prevented from crossing into the CNS because AADC in endothelial cells and pericytes of CNS vessels catalyzes them to form monoamines. These are then trapped in the endothelial cells and eventually broken down by MAO. Only when the concentration of blood-borne monoamine precursors is high enough to saturate activities of vessel AADC and MAO, which does not occur under normal physiological conditions, do these precursors or monoamines cross the blood-brain barrier (BBB) and get into CNS parenchyma (Hardebo et al. 1979b; Hardebo et al. 1980b). Under normal physiological conditions endogenous monoamines and their precursors are at much higher concentrations in the CNS than in the blood (>100-fold higher), and thus the major role of the enzymes AADC and MAO in CNS vessel endothelial cells is likely to take up and metabolize excess monoamines and precursors from the CNS and dispose of them (Enbaek et al. 1978; Hardebo et al. 1980a; Kema et al. 2000; Spatz et al. 1998).

In the normal spinal cord, besides the abundant monoamine fibers and blood vessels containing AADC, some AADC-positive but TH- and TPH-negative cells are found. They are juxtaposed to the ependymal cells of the central canal, with round-to-oval cell bodies and short processes extending into the lumen of the central canal. These cells were first determined by Jaeger and termed as D1 cells, together with other such cells along the neural axis (D2-D14), including in the striatum (Jaeger et al. 1984; Jaeger et al. 1983). Because of their properties of lacking TH and TPH, they are incapable of producing monoamines from the endogenous precursors of tyrosine and tryptophan respectively. Their short processes form a bulbous enlargement into the lumen of central canal, which appears to be similar with cerebro-spinal fluid (CSF) contacting neurons (Karasawa et al. 1995). D cells often line up to the blood vessels, central canal, or ventricles; in this regard they are thought to be part of the amine precursor uptake and decarboxylase system (APUD) that has an endocrine function of discharging amines into the blood. Moreover, D cells are found to express TAAR₁ and TAAR₄ as well as production of TAs, which could play a critical role in recruiting locomotor-like activities in the neonatal spinal cord (Gozal et al. 2014).

Spinal cord injury (SCI) and monoamines after spinal cord injury

Spinal cord injury (SCI) is one of the most devastating injuries as there is no cure and patients have to experience life-long treatment and rehabilitation. Transection of the spinal cord destroys almost all supraspinal descending innervations of the spinal cord (Carlsson et al. 1964; Murray et al. 2010). The cord caudal to the lesion site initially suffers hyporeflexia or areflexia, resulting in complete muscle paralysis, but then gradually develops into a hyperreflexia state causing involuntary muscle spasms in the following weeks (Dietz 2000; Lance 1980; Sherrington 1910).

One reason for this phenomenon is that a massive elimination of monoamines appears within days after SCI, together with a loss of almost all monoamine fibres, leaving the lower motoneurons nearly incapable of firing action potentials and contributes to spinal shock (Ditunno et al. 2004). However, over the months after SCI, monoamine receptors become capable of producing activities without binding to monoamine ligands (constitutive activity) and supersensitive to residual monoamines (Murray et al. 2010). However there is no sign of monoamine fibre recovery. Other than loss of monoamines, some of the key enzymes involved in monoamine synthesis are also eliminated with monoamine fibres, including TPH and TH (Clineschmidt et al. 1971; Magnusson 1973; Takeoka et al. 2010).

AADC after Parkinson's Disease (PD) and spinal cord injury

A similar situation to monoamines after SCI occurs with Parkinson's disease (PD): normal DA innervations of the striatum are lost, but somehow L-DOPA medication still leads to production of DA in the striatum (Goldstein et al. 1982; Ikemoto et al. 1997; Lidbrink et al. 1974). The origin of this AADC after loss of monoamine innervation has been extensively investigated in the striatum in relation to PD (Ikemoto 2004; Ikemoto et al. 1997; Karasawa et al. 1995; Kitahama et al. 2007; Mura et al. 1995; Mura et al. 2000; Ugrumov 2009). In the striatum (and arcuate nucleus), destruction of monoamine fibers (DA fibers; with 6-hydroxydopamine) leads to an upregulation of AADC activity and, in particular, an emergence of a population of AADC-containing neurons, similar to the D cells described before (Ershov et al. 2005; Mura et al. 1995). This suggests that AADC activity increases when levels of monoamines are reduced, as appears to generally occur with alterations of monoamines (Berry 2004; Grandy 2007). Considering these pieces of evidence, ectopic upregulation of AADC activity could also happen after SCI.

Despite the elimination of monoamine innervations with spinal transection, repeated studies have shown that exogenous application of the monoamine precursors 5-HTP or L-DOPA leads to synthesis of monoamines (Barbeau et al. 1990; Bedard et al. 1979; Chandler et al. 1984; Guertin 2009; Hayashi et al. 2010; Tremblay et al. 1985; Viala et al. 1971). Recently, Hayashi showed that 5-HTP, but not direct 5-HT_{2C} or 5-HT_{1A} receptor agonists, increased weight-supported stepping of spinal contused adult rats, suggesting the potential possibility of 5-HTP as a treatment to enhance motor function after SCI (Hayashi et al. 2010). However the mechanism of 5-HTP's effects is vague in this study, though they suggested 5-HTP has to be converted to 5-HT to be effective. Bedard and Barbeau also have shown that application of 5-HTP to transected spinal rats increased their hindlimb motor output, and even improved hindlimb rhythmic activities. This motor effect of 5-HTP is antagonized by the 5-HT receptor antagonist, cyproheptadine (Barbeau et al. 1990; Bedard et al. 1979). These studies indicate that after transection, even without monoamine fibres, substantial functional AADC is recovered caudally to the injury site, converting 5-HTP to 5-HT for function. However, the locations of the recovered AADC remain uncertain after SCI. Thus, Chapter 2 mainly focuses on finding locations where AADC recovers after spinal cord transection in rats and whether AADC is upregulated in different structures to compensate for the loss of brain stem monoamine innervations and associated AADC. Then in Chapter 3, we investigate the physiological function of recovered AADC after SCI.

Blood flow control in the central nervous system

The mammalian CNS is susceptible to damage when its blood supply is compromised even for very short periods. To meet the large demand of oxygen and energy from neuronal activities and

metabolic processes, 20% of circulating blood goes into the brain, and the CNS has the first priority for receiving blood supply over any other organs (Zlokovic 2011). As well, arteries in the CNS avoid anastomoses to arteries outside of the system, preventing outer arteries taking over when CNS arteries are occluded. Because of the similarity of its spinal cord vasculature's anatomy to humans, the rat is a good model with which to study blood flow regulation in the spinal cord (Hu et al. 2014; Koyanagi et al. 1993; Tveten 1976). The single anterior spinal artery (ASA) branches from the vertebral artery and feeds two-thirds of the blood into the spinal cord (Gillilan 1958; Sliwa et al. 1992; Turnbull et al. 1966). The paired posterior spinal arteries (PSA) serve mostly at the dorsal horn and dorsal column, which arises from both the vertebral artery and the posterior inferior cerebellar artery. The arterial vasocorona connects ASA and PSA serving white matter on the lateral side of the spinal cord (Sliwa et al. 1992). Spinal veins run through the entire cord from caudal to rostral, and thus injury to spinal veins may cause further spreading damage in the cord (Lazorthes et al. 1971; Martirosyan et al. 2011).

Blood flow regulation mechanisms are extensively established in brain. Though fewer studies have been conducted in the spinal cord, the spinal cord is always considered as a microcosm of the brain (Hickey et al. 1986). Analogous to peripheral blood vessels, the vasculature of the CNS has a basal tone that conserves blood from non-active areas, in that the vessels are pre-constricted and are ready to dilate when tissues nearby require energy (Lofving et al. 1956). Monoamines, such as 5-HT and NA, play a critical role in providing this basal vessel tone via 5-HT and adrenergic receptors (Bonvento et al. 1991; Chan-Palay 1976; Edvinsson et al. 1984; Griffith et al. 1982; Hamilton et al. 2010; Peerless et al. 1971; Peppiatt et al. 2006; Teng et al. 2002). However, unlike sympathetic derived NA, which regulates widespread vessel tone in the

periphery system, the autonomic system nerves end at the pia mater (Chang et al. 1989; Jackowski et al. 1989). As a consequence, monoamines released from brainstem-derived monoamine fibres take over to help setting up CNS basal vessel tone. Also, without the autonomic system, CNS blood flow regulation is fully dependent on the local homeostatic environment (Lassen 1959; Peterson et al. 2011; Willie et al. 2014). This autoregulation system provides a fast regional blood flow control to only the places that are active and require oxygen and energy, by means of cerebral pressure autoregulation, flow-metabolic coupling and neurovascular coupling. Cerebral pressure autoregulation ensures a constant blood supply into the CNS against a large variability of arteriole and capillary basal tone. It is only sensitive to cerebral perfusion pressure (CPP), involving smooth muscle cells' (SMCs) stretch responses and endothelium mechanoreceptor properties (Faraci et al. 1990; Harder 1984; Knot et al. 1998; Lassen 1959; Osol et al. 1985). Neuronal activities release a variety of vasodilators such as nitric oxide (NO), glutamate and PGE2 (Bredt et al. 1989; Buchanan et al. 1993; Faraci et al. 1994; Iadecola et al. 1997; Lacroix et al. 2015; Palmer et al. 1987; Schmidt et al. 1993; Tanaka et al. 1993). This induces a transient functional hyperemia at a local active area, and thus is called neurovascular coupling. More and more studies suggest that astrocytes and microglia emerge to have major functions in communicating neuronal activities to parenchymal vasculatures (Attwell et al. 2010; Carmignoto et al. 2010; Filosa et al. 2015; Gordon et al. 2007; Iadecola et al. 2007). Neurovascular coupling saves a considerable amount of oxygen and energy, considering the limited energy reserves, and is thought to form the basis of functional magnetic resonance imaging (fMRI) (Khanna et al. 2015; Ogawa et al. 1990a; Ogawa et al. 1990b; Raichle 1998; Roy et al. 1890). Flow-metabolism coupling responds to neuronal metabolites, such as CO₂ and adenosine, to assure metabolic activity does not exceed the capacity of the blood supply, and

eliminates harmful metabolites (Forrester et al. 1979; Phillis 2004). Traditionally, arteries and arterioles are considered to take major actions controlling CNS blood flow, because they are covered by contractile smooth muscle cells (Faraci et al. 1990; Harder 1984; Knot et al. 1998). SMCs uniformly wrap arteries and arterioles in distinctive bands and are sensitive to mechanical force and vasoactive substances. When arterioles branch to form small capillaries, the SMCs disappear, resulting originally in ideas about passive acceptance of blood in capillaries. However, recent studies indicate that SMCs are replaced by sparsely spaced pericytes on capillaries, and capillaries are actually the major sites for CNS blood flow autoregulation (Hall et al. 2014; Hamilton et al. 2010; Peppiatt et al. 2006), which will be discussed later in this thesis.

Basal vessel tone after spinal cord injury

With severe SCI, vessels and neurons caudal to the injury survive, but are essentially orphaned, losing contact with the brain and brainstem-derived axons, including losing monoamine innervation that normally arises entirely from the brainstem (Carlsson et al. 1964; Murray et al. 2010). Vasculature is directly damaged by traumatic SCI and undergoes well-documented changes, such as endothelial cell death, increase in permeability of BBB, and the disturbance of autoregulation (Casella et al. 2006; Popovich et al. 1996; Senter et al. 1978). In the meantime, angiogenesis is observed after SCI, which might inhibit cavity formation and enhance functional recovery (Imperato-Kalmar et al. 1997; Kundi et al. 2013; Loy et al. 2002; Shingu et al. 1989; Zhang et al. 1997). However, these studies mostly focus on the acute stage and close to the injury site after SCI, and little is known about those uninjured vessels far away caudal to the injury site. Some uninjured spinal neurons undergo remarkable adaptations that compensate for loss of supraspinal innervation after SCI, including adaptations in monoamine receptors (Murray

et al. 2010). These adaptations contribute both to recovery of motor function and pathological activity in the form of muscle spasms. Therefore, in Chapter 3, using this approach, we explore whether similar plasticity happens in blood vessels or whether there are alternate mechanisms that compensate for loss of monoamine innervation of blood vessels after severe SCI. Also we investigate here whether vessel tone is different after SCI.

Pericytes

Pericytes are a group of cells loosely wrapping around arterioles, venules and capillaries at the abluminal side of endothelial cells in the CNS. They have distinctive hemispheric somas and fine finger-like processes that make direct physical and signaling contact with endothelial cells (Dalkara et al. 2015; Fisher 2009; Hirschi et al. 1996; Krueger et al. 2010). They are traditionally considered to play multiple crucial roles in angiogenesis, capillary stabilization and maintaining BBB integrity (Balabanov et al. 1999; Dore-Duffy et al. 2000; Lai et al. 2005; Lindahl et al. 1997). Cell culture experiments even suggest pericytes have stem cell properties in adult brain, which show that they proliferated into different morphology spheres expressing neuron and glia biomarkers (Dore-Duffy et al. 2006). In addition to these functions, considering that capillaries make contact to much more metabolically active cells and that most monoamine innervations (65% of NA fibres) terminate closer to capillaries rather than arterioles, pericytes may have a major function in regulating CNS blood flow (Cohen et al. 1997; Hamilton et al. 2010; Hirschi et al. 1996; Kelley et al. 1987; Peppiatt et al. 2006). Based on capillary pericytes' location and morphology, they are divided into three different types: precapillary pericyte, midcapillary pericyte and postcapillary pericyte. Precapillary and postcapillary pericytes gradually transition to smooth muscles, so that they are classified as transitional pericytes. It has

long been known that these transitional pericytes express smooth muscle α -actin (SMA), while the real capillary pericytes, midpericytes, have been shown more recently to express SMA (Bandopadhyay et al. 2001; DeNofrio et al. 1989; Herman et al. 1985; Nehls et al. 1991; Yemisci et al. 2009). Capillary pericytes are pre-constricted by centrally-derived monoamines, such as NA, which sets up the basal capillary tone under normal conditions, even though not all pericytes respond to NA in an in vitro study (Hall et al. 2014; Peppiatt et al. 2006). This capillary tone (with pericytes) provides comparable resistance to blood flow as the arterioles do, which contributes to blood distribution. Besides, capillaries are also dilated by neuronal activities and metabolites to perform functional hyperemia at the sitting region of the pericytes' processes, which respond around 3 seconds earlier than arterioles in vivo (Hall et al. 2014). More recently, Attwell's group found that pericytes are extremely susceptible to ischemia. When the brain suffers from local ischemia, which shuts down both oxygen and energy supply, pericytes at the ischemic region die within 15 minutes and stay in rigor state, resulting in a long lasting resistance on the capillary bed (Hall et al. 2014; Yemisci et al. 2009). Death of pericytes in rigor could be a major factor resulting in the reduction of cerebral blood flow during the reperfusion process after ischemia, even though blood supply in arterioles is restored to normal. Unlike these thorough studies on cerebral pericytes, pericytes are still poorly studied in the spinal cord. So in Chapter 3, we also explore roles of pericytes in regulating capillary tone and blood flow after SCI.

Outline of the thesis

In Chapter 2, we examine where AADC is expressed after spinal cord transection in rats (using immune-labeling). We also examine whether it is upregulated in different structures, including D cells and blood vessels, to compensate for loss of brain stem monoamine innervation and associated AADC. We then explore the functional role of these sources of AADC in synthesis of 5-HT from exogenously applied 5-HTP. We find a clear upregulation of AADC expression and activity with injury, especially in blood vessels. However, D-cell AADC expression is unexpectedly decreased and instead we find a new class of AADC-containing neurons after injury. Both these AADC-containing vessels and neurons affect spinal cord function, increasing motoneuron activity (spasm) when we add exogenous precursors, especially when we block MAO. However, we find no evidence that endogenous precursors can produce adequate monoamines, either classical monoamines or TAs, to affect motor function. Chapter 3 focuses on the physiological functions of these upregulated AADCs after SCI. Using IR-DIC microscopy and immune-labeling, we find that TAs produced by plasma amino acids via upregulated AADC in blood vessels are substitutes for lost monoamines, and restore basal capillary tone after SCI. These TAs appear to activate traditional monoamine receptors (5-HT_{1B} and alpha₂ adrenergic receptors) rather than TAARs. They do this by acting on capillary pericytes which appear to play a critical role in regulating blood flow and capillary tone after SCI. Remarkably, we find that TAs excessively constrict capillaries (pericytes) after SCI. This leads to chronic hypoxia of the spinal cord below the injury. Specifically, by using two photon microscopy and in vivo oxygen concentration measurements, we show that both the blood flow and partial pressure of oxygen is halved after SCI. Further, we find that giving traditional monoamine receptor antagonists or AADC blockers dilate the over-constricted capillaries, brings oxygen levels back to normal, and significantly enhances motor function (spasm and locomotion) in awake rats with

SCI. Even simply giving pure oxygen enhances motor output, which provides a treatment that could be transferred easily into the clinic.

References

- Attwell D, Buchan AM, Charpak S, Lauritzen M, Macvicar BA, and Newman EA.** Glial and neuronal control of brain blood flow. *Nature* 468: 232-243, 2010.
- Balabanov R, Beaumont T, and Dore-Duffy P.** Role of central nervous system microvascular pericytes in activation of antigen-primed splenic T-lymphocytes. *J Neurosci Res* 55: 578-587, 1999.
- Bandopadhyay R, Orte C, Lawrenson JG, Reid AR, De Silva S, and Allt G.** Contractile proteins in pericytes at the blood-brain and blood-retinal barriers. *J Neurocytol* 30: 35-44, 2001.
- Barbeau H, and Rossignol S.** The effects of serotonergic drugs on the locomotor pattern and on cutaneous reflexes of the adult chronic spinal cat. *Brain Res* 514: 55-67, 1990.
- Battaglia G, Shannon M, Borgundvaag B, and Titeler M.** pH-dependent modulation of agonist interactions with [³H]-ketanserin-labelled S2 serotonin receptors. *Life Sci* 33: 2011-2016, 1983.
- Bedard P, Barbeau H, and Filion M.** Progressive increase of motor activity induced by 5-HTP in the rat below a complete section of the spinal cord. *Brain Res* 169: 393-397, 1979.
- Berry M, Juorio A, Li X-M, and Boulton A.** Aromatic L-amino acid decarboxylase: A neglected and misunderstood enzyme. *Neurochem Res* 21: 1075-1087, 1996.
- Berry MD.** Mammalian central nervous system trace amines. Pharmacologic amphetamines, physiologic neuromodulators. *J Neurochem* 90: 257-271, 2004.
- Berry MD.** The potential of trace amines and their receptors for treating neurological and psychiatric diseases. *Rev Recent Clin Trials* 2: 3-19, 2007.
- Best J, Nijhout HF, and Reed M.** Serotonin synthesis, release and reuptake in terminals: a mathematical model. *Theor Biol Med Model* 7: 1-26, 2010.
- Bjorklund A, and Dunnett SB.** Dopamine neuron systems in the brain: an update. *Trends Neurosci* 30: 194-202, 2007.
- Bonvento G, MacKenzie ET, and Edvinsson L.** Serotonergic innervation of the cerebral vasculature: relevance to migraine and ischaemia. *Brain Res Brain Res Rev* 16: 257-263, 1991.
- Borowsky B, Adham N, Jones KA, Raddatz R, Artymyshyn R, Ogozalek KL, Durkin MM, Lakhani PP, Bonini JA, Pathirana S, Boyle N, Pu X, Kouranova E, Lichtblau H, Ochoa FY, Branchek TA, and Gerald C.** Trace amines: identification of a family of mammalian G protein-coupled receptors. *Proc Natl Acad Sci U S A* 98: 8966-8971, 2001.
- Bortolato M, Chen K, and Shih JC.** Monoamine oxidase inactivation: from pathophysiology to therapeutics. *Adv Drug Deliv Rev* 60: 1527-1533, 2008.
- Boulton AA.** Identification, distribution, metabolism, and function of meta and para tyramine, phenylethylamine and tryptamine in brain. *Adv Biochem Psychopharmacol* 15: 57-67, 1976.
- Boulton AA.** The properties and potential function of some brain trace amines. *Prog Clin Biol Res* 39: 291-303, 1980.
- Boulton AA, Juorio AV, and Downer RG.** *Trace amines: comparative and clinical neurobiology.* Springer Science & Business Media, 2012.
- Branchek TA, and Blackburn TP.** Trace amine receptors as targets for novel therapeutics: legend, myth and fact. *Curr Opin Pharmacol* 3: 90-97, 2003.
- Bredt DS, and Snyder SH.** Nitric oxide mediates glutamate-linked enhancement of cGMP levels in the cerebellum. *Proc Natl Acad Sci U S A* 86: 9030-9033, 1989.
- Buchanan JE, and Phillis JW.** The role of nitric oxide in the regulation of cerebral blood flow. *Brain Res* 610: 248-255, 1993.

Bunzow JR, Sonders MS, Arttamangkul S, Harrison LM, Zhang G, Quigley DI, Darland T, Suchland KL, Pasumamula S, Kennedy JL, Olson SB, Magenis RE, Amara SG, and Grandy DK. Amphetamine, 3,4-methylenedioxymethamphetamine, lysergic acid diethylamide, and metabolites of the catecholamine neurotransmitters are agonists of a rat trace amine receptor. *Mol Pharmacol* 60: 1181-1188, 2001.

Burden D, and Philips S. Kinetic measurements of the turnover rates of phenylethylamine and tryptamine in vivo in the rat brain. *J Neurochem* 34: 1725-1732, 1980.

Carlsson A, Falck B, Fuxe K, and Hillarp Nr. Cellular localization of monoamines in the spinal cord. *Acta physiologica Scandinavica* 60: 112-119, 1964.

Carmignoto G, and Gomez-Gonzalo M. The contribution of astrocyte signalling to neurovascular coupling. *Brain Res Rev* 63: 138-148, 2010.

Casella GT, Bunge MB, and Wood PM. Endothelial cell loss is not a major cause of neuronal and glial cell death following contusion injury of the spinal cord. *Exp Neurol* 202: 8-20, 2006.

Chan-Palay V. Serotonin axons in the supra- and subependymal plexuses and in the leptomeninges; their roles in local alterations of cerebrospinal fluid and vasomotor activity. *Brain Res* 102: 103-130, 1976.

Chandler SH, Baker LL, and Goldberg LJ. Characterization of synaptic potentials in hindlimb extensor motoneurons during L-DOPA-induced fictive locomotion in acute and chronic spinal cats. *Brain Res* 303: 91-100, 1984.

Chang JY, Ekblad E, Kannisto P, and Owman C. Serotonin uptake into cerebrovascular nerve fibers of rat, visualization by immunohistochemistry, disappearance following sympathectomy, and release during electrical stimulation. *Brain Res* 492: 79-88, 1989.

Clineschmidt B, Pierce J, and Lovenberg W. Tryptophan hydroxylase and serotonin in spinal cord and brain stem before and after chronic transection. *J Neurochem* 18: 1593-1596, 1971.

Cohen Z, Molinatti G, and Hamel E. Astroglial and vascular interactions of noradrenaline terminals in the rat cerebral cortex. *J Cereb Blood Flow Metab* 17: 894-904, 1997.

Dahlstroem A, and Fuxe K. Evidence for the existence of monoamine-containing neurons in the central nervous system. I. Demonstration of monoamines in the cell bodies of brain stem neurons. *Acta Physiol Scand Suppl* SUPPL 232:231-255, 1964.

Dalkara T, and Alarcon-Martinez L. Cerebral microvascular pericytes and neuroglial signaling in health and disease. *Brain Res* 1623:3-17, 2015.

Davis BA, and Boulton AA. The trace amines and their acidic metabolites in depression--an overview. *Prog Neuropsychopharmacol Biol Psychiatry* 18: 17-45, 1994.

DeNofrio D, Hooek TC, and Herman IM. Functional sorting of actin isoforms in microvascular pericytes. *J Cell Biol* 109: 191-202, 1989.

Dietz V. Spastic movement disorder. *Spinal Cord* 38: 389-393, 2000.

Ditunno JF, Little JW, Tessler A, and Burns AS. Spinal shock revisited: a four-phase model. *Spinal Cord* 42: 383-395, 2004.

Dore-Duffy P, Katychew A, Wang X, and Van Buren E. CNS microvascular pericytes exhibit multipotential stem cell activity. *J Cereb Blood Flow Metab* 26: 613-624, 2006.

Dore-Duffy P, Owen C, Balabanov R, Murphy S, Beaumont T, and Rafols JA. Pericyte migration from the vascular wall in response to traumatic brain injury. *Microvasc Res* 60: 55-69, 2000.

Dyck LE, Yang CR, and Boulton AA. The biosynthesis of p-tyramine, m-tyramine, and beta-phenylethylamine by rat striatal slices. *J Neurosci Res* 10: 211-220, 1983.

Edvinsson L, Birath E, Uddman R, Lee TJ, Duverger D, MacKenzie ET, and Scatton B. Indoleaminergic mechanisms in brain vessels; localization, concentration, uptake and in vitro responses of 5-hydroxytryptamine. *Acta Physiol Scand* 121: 291-299, 1984.

Enbaek F, and Magnussen I. Determination of 5-hydroxytryptophan in plasma by high-performance liquid chromatography and fluorometric detection after phthaldialdehyde reaction. *Clin Chem* 24: 376-378, 1978.

Ershov P, Ugrumov M, Calas A, Krieger M, and Thibault J. Degeneration of dopaminergic neurons triggers an expression of individual enzymes of dopamine synthesis in non-dopaminergic neurons of the arcuate nucleus in adult rats. *J Chem Neuroanat* 30: 27-33, 2005.

Faraci FM, and Brian JE, Jr. Nitric oxide and the cerebral circulation. *Stroke* 25: 692-703, 1994.

Faraci FM, and Heistad DD. Regulation of large cerebral arteries and cerebral microvascular pressure. *Circ Res* 66: 8-17, 1990.

Filosa JA, Morrison HW, Iddings JA, Du W, and Kim KJ. Beyond neurovascular coupling, role of astrocytes in the regulation of vascular tone. *Neurosci* 2015.

Fisher M. Pericyte signaling in the neurovascular unit. *Stroke* 40: S13-15, 2009.

Forrester T, Harper AM, MacKenzie ET, and Thomson EM. Effect of adenosine triphosphate and some derivatives on cerebral blood flow and metabolism. *J Physiol* 296: 343-355, 1979.

Fritschy JM, and Grzanna R. Demonstration of two separate descending noradrenergic pathways to the rat spinal cord: evidence for an intragriseal trajectory of locus coeruleus axons in the superficial layers of the dorsal horn. *J Comp Neurol* 291: 553-582, 1990.

Gillilan LA. The arterial blood supply of the human spinal cord. *J Comp Neurol* 110: 75-103, 1958.

Goldstein M, Lieberman A, and Pearson J. Relatively high levels of dopamine in nucleus accumbens of levodopa treated patients with Parkinson's disease. *J Neural Transm* 54: 129-134, 1982.

Gordon GR, Mulligan SJ, and MacVicar BA. Astrocyte control of the cerebrovasculature. *Glia* 55: 1214-1221, 2007.

Gozal EA, O'Neill BE, Sawchuk MA, Zhu H, Halder M, Chou CC, and Hochman S. Anatomical and functional evidence for trace amines as unique modulators of locomotor function in the mammalian spinal cord. *Front Neural Circuits* 8: 134, 2014.

Gozlan H, El Mestikawy S, Pichat L, Glowinski J, and Hamon M. Identification of presynaptic serotonin autoreceptors using a new ligand: ³H-PAT. *Nature* 305: 140-142, 1983.

Grandy DK. Trace amine-associated receptor 1: Family archetype or iconoclast? *Pharmacol Ther* 116: 355-390, 2007.

Griffith S, Lincoln J, and Burnstock G. Serotonin as a neurotransmitter in cerebral arteries. *Brain Res* 247: 388-392, 1982.

Guertin PA. Recovery of locomotor function with combinatory drug treatments designed to synergistically activate specific neuronal networks. *Curr Med Chem* 16: 1366-1371, 2009.

Hall CN, Reynell C, Gesslein B, Hamilton NB, Mishra A, Sutherland BA, O'Farrell FM, Buchan AM, Lauritzen M, and Attwell D. Capillary pericytes regulate cerebral blood flow in health and disease. *Nature* 508: 55-60, 2014.

Hamilton NB, Attwell D, and Hall CN. Pericyte-mediated regulation of capillary diameter: a component of neurovascular coupling in health and disease. *Front Neuroenergetics* 2: 2010.

Hardebo J, Emson P, Falck B, Owman C, and Rosengren E. Enzymes related to monoamine transmitter metabolism in brain microvessels. *J Neurochem* 35: 1388-1393, 1980a.

Hardebo J, Falck B, and Owman C. A comparative study on the uptake and subsequent decarboxylation of monoamine precursors in cerebral microvessels. *Acta Physiol Scand* 107: 161-167, 1979a.

Hardebo JE, Falck B, Owman C, and Rosengren E. Studies on the enzymatic blood-brain barrier: Quantitative measurements of DOPA decarboxylase in the wall of microvessels as related to the parenchyma in various CNS regions. *Acta Physiol Scandinavica* 105: 453-460, 1979b.

Hardebo JE, and Owman C. Barrier mechanisms for neurotransmitter monoamines and their precursors at the blood-brain interface. *Ann Neurol* 8: 1-11, 1980b.

Harder DR. Pressure-dependent membrane depolarization in cat middle cerebral artery. *Circ Res* 55: 197-202, 1984.

Harvey PJ, Li X, Li Y, and Bennett DJ. 5-HT₂ receptor activation facilitates a persistent sodium current and repetitive firing in spinal motoneurons of rats with and without chronic spinal cord injury. *J Neurophysiol* 96: 1158-1170, 2006.

Hayashi Y, Jacob-Vadakot S, Dugan E, McBride S, Olexa R, Simansky K, Murray M, and Shumsky J. 5-HT precursor loading, but not 5-HT receptor agonists, increases motor function after spinal cord contusion in adult rats. *Exp Neurol* 221: 68-78, 2010.

Heckmann CJ, Gorassini MA, and Bennett DJ. Persistent inward currents in motoneuron dendrites: implications for motor output. *Muscle Nerve* 31: 135-156, 2005.

Heller B, Fischer E, and Martin R. Therapeutic action of D-phenylalanine in Parkinson's disease. *Arzneimittelforschung* 26: 577-579, 1976.

Herman IM, and D'Amore PA. Microvascular pericytes contain muscle and nonmuscle actins. *J Cell Biol* 101: 43-52, 1985.

Hickey R, Albin MS, Bunegin L, and Gelineau J. Autoregulation of spinal cord blood flow: is the cord a microcosm of the brain? *Stroke* 17: 1183-1189, 1986.

Hirschi KK, and D'Amore PA. Pericytes in the microvasculature. *Cardiovasc Res* 32: 687-698, 1996.

Hochman S, Garraway SM, Machacek DW, and Shay BL. 5-HT receptors and the neuromodulatory control of spinal cord function. *Motor Neurobiology of the Spinal Cord* 47-87, 2001.

Hu J, Cao Y, Wu T, Li D, and Lu H. High-resolution three-dimensional visualization of the rat spinal cord microvasculature by synchrotron radiation micro-CT. *Med Phys* 41: 101904, 2014.

Iadecola C, and Nedergaard M. Glial regulation of the cerebral microvasculature. *Nat Neurosci* 10: 1369-1376, 2007.

Iadecola C, Yang G, Ebner TJ, and Chen G. Local and propagated vascular responses evoked by focal synaptic activity in cerebellar cortex. *J Neurophysiol* 78: 651-659, 1997.

Ikemoto K. Significance of human striatal D-neurons: implications in neuropsychiatric functions. *Prog Neuropsychopharmacol Biol Psych* 28: 429-434, 2004.

Ikemoto K, Kitahama K, Jouvet A, Arai R, Nishimura A, Nishi K, and Nagatsu I. Demonstration of L-dopa decarboxylating neurons specific to human striatum. *Neurosci Lett* 232: 111-114, 1997.

Imperato-Kalmar EL, McKinney RA, Schnell L, Rubin BP, and Schwab ME. Local changes in vascular architecture following partial spinal cord lesion in the rat. *Exp Neurol* 145: 322-328, 1997.

Jackowski A, Crockard A, and Burnstock G. 5-Hydroxytryptamine demonstrated immunohistochemically in rat cerebrovascular nerves largely represents 5-hydroxytryptamine uptake into sympathetic nerve fibres. *Neurosci* 29: 453-462, 1989.

Jacobs BL, and Azmitia EC. Structure and function of the brain serotonin system. *Physiol Rev* 72: 165-229, 1992.

Jaeger C, Ruggiero D, Albert V, Joh T, and Reis D. Immunocytochemical localization of aromatic-L-amino acid decarboxylase. *Handbook of Chemical Neuroanatomy* 2: 387-408, 1984.

Jaeger C, Teitelman G, Joh T, Albert V, Park D, and Reis D. Some neurons of the rat central nervous system contain aromatic-L-amino-acid decarboxylase but not monoamines. *Science* 219: 1233-1235, 1983.

Kalaria RN, and Harik SI. Blood-Brain barrier monoamine oxidase: enzyme characterization in cerebral microvessels and other tissues from six mammalian species, including human. *J Neurochem* 49: 856-864, 1987.

Karasawa N, Arai R, Isomura G, Nagatsu T, and Nagatsu I. Chemical features of monoaminergic and non-monoaminergic neurons in the brain of laboratory shrew (*Suncus murinus*) are changed by systemic administration of monoamine precursors. *Neurosci Res* 24: 67-74, 1995.

Kelley C, D'Amore P, Hechtman HB, and Shepro D. Microvascular pericyte contractility in vitro: comparison with other cells of the vascular wall. *J Cell Biol* 104: 483-490, 1987.

Kema IP, de Vries EG, and Muskiet FA. Clinical chemistry of serotonin and metabolites. *J Chromatogr B: Biomed Sci Appl* 747: 33-48, 2000.

Khanna N, Altmeyer W, Zhuo J, and Steven A. Functional Neuroimaging: Fundamental Principles and Clinical Applications. *Neuroradiol J* 28: 87-96, 2015.

Kitahama K, Geffard M, Araneda S, Arai R, Ogawa K, Nagatsu I, and Pequignot J-M. Localization of L-DOPA uptake and decarboxylating neuronal structures in the cat brain using dopamine immunohistochemistry. *Brain Res* 1167: 56-70, 2007.

Knight AR, Misra A, Quirk K, Benwell K, Revell D, Kennett G, and Bickerdike M. Pharmacological characterisation of the agonist radioligand binding site of 5-HT(2A), 5-HT(2B) and 5-HT(2C) receptors. *Naunyn Schmiedebergs Arch Pharmacol* 370: 114-123, 2004.

Knot HJ, and Nelson MT. Regulation of arterial diameter and wall $[Ca^{2+}]$ in cerebral arteries of rat by membrane potential and intravascular pressure. *J Physiol* 508 (Pt 1): 199-209, 1998.

Kopin IJ. False adrenergic transmitters. *Annu Rev Pharmacol* 8: 377-394, 1968.

Kopin IJ, Fischer JE, Musacchio J, and Horst WD. Evidence for a false neurochemical transmitter as a mechanism for the hypotensive effect of monoamine oxidase inhibitors. *Proc Natl Acad Sci U S A* 52: 716-721, 1964.

Koyanagi I, Tator CH, and Lea PJ. Three-dimensional analysis of the vascular system in the rat spinal cord with scanning electron microscopy of vascular corrosion casts. Part 1: Normal spinal cord. *Neurosurgery* 33: 277-283; discussion 283-274, 1993.

Krueger M, and Bechmann I. CNS pericytes: concepts, misconceptions, and a way out. *Glia* 58: 1-10, 2010.

Kundi S, Bicknell R, and Ahmed Z. The role of angiogenic and wound-healing factors after spinal cord injury in mammals. *Neurosci Res* 76: 1-9, 2013.

Lacroix A, Toussay X, Anenberg E, Lecrux C, Ferreira N, Karagiannis A, Plaisier F, Chausson P, Jarlier F, Burgess SA, Hillman EM, Tegeder I, Murphy TH, Hamel E, and Cauli B. COX-2-derived prostaglandin E2 produced by pyramidal neurons contributes to neurovascular coupling in the rodent cerebral cortex. *J Neurosci* 35: 11791-11810, 2015.

Lai CH, and Kuo KH. The critical component to establish in vitro BBB model: Pericyte. *Brain Res Brain Res Rev* 50: 258-265, 2005.

Lance JW. The control of muscle tone, reflexes, and movement: Robert Wartenberg Lecture. *Neurol* 30: 1303-1313, 1980.

Lassen NA. Cerebral blood flow and oxygen consumption in man. *Physiol Rev* 39: 183-238, 1959.

Lazorthes G, Gouaze A, Zadeh JO, Santini JJ, Lazorthes Y, and Burdin P. Arterial vascularization of the spinal cord. Recent studies of the anastomotic substitution pathways. *J Neurosurg* 35: 253-262, 1971.

Lidbrink P, and Fuxe K. Selective reserpine-resistant accumulation of catecholamines in central dopamine neurones after DOPA administration. *Brain Res* 67: 439-456, 1974.

Lindahl P, Johansson BR, Leveen P, and Betsholtz C. Pericyte loss and microaneurysm formation in PDGF-B-deficient mice. *Science* 277: 242-245, 1997.

Lindemann L, Ebeling M, Kratochwil NA, Bunzow JR, Grandy DK, and Hoener MC. Trace amine-associated receptors form structurally and functionally distinct subfamilies of novel G protein-coupled receptors. *Genomics* 85: 372-385, 2005.

Lofving B, and Mellander S. Some aspects of the basal tone of the blood vessels. *Acta Physiol Scand* 37: 134-141, 1956.

Loy DN, Crawford CH, Darnall JB, Burke DA, Onifer SM, and Whittemore SR. Temporal progression of angiogenesis and basal lamina deposition after contusive spinal cord injury in the adult rat. *J Comp Neurol* 445: 308-324, 2002.

Magnusson T. Effect of chronic transection on dopamine, noradrenaline and 5-hydroxytryptamine in the rat spinal cord. *Naunyn Schmiedebergs Arch Pharmacol* 278: 13-22, 1973.

Martirosyan NL, Feuerstein JS, Theodore N, Cavalcanti DD, Spetzler RF, and Preul MC. Blood supply and vascular reactivity of the spinal cord under normal and pathological conditions. *J Neurosurg Spine* 15: 238-251, 2011.

Miller GM. The emerging role of trace amine-associated receptor 1 in the functional regulation of monoamine transporters and dopaminergic activity. *J Neurochem* 116: 164-176, 2011.

Mura A, Jackson D, Manley MS, Young SJ, and Groves PM. Aromatic L-amino acid decarboxylase immunoreactive cells in the rat striatum: a possible site for the conversion of exogenous L-DOPA to dopamine. *Brain Res* 704: 51-60, 1995.

Mura A, Linder J, Young S, and Groves P. Striatal cells containing aromatic L-amino acid decarboxylase: an immunohistochemical comparison with other classes of striatal neurons. *Neurosci* 98: 501-511, 2000.

Murray KC, Nakae A, Stephens MJ, Rank M, D'Amico J, Harvey PJ, Li X, Harris RLW, Ballou EW, and Anelli R. Recovery of motoneuron and locomotor function after spinal cord injury depends on constitutive activity in 5-HT_{2C} receptors. *Nature medicine* 16: 694-700, 2010.

Narang D, Tomlinson S, Holt A, Mousseau DD, and Baker GB. Trace amines and their relevance to psychiatry and neurology: a brief overview. *Bull Clin Psychopharmacol* 21: 73-79, 2011.

Nehls V, and Drenckhahn D. Heterogeneity of microvascular pericytes for smooth muscle type alpha-actin. *J Cell Biol* 113: 147-154, 1991.

Ogawa S, and Lee TM. Magnetic resonance imaging of blood vessels at high fields: in vivo and in vitro measurements and image simulation. *Magn Reson Med* 16: 9-18, 1990a.

Ogawa S, Lee TM, Nayak AS, and Glynn P. Oxygenation-sensitive contrast in magnetic resonance image of rodent brain at high magnetic fields. *Magn Reson Med* 14: 68-78, 1990b.

Osol G, and Halpern W. Myogenic properties of cerebral blood vessels from normotensive and hypertensive rats. *Am J Physiol* 249: H914-921, 1985.

Palmer RM, Ferrige AG, and Moncada S. Nitric oxide release accounts for the biological activity of endothelium-derived relaxing factor. *Nature* 327: 524-526, 1987.

Paterson IA, Juorio AV, and Boulton AA. 2-Phenylethylamine: a modulator of catecholamine transmission in the mammalian central nervous system? *J Neurochem* 55: 1827-1837, 1990.

Peerless SJ, and Yasargil MG. Adrenergic innervation of the cerebral blood vessels in the rabbit. *J Neurosurg* 35: 148-154, 1971.

Peppiatt CM, Howarth C, Mobbs P, and Attwell D. Bidirectional control of CNS capillary diameter by pericytes. *Nature* 443: 700-704, 2006.

Perrier J-F, and Delgado-Lezama R. Synaptic release of serotonin induced by stimulation of the raphe nucleus promotes plateau potentials in spinal motoneurons of the adult turtle. *J Neurosci* 25: 7993-7999, 2005.

Peterson EC, Wang Z, and Britz G. Regulation of cerebral blood flow. *Int J Vasc Med* 2011: 823525, 2011.

Phillis JW. Adenosine and adenine nucleotides as regulators of cerebral blood flow: roles of acidosis, cell swelling, and KATP channels. *Crit Rev Neurobiol* 16: 237-270, 2004.

Popovich PG, Horner PJ, Mullin BB, and Stokes BT. A quantitative spatial analysis of the blood-spinal cord barrier. I. Permeability changes after experimental spinal contusion injury. *Exp Neurol* 142: 258-275, 1996.

Potkin SG, Wyatt RJ, and Karoum F. Phenylethylamine (PEA) and phenylacetic acid (PAA) in the urine of chronic schizophrenic patients and controls. *Psychopharmacol Bull* 16: 52-54, 1980.

Raichle ME. Behind the scenes of functional brain imaging: a historical and physiological perspective. *Proc Natl Acad Sci U S A* 95: 765-772, 1998.

Rajaofetra N, Sandillon F, Geffard M, and Privat A. Pre- and post-natal ontogeny of serotonergic projections to the rat spinal cord. *J Neurosci Res* 22: 305-321, 1989.

Roy CS, and Sherrington CS. On the Regulation of the Blood-supply of the Brain. *J Physiol* 11: 85-158 117, 1890.

Saavedra J. β -Phenylethylamine, phenylethanolamine, tyramine and octopamine. In: *Catecholamines II* Springer, 1989, p. 181-210.

Schmidt BJ, and Jordan LM. The role of serotonin in reflex modulation and locomotor rhythm production in the mammalian spinal cord. *Brain Res Bull* 53: 689-710, 2000.

Schmidt HH, Lohmann SM, and Walter U. The nitric oxide and cGMP signal transduction system: regulation and mechanism of action. *Biochim Biophys Acta* 1178: 153-175, 1993.

Senter HJ, and Venes JL. Altered blood flow and secondary injury in experimental spinal cord trauma. *J Neurosurg* 49: 569-578, 1978.

Shen Y, Monsma FJ, Jr., Metcalf MA, Jose PA, Hamblin MW, and Sibley DR. Molecular cloning and expression of a 5-hydroxytryptamine₇ serotonin receptor subtype. *J Biol Chem* 268: 18200-18204, 1993.

Sherrington CS. Flexion-reflex of the limb, crossed extension-reflex, and reflex stepping and standing. *J Physiol* 40: 28-121, 1910.

Shimazu S, and Miklya I. Pharmacological studies with endogenous enhancer substances: beta-phenylethylamine, tryptamine, and their synthetic derivatives. *Prog Neuropsychopharmacol Biol Psychiatry* 28: 421-427, 2004.

Shingu H, Kimura I, Nasu Y, Shiotani A, Oh-hama M, Hijioka A, and Tanaka J. Microangiographic study of spinal cord injury and myelopathy. *Paraplegia* 27: 182-189, 1989.

Sliwa JA, and Maclean IC. Ischemic myelopathy: a review of spinal vasculature and related clinical syndromes. *Arch Phys Med Rehabil* 73: 365-372, 1992.

Spatz M, and McCARRON RM. *Blood-brain barrier and monoamines, revisited.* Cambridge University Press, Cambridge, UK Blood-brain barrier and monoamines, revisited, 1998.

Takeoka A, Kubasak MD, Zhong H, Kaplan J, Roy RR, and Phelps PE. Noradrenergic innervation of the rat spinal cord caudal to a complete spinal cord transection: effects of olfactory ensheathing glia. *Exp Neurol* 222: 59-69, 2010.

Tanaka K, Fukuuchi Y, Gomi S, Mihara B, Shirai T, Nogawa S, Nozaki H, and Nagata E. Inhibition of nitric oxide synthesis impairs autoregulation of local cerebral blood flow in the rat. *Neuroreport* 4: 267-270, 1993.

Teng GQ, Nauli SM, Brayden JE, and Pearce WJ. Maturation alters the contribution of potassium channels to resting and 5HT-induced tone in small cerebral arteries of the sheep. *Brain Res Dev Brain Res* 133: 81-91, 2002.

Tremblay LE, Bédard PJ, Maheux R, and Di Paolo T. Denervation supersensitivity to 5-hydroxytryptamine in the rat spinal cord is not due to the absence of 5-hydroxytryptamine. *Brain Res* 330: 174-177, 1985.

Turnbull IM, Brieg A, and Hassler O. Blood supply of cervical spinal cord in man. A microangiographic cadaver study. *J Neurosurg* 24: 951-965, 1966.

Tveten L. Spinal cord vascularity. III. The spinal cord arteries in man. *Acta radiologica: Diagnosis* 17: 257-273, 1976.

U'Prichard DC, Greenberg DA, and Snyder SH. Binding characteristics of a radiolabeled agonist and antagonist at central nervous system alpha noradrenergic receptors. *Mol Pharmacol* 13: 454-473, 1977.

Ugrumov M. Non-dopaminergic neurons partly expressing dopaminergic phenotype: distribution in the brain, development and functional significance. *J Chem Neuroanat* 38: 241-256, 2009.

Viala D, and Buser P. Methods of obtaining locomotor rhythms in the spinal rabbit by pharmacological treatments (DOPA, 5-HTP, D-amphetamine). *Brain Res* 35: 151, 1971.

Warsh J, and Stancer H. Brain and peripheral metabolism of 5-hydroxytryptophan-14C following peripheral decarboxylase inhibition. *J Pharmacol Exp Ther* 197: 545-555, 1976.

Willie CK, Tzeng YC, Fisher JA, and Ainslie PN. Integrative regulation of human brain blood flow. *J Physiol* 592: 841-859, 2014.

Xie Z, and Miller GM. Beta-phenylethylamine alters monoamine transporter function via trace amine-associated receptor 1: implication for modulatory roles of trace amines in brain. *J Pharmacol Exp Ther* 325: 617-628, 2008.

Xie Z, and Miller GM. Trace amine-associated receptor 1 as a monoaminergic modulator in brain. *Biochem Pharmacol* 78: 1095-1104, 2009.

Xie Z, and Miller GM. Trace amine-associated receptor 1 is a modulator of the dopamine transporter. *J Pharmacol Exp Ther* 321: 128-136, 2007.

Yemisci M, Gursoy-Ozdemir Y, Vural A, Can A, Topalkara K, and Dalkara T. Pericyte contraction induced by oxidative-nitrative stress impairs capillary reflow despite successful opening of an occluded cerebral artery. *Nat Med* 15: 1031-1037, 2009.

Zhang Z, and Guth L. Experimental spinal cord injury: Wallerian degeneration in the dorsal column is followed by revascularization, glial proliferation, and nerve regeneration. *Exp Neurol* 147: 159-171, 1997.

Zlokovic BV. Neurovascular pathways to neurodegeneration in Alzheimer's disease and other disorders. *Nat Rev Neurosci* 12: 723-738, 2011.

Chapter 2: Synthesis, transport and metabolism of serotonin from exogenously applied 5-HTP after spinal cord injury in rats.

Introduction

Descending brainstem-derived monoamines, such as serotonin (5-hydroxytryptamine, 5-HT) and noradrenaline (NA) play a powerful role in modulating the excitability of motoneurons in the spinal cord (Harvey et al. 2006; Heckman et al. 2005; Hochman et al. 2001; Jacobs et al. 1992; Murray et al. 2010; Perrier et al. 2005; Schmidt et al. 2000). 5-HT, particularly, increases motoneurons' resting membrane potential and facilitates low-voltage gated persistent inward currents composed of sodium (Na PIC) and calcium (Ca PIC), allowing motoneurons to depolarize more easily and therefore generate appropriate muscle contractions (Harvey et al. 2006; Heckman et al. 2005). In normal rats, spinal monoamines are primarily produced in the terminals of descending brainstem fibres (Carlsson et al. 1964; Jacobs et al. 1992), which contain the necessary biosynthesis enzymes, including tryptophan hydroxylase (TPH) that converts tryptophan to 5-hydroxytryptophan (5-HTP), tyrosine hydroxylase (TH) that converts tyrosine to L-dihydroxyphenylalanine (L-DOPA), and aromatic acid decarboxylase (AADC) that converts 5-HTP to 5-HT and L-DOPA to dopamine (DA); they also contain monoamine oxidase (MAO) that metabolises monoamines (Best et al. 2010; Gozal 2010; Hardebo et al. 1980b; Ikemoto 2004). Transection of the spinal cord destroys all supraspinal innervation of the spinal cord, leading to the loss of most monoamine fibers caudal to the lesion site (Carlsson et al. 1964; Murray et al. 2010) together with a dramatic loss of monoamines and some of the key enzymes involved in monoamines synthesis, including TPH and TH (Clineschmidt et al. 1971; Magnusson 1973; Takeoka et al. 2010).

Despite the elimination of monoamine fibre innervation with spinal transection, repeated studies (Barbeau et al. 1990; Bedard et al. 1979; Chandler et al. 1984; Guertin 2009; Hayashi et al. 2010;

Tremblay et al. 1985; Viala et al. 1971) have shown that exogenous application of the monoamine precursors 5-HTP or L-DOPA leads to synthesis of monoamines that in turn activate monoamine receptors and ultimately improve motor activity (locomotion or changes in spasms), suggesting that substantial functional AADC still remains in the spinal cord converting these precursors to monoamines. A similar situation occurs with Parkinson's disease (PD): normal DA innervation of the striatum is lost, but somehow L-DOPA medication still leads to production of DA in the striatum (Goldstein et al. 1982; Ikemoto et al. 1997; Lidbrink et al. 1974). The origin of this AADC after loss of monoamine innervation has been extensively investigated in the striatum in relation to PD (Ikemoto 2004; Ikemoto et al. 1997; Karasawa et al. 1995; Kitahama et al. 2007; Mura et al. 1995; Mura et al. 2000; Ugrumov 2009), but remains uncertain after spinal cord injury (Jaeger et al. 1983). In the striatum (and arcuate nucleus) destruction of monoamine fibres (DA fibres; with 6-hydroxydopamine) leads to an upregulation of AADC activity, and in particular an emergence of a population of AADC-containing neurons, similar to the D-cells described further below (Ershov et al. 2005; Mura et al. 1995). This suggests that AADC activity increases when levels of monoamines are reduced, as appears to generally occur with alterations of monoamines (Berry 2004; Grandy 2007). We investigate here whether a similar compensation happens with spinal cord injury. We explore both where AADC remains in the spinal cord after injury, and whether this AADC can make functional amounts of 5-HT.

In the normal spinal cord, besides the abundant monoamine fibres that contain AADC, some AADC-positive cells are found juxtaposed to the ependymal cells of the central canal, with processes extending into the lumen of the central canal. These have been termed D1-cells,

together with other such cells along the neural axis (D2 – D14), including in the striatum (Jaeger et al. 1984; Jaeger et al. 1983). D-cells are characterized primarily by being monoenzymatic (AADC-only), lacking TH and TPH, rendering them incapable of making monoamines from endogenous precursors (tyrosine and tryptophan respectively) (Jaeger et al. 1984; Jaeger et al. 1983). They often oppose the blood vessels, central canal or ventricles, and in this regard are thought to be part the amine precursor uptake and decarboxylase system (APUD) that has an endocrine function of discharging amines into the blood and CSF (Karasawa et al. 1995). They are anatomically reminiscent of the dopaminergic cells that contact the central canal in lower animals (Acerbo et al. 2003). D-cells could be the site of monoamine synthesis with exogenous application of precursors like 5-HTP after spinal cord injury, though they do seem spatially distant from motoneurons and relatively few in number, raising a question of how they can affect motor function.

AADC is also abundant in the liver, kidney, gastrointestinal tract and blood vessels (Berry et al. 1996). In the liver and kidney, AADC is thought to play a role in disposing of excess monoamine precursors and amino acids: here cells take up precursors and AADC catalyzes them to form 5-HT, catecholamines and trace amines, which are then either directly discarded into the urine (kidney) or further broken down by MAO (liver) (Berry et al. 1996). Peripheral AADC like this consumes a large fraction of systemically applied precursors 5-HTP or L-DOPA (Warsh et al. 1976), and thus in clinical practice it is common to block peripheral AADC with substances like carbidopa that do not easily cross the blood-brain barrier (BBB), in order to allow more effective delivery of 5-HTP or L-DOPA medications to the brain, especially in treatment of PD (Jonkers et al. 2001).

CNS blood vessels also contain some AADC, as well as abundant MAO, which are together thought to perform a similar function of regulating excess monoamine precursors, as seen in the periphery (liver and kidney), and thus function as a *monoamine trapping and disposal system* (Hardebo et al. 1980b; Kalaria et al. 1987; Spatz et al. 1998). Specifically, exogenously injected circulating monoamine precursors are normally prevented from crossing into the CNS because AADC in endothelial cells and pericytes of CNS vessels catalyzes them to form monoamines, which are then trapped in the endothelial cells and eventually broken down by MAO. Only when the concentration of blood-borne monoamine precursors is high enough to saturate activities of vessel AADC and MAO (which does not occur under normal physiological conditions) do these precursors or monoamines cross the BBB and get into CNS parenchyma (Hardebo et al. 1979b; Hardebo et al. 1980b). Under normal physiological conditions endogenous monoamines and their precursors are at much higher concentrations in the CNS than in the blood (>100 fold higher), and thus the major role of the AADC and MAO enzymes in the brain vessel endothelial cells is likely to take up and metabolize excess monoamines and precursors from the CNS and thus dispose of them (Engbaek et al. 1978; Hardebo et al. 1980b; Kema et al. 2000; Spatz et al. 1998). This role may well reverse with spinal cord injury, whereby endothelial cells may provide amines to the spinal cord, because central monoamines and their precursors are largely eliminated by injury, and this is an idea that we investigate in the present paper.

While both peripheral and central AADC produces 5-HT from exogenously applied 5-HTP, this AADC is unlikely to endogenously produce 5-HT that can affect the spinal cord after spinal transection, for several reasons. First, peripherally synthesized 5-HT is mostly transported, stored

in vesicles or metabolized before it gets into the circulation, and what little 5-HT does enter the circulation (from gut) is avidly transported into platelets, leaving serum 5-HT levels very low (Kema et al. 2000; Paasonen 1965), and this remaining 5-HT does not easily cross the BBB (Oldendorf 1971). Second, while 5-HTP does easily cross the BBB (by the amino acid L-transport system)(Gomes et al. 1999; Hawkins et al. 2006), very little if any is normally detected in serum (Coppi et al. 1989; Engbaek et al. 1978; Kema et al. 2000; Tyce et al. 1981), and thus AADC-containing cells in the spinal cord (D-cells and vessels) are unlikely to receive adequate endogenous 5-HTP to make 5-HT. Finally, there is not likely a significant source of 5-HTP intrinsic to the spinal cord after transection, considering that most TPH is lost with injury, along with the associated descending 5-HT fibres (Carlsson et al. 1964; Clineschmidt et al. 1971).

In the present study we examined where AADC is expressed after spinal cord transection in rats (using immunolabelling), and whether it is upregulated in different structures, including D-cells and blood vessels, to compensate for loss of brainstem monoamine innervation and associated AADC. We then explored the functional role of these sources of AADC in synthesis of 5-HT from either exogenously applied 5-HTP, or endogenous 5-HTP. We found a clear upregulation of AADC expression and activity with injury, especially in blood vessels. However, D-cell AADC expression was unexpectedly decreased, and instead we found a new class of AADC-containing neurons after injury. Both these AADC-containing vessels and neurons affected spinal cord function, increasing motoneuron activity (spasms) when we added exogenous precursors, especially when we blocked MAO. However, we found no evidence that endogenous 5-HTP could produce adequate 5-HT to affect motor function. This does not, however, rule out other endogenous functions of AADC after spinal cord injury, including the production of trace

amines, like tryptamine, from dietary amino acids, like tryptophan (Berry 2004; Grandy 2007), as we examine in a later paper (Li and Bennett, in preparation).

Methods

Adult female rats with spinal cord injury (SCI) were studied and compared to age-matched uninjured normal rats (3.5–5 months old). For the chronic SCI, adult rats were transected at the S2 sacral level at about 2 months of age, and experiments commenced after their affected muscles became spastic (1.5–3 months after injury), as detailed previously (Bennett et al. 1999; Bennett et al. 2004). The affected sacrocaudal spinal cord was evaluated with histological methods and compared to normal cords and sections of cord rostral to the injury. Also, recordings were made from muscle, motoneurons and associated ventral roots of the sacrocaudal spinal cord of spastic adult rats (Bennett et al. 2004; Murray et al. 2010). Some recordings were made from the whole sacrocaudal spinal cord that was removed from the chronic spinal or normal rats and maintained *in vitro*, while others were made with EMG recordings in the awake rats (Murray et al. 2010). Some rats were additionally studied only 1 to 2 days after sacral transection (acute spinal). All experimental procedures were approved by the University of Alberta Animal Care and Use Committee: Health Sciences.

In vitro preparation

Details of the *in vitro* experimental procedures have been described previously (Murray et al. 2010; Murray et al. 2011b). Briefly, all the rats were anesthetized with urethane (0.18 g/100 g; with a maximum dose of 0.45 g), and the sacrocaudal spinal cord was removed and transferred to a dissection chamber containing modified artificial cerebrospinal fluid (mACSF). Spinal roots were removed, except the sacral S4 and caudal Ca1 ventral roots and the Ca1 dorsal roots. After 1.5 h in the dissection chamber (at 20°C), the cord was transferred to a recording chamber containing normal ACSF (nACSF) maintained near 24°C, with a flow rate > 5 ml/min. A 45

minute period in nACSF was given to wash out the residual anesthetic and mACSF before recording, at which time the nACSF was recycled in a closed system.

Ventral root reflex recording and averaging

Dorsal and ventral roots were mounted on silver-silver-chloride wires above the nACSF of the recording chamber and covered with a 5:1 mixture of petroleum jelly and mineral oil for monopolar stimulation and recording (Murray et al. 2011b). We evoked ventral root reflexes with a low-threshold Ca1 dorsal root stimulation (single pulse, 0.1 ms, 0.02 mA, corresponding to 3 times afferent threshold, T) using a constant current stimulator (Isoflex, Israel). This stimulation intensity ($3 \times T$) is compatible with activation of low-threshold group I and II ($A\beta$) afferents, with a major cutaneous component (Murray et al. 2010; Murray et al. 2011b). The stimulation was repeated five times at 10 second intervals for each trial. The ventral root recordings were amplified ($\times 2,000$), high-pass filtered at 100 Hz, low-pass filtered at 3 kHz, and recorded with a data-acquisition system sampling at 6.7 kHz (Axonscope 8, Axon Instruments). Ventral root reflexes were quantified using custom written software (Matlab, MathWorks, Natick, MA). That did the following: data were high pass filtered at 800 Hz and rectified to allow averaging. We quantified the long-latency, long-lasting reflex (LLR) by averaging the rectified response 500–4,000 ms after stimulus, a period where the response is mainly determined by the motoneuron Ca PIC activity and not by stimulus-evoked synaptic inputs (Murray et al. 2011a; Murray et al. 2011b). Ventral root activity was averaged for all five stimuli in a trial. Also, background activity 300 ms prior to each stimulation was quantified similarly. This recording procedure was repeated at 12 min intervals, and agonists were added immediately after each recording, giving them time to fully act by the next recording session. Cumulative dose–response

relations were computed by increasing agonist doses at these 12 min intervals (0.003, 0.01, 0.03, 0.1, etc μM doses used). The effects of agonists on the reflexes were reversible on washout of the agonist, but full recovery to baseline only occurred after several hours, likely because of the large size of the whole cord preparation. Thus washout of agonists was not feasible between doses of the agonists used in the construction of dose–response relations.

Intracellular recording

Sharp intracellular electrodes were made from glass capillary tubes (1.5 mm OD, Warner GC 150F-10) using a Sutter P-87 micropipette puller and filled with a combination of 1 M potassium acetate and 1 M KCl. Electrodes were beveled down from an initial resistance of 40–80 to 26–32 M Ω using a rotary beveller (Sutter BV-10). A stepper-motor micromanipulator (660, Kopf) was used to advance the electrodes through the ventral cord surface into motoneurons. Penetrations were made with capacitance-over-compensation ringing. After penetration, motoneuron identification was made with antidromic ventral root stimulation, and noting ventral horn location, input resistance and time constant (> 6 ms for motoneurons) (Murray et al. 2010; Murray et al. 2011b). Data were collected with an Axoclamp 2b intracellular amplifier (Axon Instruments, Burlingame, CA) running in discontinuous current clamp (DCC, switching rate 4–6 kHz, output bandwidth 3.0 kHz, sample rate of 6.7 kHz) or discontinuous single-electrode voltage clamp (SEVC; gain, 0.8 – 2.5 nA/mV) modes.

Slow triangular voltage ramps (3.5 mV/s voltage clamp) were applied to the motoneurons to measure their electrical properties, as detailed previously (Murray et al. 2011b). The input resistance (R_m) was measured during the voltage ramps over a 5 mV range near rest and

subthreshold to PIC onset. Resting potential (V_m) was recorded with 0 nA bias current, after the cell had been given about 15 min to stabilize after penetration. The slow triangular voltage ramps were used to directly measure the PICs. During the upward portion of this ramp, the current response initially increased linearly with voltage in response to the passive leak conductance. A linear relation was fit in the region just below the PIC onset (5 mV below) and extrapolated to the whole range of the ramp (leak current). At depolarized potentials above the PIC onset threshold, there was a downward deviation from the extrapolated leak current, and the PIC was estimated as the difference between the leak current and the total current (leak-subtracted current). The PIC was quantified as the initial peak amplitude of this downward deviation below the leak line (leak-subtracted current). The onset voltage for the PIC was defined as the voltage at which the slope of the current response initially reached zero (Murray et al. 2011b).

Drugs and solutions

Two kinds of ACSF were used in these experiments: mACSF in the dissection dish before recording and nACSF in the recording chamber. The mACSF was composed of (in mM) 118 NaCl, 24 NaHCO₃, 1.5 CaCl₂, 3 KCl, 5 MgCl₂, 1.4 NaH₂PO₄, 1.3 MgSO₄, 25 D-glucose, and 1 kynurenic acid. The nACSF was composed of (in mM) 122 NaCl, 25 NaHCO₃, 2.5 CaCl₂, 3 KCl, 1 MgCl₂, 0.5 NaH₂PO₄, and 12 D-glucose. Both types of ACSF were saturated with 95% O₂ - 5% CO₂ and maintained at pH 7.4. The drugs added to the ACSF were: 5-HT, 5-HTP, clorgyline, pargyline, carbidopa, leucine, NSD1015 and strychnine (all from Sigma-Aldrich), and SB206553, APV, bicuculline, CNQX (all from Tocris), and TTX (TTX-citrate; Alomone). All drugs were first dissolved as a 10–50 mM stock in water before final dilution in ACSF, with the exception of

bicuculline, which was dissolved in minimal amounts of DMSO (final concentration in ACSF <0.04%; by itself, DMSO had no effect on the LLR in vehicle controls).

Spasms in awake chronic spinal rat

Tail muscle spasms were evoked with brief electrical stimulation of the skin of the tail, and recorded with tail muscle EMG (electromyogram). Percutaneous EMG wires (50 μ m stainless steel, Cooner wires, USA) were inserted in segmental tail muscles at the midpoint of the tail and recordings were made while the rat was in a Plexiglas tube, as detailed previously (Murray et al. 2011b). Muscle spasms were evoked with low threshold electrical stimulation of the skin at the distal tip of the tail (cutaneous stimulation; 0.2 ms, 10 mA pulse; 50 times reflex threshold, 50 \times T; 4 spasms evoked at 10 s intervals for a trial; trials repeated at 5 min intervals) and the tail was partly restrained from moving with a piece of masking tape connecting the midpoint of the tail to a rigid stand. EMG was sampled at 5 kHz, rectified and averaged over a 500–4,000 ms interval to quantify spasms (long lasting reflex, LLR; using Axoscope, Axon Instr., and Matlab, Mathworks). EMG over 300 ms prior to stimulation was also averaged (background). Drugs were applied in vivo by intraperitoneal injection (i.p.), and were dissolved in sterile saline. Dose-response relations were made by applying increasing drug doses at 15 min intervals, as for the in vitro preparation.

Immunolabelling

Rats were euthanized with Euthanyl (Bimeda-MTC; 700 mg/kg) and perfused intracardially with 100 ml saline containing sodium nitrite (1 g/l, Fisher) and heparin (300 IU/l, from 1,000 units/ml stock, Leo Pharma) for 3–4 minutes, followed by 400 ml 4% paraformaldehyde (PFA; in

phosphate buffer at room temperature), over about 15 mins. Spinal cords were postfixed in PFA overnight at 4°C, cryoprotected in 30% sucrose in phosphate buffer, frozen, and cut on a cryostat in horizontal or transverse 20 µm sections. Spinal cord sections were mounted on slides and rinsed in Tris-buffered saline containing 0.5% TritonX-100 (TBS-TX). All subsequent antibody applications and rinses that followed them also used TBS-TX, as we found this improved not only antibody penetration, but also removal of excess antibody after incubation. Sections were incubated overnight at 4°C with the following primary antibodies: rabbit anti-5-HT (1:5,000, Sigma S5545), mouse anti-GFAP (1:500, Millipore, MAB360), mouse anti-NeuN (1:500, Chemicon MAB377X, Alexa Fluor488 conjugated) and sheep anti-AADC (1:200, Millipore, AB119) in PBS-TX. For staining of AADC, antigen retrieval was performed by incubating slides in 10 mM citrate buffer (pH 8.5) at 80 °C for 30 mins prior to primary antibody incubation. To visualize the labeling of 5-HT, GFAP and NeuN, fluorescent secondary antibodies were used including goat anti-rabbit Texas Red (1:500, Vector, T-1000) and goat anti-mouse Alexa Fluor 488 (1:200, Invitrogen, A11029) in TPS-TX, were applied on slides for 90 min at room temperature. To visualize the AADC with fluorescent labels, tyramide amplification was additionally performed (Invitrogen, TSA Kit no. 12), which included an Alexa Fluor 488 Tyramide following ABC amplification (Vector PK-6101). Alternatively, to view DAB labelling of AADC or 5-HT biotinylated donkey anti-sheep antibody (1:2,000, Millipore, AP184B) or goat anti-rabbit 1:200, Vector ABC kit) was applied at room temperature for 2 hours in TBS-TX, followed by DAB-ABC amplification according to manufacturer guidelines (ABC, Vector PK-6101; DAB, Vector SK-4100). Image acquisition was with both conventional microscopy (for DAB) and confocal microscopy using a Leica TCS SP2 II Spectral Confocal System (for fluorescence). The latter used 1.3 µm optical sections that were collected into a z-stack over 5 –

20 μm , and subsequently projected into a single image using maximum intensity sorting (with ImageJ). Controls in which the primary antibody was omitted were used to confirm that the secondary antibody produced no labeling by itself. Clear labelling of monoamine fibres in normal rats was used as a positive control for AADC and 5-HT, and loss of these fibres in chronic spinal rats a negative control.

Immunolabelling of vessels for 5-HT and AADC was quantified by counting the numbers of labelled vessels per 20 μm section and dividing by section area, to compute vessels per unit area. As some vessels branched in a complex pattern, each portion of the branching structure between branch points was counted as a single vessel. Because the tissue was perfused with sodium nitrite at the time of fixation, vessels were dilated and clearly distinguishable from other structures. Pairs of normal and chronic spinal rat spinal cord sections were placed on the same slide during immunolabelling and tissue from all rats were photographed at a fixed exposure to reduce bias from differing immunolabelling. Vessels were only considered stained when they exceeded a fixed background staining threshold obtained in chronic spinal rats, and generally this was confirmed by the presence of pericytes that always stained the most strongly, and lined the vessel walls. Immunolabelling of neurons and D-cells for AADC or 5-HT was quantified by counting them in the same manner. Neurons were identified by their morphology, and confirmed with NeuN immunolabelling. D-cells we identified by their distinctive end-feet that protruded into the central canal.

HPLC analysis

For biochemical analysis of 5-HT and its metabolic product 5-hydroxyindole-3-acetic acid (5-HIAA), chronic spinal rats were perfused intracardially with 100 ml mACSF containing sodium nitrite and heparin for 3-4 mins, to clear blood from the spinal cord, as described above for immunolabelling. The spinal cord was then rapidly removed and placed in mACSF, as described above for in vitro recording. The cord was then incubated in varying concentrations of 5-HT in vitro for 1 hr. Roots and large surface vessels were removed, and then the cord caudal to the injury was frozen in isopentane cooled on dry ice and stored at -80°C . Subsequently, the cord was homogenized in ice-cold 0.1 N perchloric acid, centrifuged to remove precipitated protein and the concentrations of 5-HT and its acid metabolite 5-HIAA in the supernatant were determined using high pressure liquid chromatography (HPLC) with electrochemical detection according to the procedures of Baker et al.

Data analysis

Data were analyzed in Clampfit 8.0 (Axon Instruments) and Sigmaplot (Jandel Scientific) and expressed as mean \pm standard deviation (SD). A Student's *t*-test was used to test for statistical differences before and after drug applications, with a significance level of $P < 0.05$. A Kolmogorov-Smirnov test for normality was applied to each data set, with a $P = 0.05$ level set for significance. Most data sets were found to be normally distributed, as is required for a *t*-test. For those that were not normal, a Wilcoxon signed rank test was instead used with a significance level of $P < 0.05$.

Standard sigmoidal curves were fit to the relation between agonist dose and reflex responses, with doses expressed in log units and with a Hill slope of unity. The dose that produced 50% effect (EC_{50}) was measured from the curve. Also, the maximum drug-induced response (efficacy) was computed from the curve (peak of curve).

Results

AADC is upregulated in microvasculature after SCI

To examine where AADC is located after SCI, immunolabelling of AADC was performed on spinal cord segments both caudal and rostral to the sacral S2 injury site in chronic spinal rats, as well as at these locations in age-matched normal rats. In all spinal cord segments from normal rats, intense AADC labelling was seen mainly localized on descending monoamine fibres, which originate in the brainstem, consistent with AADC being a key enzyme in monoamine synthesis in normal cords. AADC-labelled fibres were seen descending in the white matter (WM, f in Fig. 2-1A) and traversing into the grey matter (GM). With a few exceptions, most other spinal cord structures had little distinct AADC staining, including a lack of AADC staining on most blood vessels and neurons in normal spinal cord (v, Fig. 2-1A). Occasionally, some blood vessels were weakly AADC-positive, and these vessels also had perivascular AADC-positive cells, which were likely pericytes (p, Fig. 2-1A). Also, as has been described before (Jaeger et al. 1983), in these normal rats AADC-positive D-cells lined the central canal, which had end feet projecting into the CSF (as detailed in a later figure).

In chronic spinal rats, AADC staining in monoamine fibres was eliminated caudal to the injury, in accordance with the severance of all descending fibres. However, a marked increase in AADC labelling showed up in almost all spinal vessels in both the WM and the GM (v, Fig. 2-1B), and pericytes on these vessels were densely stained by AADC labeling (Fig. 2-1B). These labelled vessels included spinal capillaries and small diameter veins that all lacked a smooth muscle layer (collectively termed microvessels) (Hardebo et al. 1980b). In contrast to these microvessels, the large surface pial vessels like the anterior artery or their arteriole branches did not show AADC

labelling under any conditions. To quantify the AADC in spinal microvessels, the number of AADC-labelled blood vessel branches per unit area was counted (see Methods for threshold criteria), and found to significantly increase 5-fold with injury (Fig. 2-1D). All spinal regions, including GM, WM, Ventral Horn (VH), CC and Dorsal Horn (DH), showed this 5-fold increase in AADC-positive microvessels in chronic spinal rats, compared to normal (Fig. 2-1C, D). The number of labelled pericytes (AADC-labelled) likewise increased 5-fold (not shown), as they were seen densely covering all microvessels after injury, unlike prior to injury (Fig. 2-1).

After injury AADC is upregulated in dorsolateral neurons associated with blood vessels

Unexpectedly, caudal to the spinal cord injury strong AADC labelling appeared in cells scattered through the grey matter, especially located laterally and dorsally to the central canal at the boundary of the grey matter and white matter (n, Fig. 2-1B, C, F). These AADC-positive cells were presumably neurons because of their morphology, as we verify later. These AADC-neurons were rarely found in normal spinal cords (on average 0.04 neurons/mm², corresponding to only a few neurons in the whole sacral cord), while there were many AADC neurons in each 20 µm transverse section after chronic SCI (Fig. 2-1E, significantly more). Typically, in chronic spinal rats these AADC neurons were multipolar, with soma about 10 - 20 µm in diameter, too small to be motoneurons and not often in the motor nucleus [motoneurons did sometimes weakly express AADC (Fig. 2-1C, VH), as previously reported (Gozal 2010), though at much lower levels, near the detection threshold]. Interestingly, the AADC neurons often had fine processes that contacted blood vessels (left process of neuron in Fig. 2-1F, see also Figs. 2-2I and 2-3C, described later), and thus seem to have some function related to vessels. However, these AADC-neurons were not D-cells of the central canal, lacking contact with the central canal. Indeed, the

number of D-cells of the CC decreased, rather than increased, with injury (Fig. 2-1E), as detailed in a later section.

AADC labelling rostral to the lesion in chronic spinal rats was not significantly different from that in intact animals, with a similar lack of AADC-positive neurons and vessels, and normal numbers of D-cells lining the central canal, even close to the injury site (not shown, same rats tested below injury in Fig. 2-1). This suggests that it is the loss of monamine fibres, and not the injury itself, that triggers the dramatic upregulation AADC in vessels, pericytes and neurons caudal to a chronic injury.

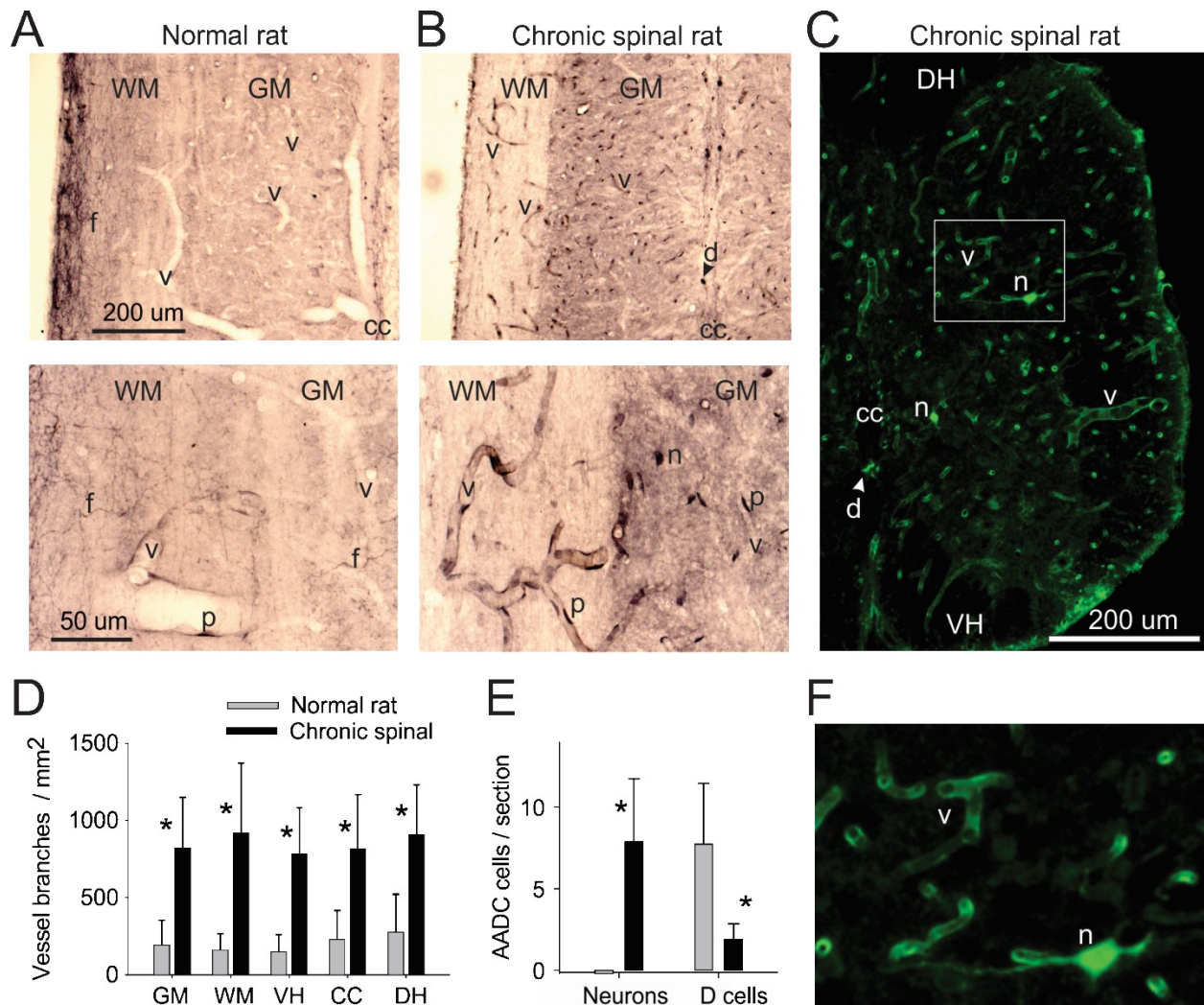


Figure 2-1. L-Amino acid decarboxylase (AADC) is upregulated in microvasculature and neurons after spinal cord injury.

A: immunolabeling for antibody to AADC (black, DAB) in horizontal section of spinal cord of normal rat. AADC is seen mainly confined to monoamine fibers (f; seen on expanded scale, *bottom*). Microvasculature (v) and pericytes (p) only weakly express AADC. D cells that are AADC positive are seen lining the central canal (CC). **B:** in chronic spinal rats, all descending monoamine fibers disappear together with their AADC labeling, but nearly all microvessels (v) in both white matter (WM) and gray matter (GM) are now intensely labeled with AADC, with the darkest labeling in pericytes (p) adhered to the vessel wall. Neurons (n) are also labeled for AADC. Some D cells (d) remain labeled. **C:** AADC immunofluorescence (green) showing distribution of AADC in transverse section of chronic spinal rat. Vessels stained with AADC are seen in the dorsal horn (DH) and ventral horn (VH). Neurons (n) expressing AADC appear with injury. D cells (d) remain only on the ventral aspect on CC (arrow). **D:** quantification of microvessel AADC staining, with a 5-fold increase in vessels after injury. **E:** quantification of number of AADC-labeled neurons and D cells per transverse section, with AADC neurons appearing only with injury and D cells decreasing in number with injury. **F:** expanded view of box in C, showing AADC neuron (n) and vessels (v).

*Significant increase compared with control, $P < 0.05$, $n \geq 5$ rats/condition.

Upregulated AADC synthesizes 5-HT from exogenous 5-HTP after SCI

To determine the functionality of the upregulated AADC after SCI, 5-HT immunolabelling was carried out in both normal and SCI rats with or without 5-HTP administration in vivo (i.p. 30 mg/kg, 25 mins before perfusion, DAB label). In normal spinal cords, without 5-HTP injection, only 5-HT fibres (brainstem-derived) were strongly labelled by the 5-HT antibody (f, Fig. 2-2C, 2G), though some diffuse background 5-HT labelling was present, as discussed below. Blood vessels were not 5-HT positive (v, white spaces), and 5-HT-positive neurons were not found (Fig. 2-2C, G). After 5-HTP was injected in these normal animals, weak 5-HT labelling was visualized on a few blood vessels and associated with a few perivascular pericytes in spinal cord (v, p, Fig. 2-2D, H). To rule out the interference of endogenous background 5-HT in characterizing the function of AADC in uninjured spinal cords, p-chlorophenylalanine (pCPA) was administered (i.p. 350 mg/kg/day) to deplete endogenous 5-HT. After two days pCPA depleted almost all endogenous 5-HT in sacral spinal cord, with only small amounts of 5-HT fibres seen near areas where monoamine fibres are normally densest (near motoneurons and central canal; Fig. 2-2K), and the diffuse background 5-HT staining was likewise reduced. After this 5-HT depletion with pCPA in uninjured rats, 5-HTP still failed to produce much 5-HT synthesis in microvessels, with only weak 5-HT labelling found in a small fraction of the microvessels, pericytes and 5-HT fibres in both the WM and the GM (Fig. 2-2L), and no production of 5-HT elsewhere, including an absence in neurons and motoneurons (Fig. 2-2L).

In untreated chronic spinal rats no 5-HT labelling was observed below the injury site (Fig. 2-2A).

The tissue was so devoid of 5-HT (white) that it was indistinguishable from tissue processed

identically for immunolabelling, but without the primary antibody (not shown), thus providing a clear control for the selectivity of the 5-HT antibody.

In contrast, in chronic spinal rats with 5-HTP injection (i.p., 30 mg/kg), blood vessels and pericytes were strongly stained by the 5-HT antibody in both the WM and the GM (Fig. 2-2B, F), consistent with their strong AADC staining (Fig. 2-1). Overall there was a significant 10-fold increase in vessels synthesizing 5-HT from 5-HTP (Fig. 2-2E). Neurons were also labeled by 5-HT and based on their morphology and medial-lateral location, we suppose that they are the same neurons that were AADC-positive (Fig. 2-2F, Fig. 2-1), as confirmed by double staining of AADC and 5-HT in a later section (Fig. 2-3). Rostral to the spinal cord transection AADC function was not different from normal, with no AADC neurons and few vessels and pericytes stained with 5-HT after 5-HTP injection, not significantly different from normal rats (Fig. 2-2E).

Diffusely distributed uptake of 5-HT in the spinal cord, separate from AADC cells

Below the injury in chronic spinal rats, weak background staining for 5-HT appeared diffusely distributed throughout the spinal cord after 5-HTP treatment (Fig. 2-2B, outside of vessels and neurons), unlike in the untreated chronic spinal rat (Fig. 2-2A), indicating that there was a weak uptake of 5-HT into many other spinal structures that do not contain AADC. In normal rats diffuse background 5-HT was also present, and this was intensified with 5-HTP application (Fig. 2-2G-H) and largely eliminated by 5-HT depletion (Fig. 2-2K, with pCPA), suggesting that there was likewise some weak uptake of 5-HT in many structures, presumably from 5-HT escaping from 5-HT fibres. When we directly incubated isolated cords of chronic spinal rats in 5-HT itself (1 μ M, for 1 hour, in vitro), there was likewise an increase in diffuse background 5-HT

immunolabelling (not shown, $n = 4/4$), confirming a general 5-HT uptake mechanism, separate from the main sites of 5-HT synthesis (AADC-containing neurons and vessels).

Diffusely distributed uptake of 5-HT in the spinal cord, verified with HPLC

Furthermore, when the isolated cords of chronic spinal rats were incubated in 1 μM 5-HT (in vitro for > 60 mins), we detected $0.36 \pm 0.06 \mu\text{M}$ 5-HT when we emulsified the whole cord and performed HPLC analysis (corresponding to $63.0 \pm 10.6 \text{ ng/g}$ tissue). The remaining 5-HT was accounted for as the 5-HT metabolite 5-HIAA, with a concentration of $0.61 \pm 0.05 \mu\text{M}$ (or $117.5 \pm 8.9 \text{ ng/g}$, $n = 4$). When we incubated the cords with MAO inhibitors (clorgyline and pargyline, 1 μM each) together with the 1 μM 5-HT, then the HPLC analysis showed a 4-fold increase in 5-HT ($1.42 \pm 0.73 \mu\text{M}$, or $250.3 \pm 129.8 \text{ ng/g}$ tissue), not different from the applied 1 μM 5-HT ($P = 1.0$, $n = 4$), and consistent with 5-HT being transported and metabolized by MAO. As expected, 5-HIAA was nearly eliminated with an MAO block ($0.16 \pm 0.11 \mu\text{M}$). Together these results indicate that the 5-HT must have diffused fairly uniformly into the spinal cord structures, whereas if the 5-HT had stayed only in the extracellular space a much lower overall concentration of 5-HT should have been seen with HPLC, considering that the extracellular space only makes up 10% of the total cord volume (0.1 μM 5-HT would have been seen, instead of about 1 μM) (Vargova et al. 2008).

In contrast, the HPLC analysis of untreated cords from chronic spinal rats (below injury) gave very low 5-HT levels ($4.2 \pm 3.4 \text{ ng/g}$, $n = 6$), near the minimum detection limit and over 200 times lower than the 5-HT in normal cords ($906.0 \pm 141.8 \text{ ng/g}$, $n = 6$, significant $P < 0.05$). Furthermore, most of this small amount of 5-HT in chronic spinal rats was likely due to blood products (platelets) remaining in the vessels of the cord, because the HPLC gave near zero 5-HT

levels in cords well perfused and cleared of blood (< 6 ng/g), and higher values (up to 30 ng/g) in cords poorly perfused. Importantly, the residual level of 5-HT in untreated rats was not significantly changed by MAO inhibitors (2.7 ± 1.3 ng/g, $P < 0.05$), unlike when the cords were incubated in 5-HT (see above), consistent with the residual 5-HT being stored in a location, like platelets, inaccessible to the diffusely located spinal cord MAO, and thus not likely to affect spinal cord function.

Exogenous 5-HT derived in periphery is not accumulated in AADC-containing cells

To rule out the possibility that in our experiments 5-HT was synthesized from 5-HTP in peripheral structures containing AADC (e.g, liver) and then leaked into the spinal cord, we injected 5-HT peripherally in chronic spinal rats (i.p. 30 mg/kg, 25 mins before perfusion), and then conducted 5-HT immunolabelling. With this 5-HT injection, we found that 5-HT immunolabelling did not occur in vessels and neurons, unlike with 5-HTP injections, and there was very little diffuse background staining (Fig. 2-2J), consistent with the relative impermeability of 5-HT across the BBB (Oldendorf 1971). This suggests that the 5-HT immunolabelling that we observe in chronic rats after 5-HTP injection is centrally produced in spinal cord blood vessels, pericytes and AADC-expressing neurons. To further verify this conclusion, the chronically injured spinal cord was removed from the rat and then incubated in 30 μ M 5-HTP in vitro (1 hr). In these isolated and 5-HTP-treated cords intense 5-HT immunolabelling was visualized in vessels, pericytes and AADC neurons (Fig. 2-2I), as in vivo. In contrast, incubation of isolated cords with 5-HT itself (1 μ M, 1 hour, in vitro) did not produce distinct 5-HT immunolabelling in vessels, pericytes and neurons, but only produced weak diffuse background 5-HT immunolabelling, as described above (not shown, $n = 4/4$), confirming that

these AADC containing sites are the source of 5-HT synthesis, and are not simply sites that accumulate 5-HT from elsewhere.

Detailed morphology of AADC neurons, seen with in vitro 5-HTP incubation

Interestingly, with in vitro 5-HTP incubation, compared to in vivo 5-HTP injections, delivery of 5-HTP to the AADC-neurons appeared more effective, with cell bodies more intensely stained, morphological structure more clear, including staining of fine processes (dendrites, Fig. 2-2I). Importantly, these fine processes often appeared in close apposition to vessels (Fig. 2-2I, n and v), suggesting that AADC-neurons may somehow interact with blood vessels, as already noted.

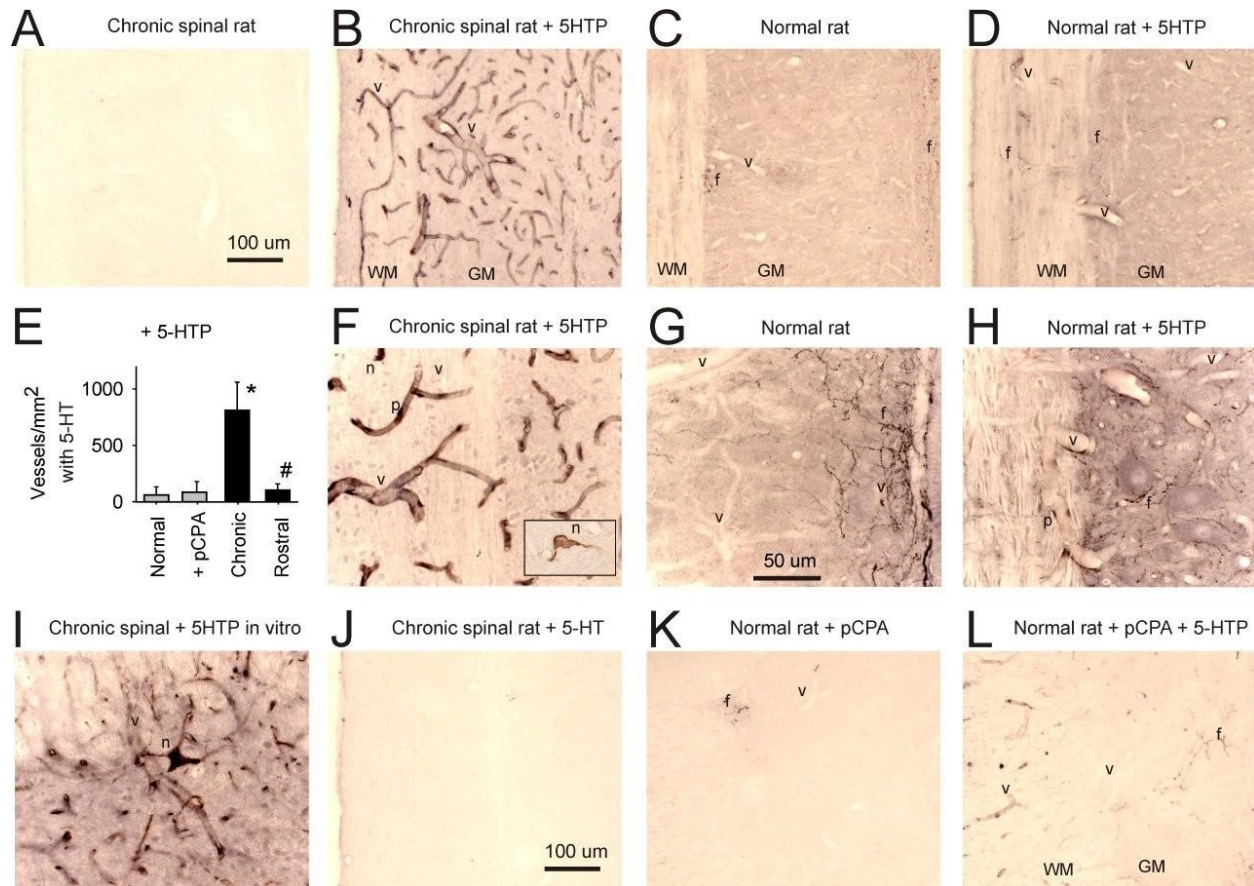


Figure 2-2. Serotonin (5-hydroxytryptamine, 5-HT) synthesis from exogenous 5-hydroxytryptophan (5-HTP) in chronic spinal rats.

A: in untreated chronic spinal rats no 5-HT immunolabeling is seen in the spinal cord caudal to the lesion (5-HT labeled black with DAB, horizontal sections). **B:** injection of 5-HTP (i.p., 30 mg/kg, 25 min prior to fixation) leads to synthesis of 5-HT in locations where we also see AADC, including on the microvasculature (v), in both WM and GM. However, there is also diffuse 5-HT labeling throughout the spinal cord (darker than A). Expanded image shown in F. **C:** in untreated normal rats, brainstem-derived monoamine fibers have 5-HT labeling, and there is some diffuse background labeling of 5-HT. Expanded image shown in G. **D:** injection of 5-HTP in these normal rats causes a somewhat more intense diffuse 5-HT labeling, but very few microvessels are labeled. Expanded image shown in H. **E:** quantification of the number of 5-HT-labeled microvessels in rats treated with 5-HTP and examined under the following conditions: normal rat caudal to injury, normal rat with endogenous 5-HT depleted with *p*-chlorophenylalanine (pCPA, 350 mg/kg/day, 2 days prior), chronic spinal rat caudal to injury, and chronic spinal rat rostral to injury. *Significantly greater than normal rat, #significantly less than chronic spinal caudal cord, $P < 0.05$, $n \geq 5$ rats/condition. **F:** expanded image of chronic spinal rat treated with 5-HTP (30 mg/kg), showing vessels (v), pericytes (p), and neurons (n) labeled for 5-HT. *Inset:* the labeled neuron is from a different rat injected with a lower dose of 5-HTP (3 mg/kg). **G and H:** expanded images of normal rats showing 5-HT-labeled fibers with and without 5-HTP and a relative lack of 5-HT-labeled vessels. **I:** immunolabeling for 5-HT in spinal cord of chronic spinal rat maintained in vitro and incubated in 5-HTP (30 μ M for 1 h), showing 5-HT synthesized in situ in vessels (v) and neurons (n). **J:** lack of 5-HT immunolabeling in chronic spinal rat injected with 5-HT (i.p., 30 mg/kg, 25 min prior to fixation). **K:** relative lack of 5-HT immunolabeling in normal rat treated with pCPA, except in a few fibers near the motor nucleus. **L:** injection of 5-HTP in pCPA-treated normal rats leads to 5-HT-labeling in only a few fibers. $n \geq 5$ for A-L.

5-HT is not endogenously produced by spinal cord AADC after spinal cord injury

We next used double fluorescence immunolabelling of 5-HT and AADC to verify that synthesis of 5-HT from exogenous 5-HTP (via AADC) is the sole source of 5-HT after spinal cord injury, unlike in normal rats. In untreated normal rats, both 5-HT (red) and AADC (green) antibodies mostly labelled brainstem-derived monoamine fibres (f, Fig. 2-3A), with 5-HT fibres making up a substantial fraction of the total monoamine fibres (AADC-labelled), while the remaining fibres were presumably of catecholamine origin. In contrast, in untreated chronic spinal rats no 5-HT fluorescence label was seen caudal to the injury (Fig. 2-3B, as also seen with DAB in Fig. 2-2), whereas in these same sections double labelling revealed AADC-positive vessels and neurons (Fig. 2-3B).

Application of 5-HTP (i.p. 30 mg/kg, in vivo 25 mins before perfusion) in these chronic spinal rats revealed that 5-HT synthesis (red) always co-localized with the enzyme AADC (green; Fig. 2-3C). When we lowered the 5-HTP dose to a level near the minimum to have physiological effects (3 mg/kg, 25 mins prior to perfusion, as detailed later) we still saw both vessel and neuronal synthesis of 5-HT (Fig. 2-2F, inset). This indicates that we can detect 5-HT with our immunolabelling with near minimal functional amounts of 5-HTP, and thus the lack of 5-HT labelling in untreated chronic spinal rats indicates that there is no functional endogenous 5-HTP or accumulation of 5-HT.

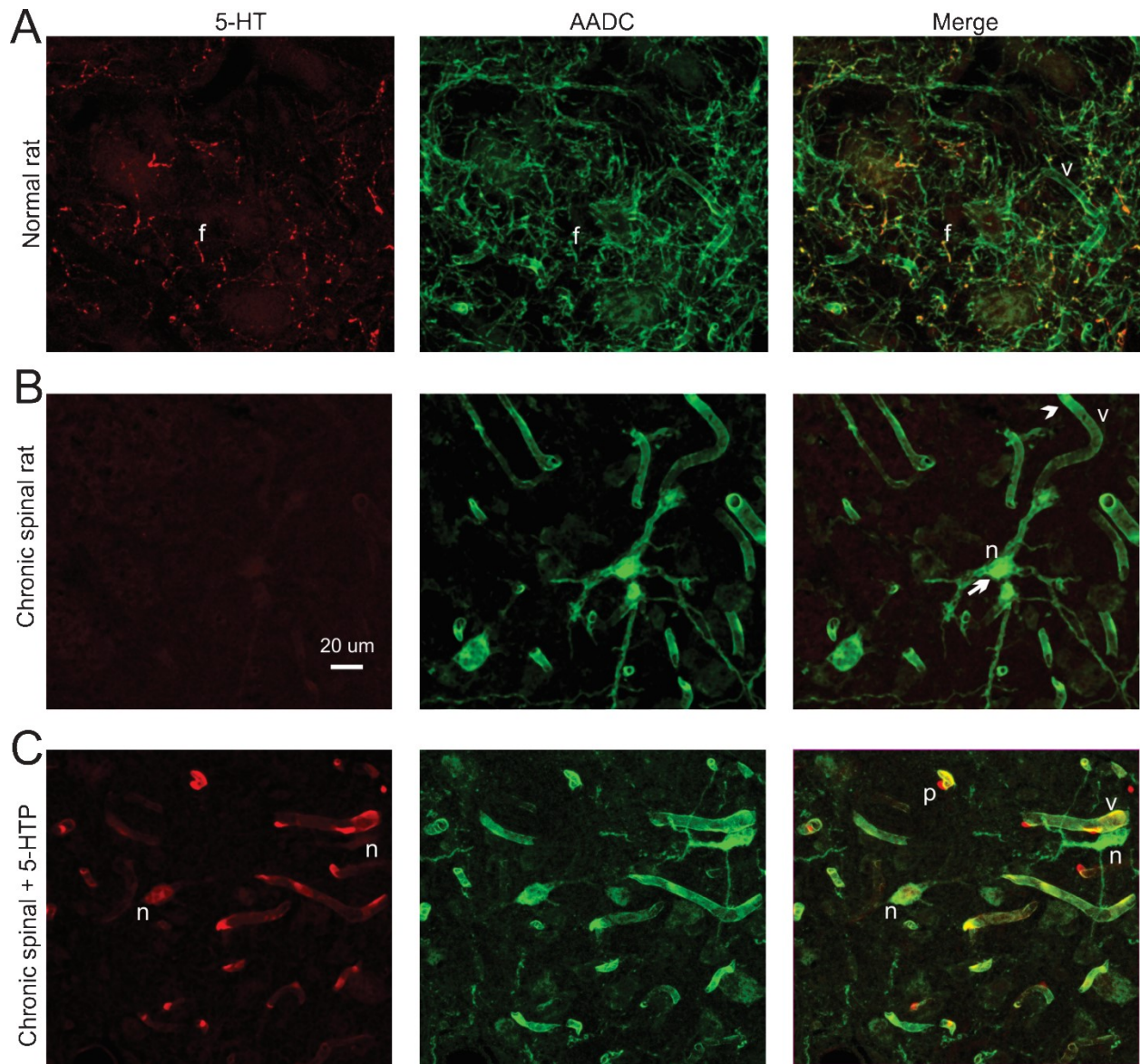


Figure 2-3. 5-HT is not endogenously synthesized by AADC after injury.

A: double immunofluorescence labeling for 5-HT (red) and AADC (green) in the spinal cord of a normal rat (ventral horn), showing a dense network of AADC-positive monoamine fibers (f), some of which are 5-HT fibers (double stained orange). A few vessels (v) are weakly AADC positive, but these do not synthesize 5-HT endogenously (not labeled red). **B:** double labeling of untreated chronic spinal rats, showing that AADC neurons (n) and vessels (v) do not endogenously produce 5-HT (no red). **C:** in contrast, injection of exogenous 5-HTP leads to exogenous 5-HT synthesis in vessels (v) and neurons (n) double-labeled with AADC. Pericytes (p) appear to accumulate 5-HT out of proportion to the AADC and sometimes partly detach from vessels. All images on same scale. Same rats as in Fig. 2-2.

Variability of 5-HT synthesis in AADC-containing neurons, vessels and pericytes

Interestingly, even with our standard dose of in vivo 5-HTP injection (30 mg/kg), the intensity of 5-HT labelling was sometimes weaker in neurons compared to vessels and pericytes, even though the AADC labelling was not (Fig. 2-3C, Fig. 2-4A). We suspect that the 25 mins that we waited after 5-HTP injection was not always enough to allow adequate amounts of 5-HTP to move across the BBB from vessels to neurons, because when 5-HTP was applied for longer periods, more intense and uniform neuronal 5-HT staining occurred (not shown, $n = 3/3$), and when cords were incubated for long periods (60 mins) in vitro with 5-HTP we saw more detailed morphology labelled with 5-HT in AADC-neurons, as described above (Fig. 2-2I).

On the contrary, pericytes stood out as a location where 5-HT fluorescence was always relatively more intense than the AADC fluorescence in 5-HTP-injected chronic spinal rats (Figs. 2-3C and 2-4A), suggesting that 5-HT is somehow accumulated in pericytes, in addition to being synthesized there.

Carbidopa blocks vessel but not neuronal AADC activity

To demonstrate that AADC neurons alone have the ability to transform exogenous 5-HTP into 5-HT, carbidopa was employed to selectively impede the function of AADC in vessels.

Carbidopa (50 mg/kg), which is a peripheral and vessel AADC inhibitor that does not readily cross the BBB (Hardebo et al. 1979b; Hardebo et al. 1980b), was given together with 5-HTP (30 mg/kg, 25 mins prior to perfusion, and 30 mins after carbidopa). After this treatment with carbidopa, only the AADC-neurons were 5-HT positive (n , Fig. 2-4B; not significantly different in number than without carbidopa, Fig. 2-4C), and vessels no longer synthesized 5-HT

(significant reduction in stained vessels, Fig. 2-4C), consistent with previous reports that this dose of carbidopa blocks CNS vessel AADC function (Hardebo et al. 1979b). In contrast, the AADC immunolabelling staining pattern (Fig. 2-4B) remained similar compared to spinal cords of chronic spinal rats treated with only 5-HTP (Fig. 2-4A): microvessels, pericytes and the AADC neurons were labeled. Furthermore, in the presence of carbidopa, 5-HT labelling in the AADC neurons became more pronounced (n, Fig. 2-4B) compared to in chronic spinal rats treated with only 5-HTP (n, Fig. 2-3A): the cell bodies were more intensely stained and fine processes of dendrites and axons were more easily visible. In addition, most of these 5-HT processes co-localized substantially with AADC (Fig. 2-4B arrow). By blocking peripheral (e.g. liver) and vessel AADC with carbidopa, much less 5-HTP is known to be metabolized in the periphery, and thus much more is available to reach the spinal cord (see Discussion); this would explain the increased synthesis of 5-HT in neurons.

Leucine blocks neuronal but not vessel AADC synthesis of 5-HT from 5-HTP

We also incubated the isolated sacrocaudal cord from chronic spinal rats in vitro with 5-HTP (30 μ M) together with leucine (3 mM, 30 mins prior to 5-HTP), which competitively blocks the movement of 5-HTP via the L-transport system, one of the major transporters of amino acids and monoamine precursors (Gomes et al. 1999; Hawkins et al. 2006). In these cords, there was hardly any AADC neurons labelled with 5-HT (significant reduction compared to without leucine), but microvessels and pericytes were still strongly labelled for 5-HT (Fig. 2-4C). Thus, transport of 5-HTP into AADC cells is mostly dependent on the L-transport system, whereas transport of 5-HTP into vessels must utilize multiple transport systems in addition to the L-

system, as has been reported before (Hawkins et al. 2006). These data also demonstrate that 5-HT can be produced in vessels alone, not depending on AADC cells.

New class of AADC neurons are NeuN positive and GFAP negative

To further characterize the new class of AADC cells that we find after injury, we labelled AADC cells with 5-HT (after a 5-HTP injection) and double labelled with either NeuN (neuron specific) or GFAP (astrocyte specific). As shown in Fig. 2-4D, the 5-HT-producing AADC cells co-labelled with NeuN, confirming our previous suggestion that these are AADC neurons. These rats tested with NeuN were also treated with carbidopa, to optimize the 5-HT produced in AADC neurons, as discussed above.

In 5-HTP treated chronic spinal rats, AADC cells (5-HT positive) did not colocalize with GFAP (n, in Fig. 2-4E), indicating that they were not astrocytes. Additionally, vessels that synthesized 5-HT did not stain for GFAP, indicating the vessel AADC and 5-HT synthesis was not caused by astrocytes, even though astrocytes did surround vessels (arrow in Fig. 2-4E).

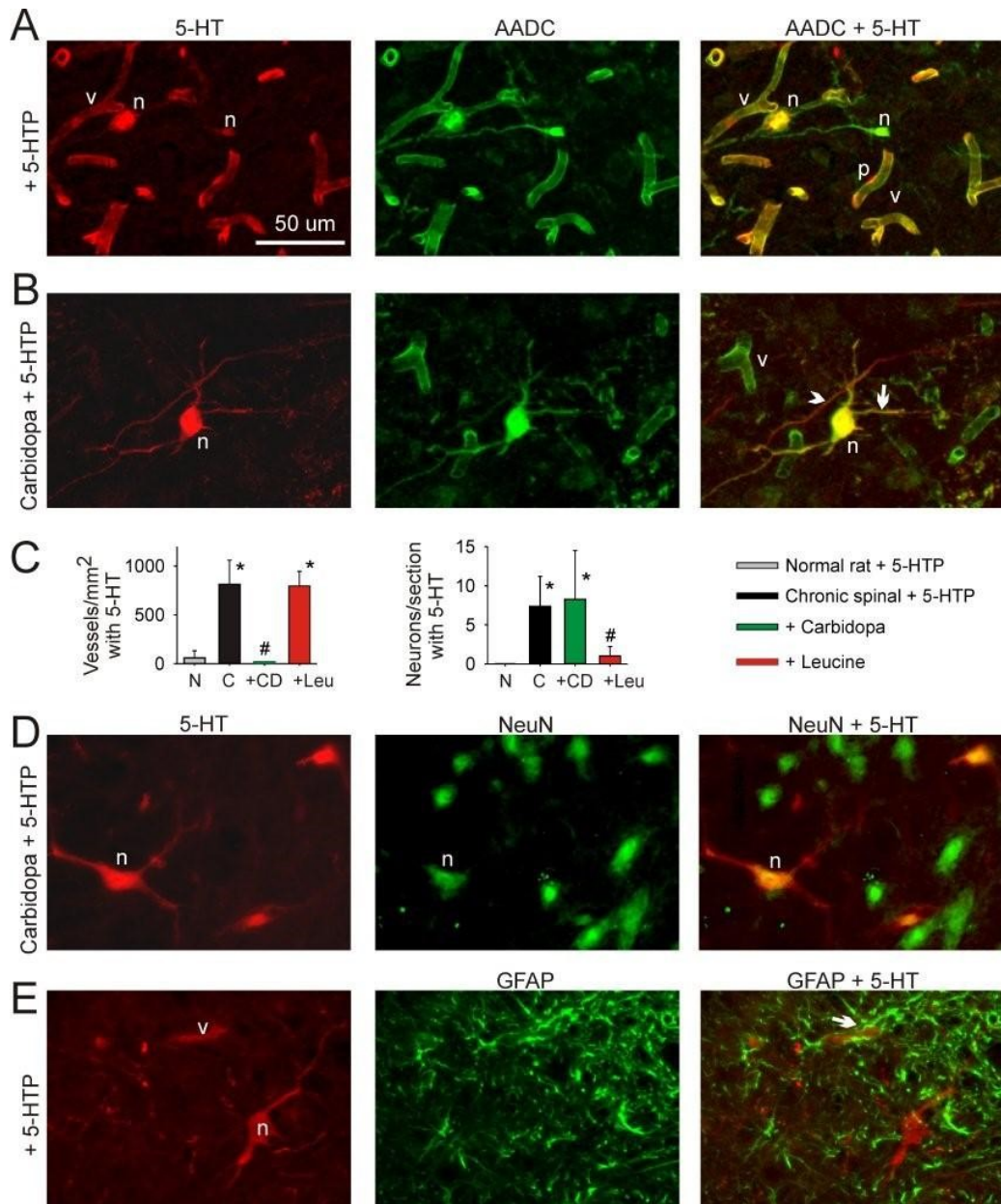


Figure 2-4. Characterization of AADC neurons that appear after spinal cord injury.

A: double labeling of 5-HT (red) and AADC (green) in chronic spinal rat treated with 5-HTP (30 mg/kg ip), showing 5-HT synthesis in vessels (v) and neurons (n) also labeled for AADC. Transverse section lateral to central canal. **B:** in chronic spinal rats pretreated with carbidopa (50 mg/kg 30 min prior) and then given 5-HTP, AADC-labeled vessels no longer synthesize 5-HT, whereas AADC-labeled neurons continue to synthesize 5-HT. **C:** quantification of the number of 5-HT-labeled vessels (per mm²) and neurons (per transverse section) in rats treated in vivo with 5-HTP under the following conditions: normal rat (N), chronic spinal rat (C), chronic spinal rat treated with carbidopa (CD), and chronic spinal rat treated with leucine (Leu, in vitro 5-HT and leucine, in this case only), *n* = 5–8 rats/condition. **D:** double labeling with 5-HT and NeuN in chronic spinal rat treated with 5-HTP (and carbidopa), showing that AADC cells that synthesize 5-HT are indeed AADC neurons. **E:** double labeling with 5-HT and glial fibrillary acidic protein (GFAP) in chronic spinal rats treated with 5-HTP, showing that 5-HT is not synthesized in astrocytes, even though these surround the AADC-containing vessels (v) and neurons (n).

D-cells in the central canal disappear with spinal cord injury

While AADC staining increased dramatically in microvessels, pericytes and neurons after injury, the number of AADC positive D-cells in the central canal significantly decreased (Fig. 2-1E), as already mentioned. Furthermore, the remaining D-cells were only observed at the ventral side of the central canal (CC in Fig. 2-5B-C), whereas they normally lined the whole central canal on dorsal and ventral aspects (Fig. 2-5A) (Jaeger et al. 1983). The remaining D-cells did not endogenously produce 5-HT (not shown), as in normal rats (Fig. 2-5A), but could produce 5-HT when the rat was injected with 5-HTP (arrow Fig. 2-5B), allowing us to further characterize these cells with double 5-HT and NeuN or GFAP immunolabelling (for technical reasons we were never able to get the AADC antibody itself to work as a co-label with NeuN or GFAP). Interestingly, we found that in these 5-HTP injected rats (normal or injured), D-cells were not NeuN-positive (arrow Fig. 2-5C). However, NeuN sometimes failed to even label motoneurons (not shown), so a negative NeuN finding does not necessarily rule out the original conclusions of Jaeger that these cells are neuron-like (Jaeger et al. 1983). Furthermore, we found that these D-cells did not co-localize GFAP (Fig. 2-5D), indicating that they were not of glial origin.

We wondered whether the loss of D-cells might be caused by D-cells migrating away from the central canal into the grey matter and producing the new AADC-positive neurons that we observe after injury. Thus, we examined AADC labelling at just 1 to 2 days after spinal cord injury. However, in none of these acutely injured rats ($n = 4/4$) did we detect D-cells leaving the central canal area (near central canal, but not in contact with CSF), and furthermore, AADC positive neurons began appearing far from the central canal, even at this early time point after

injury (data not shown). Thus, the AADC neurons likely arose from existing neurons in the grey matter and not from migrating D-cells of the central canal.

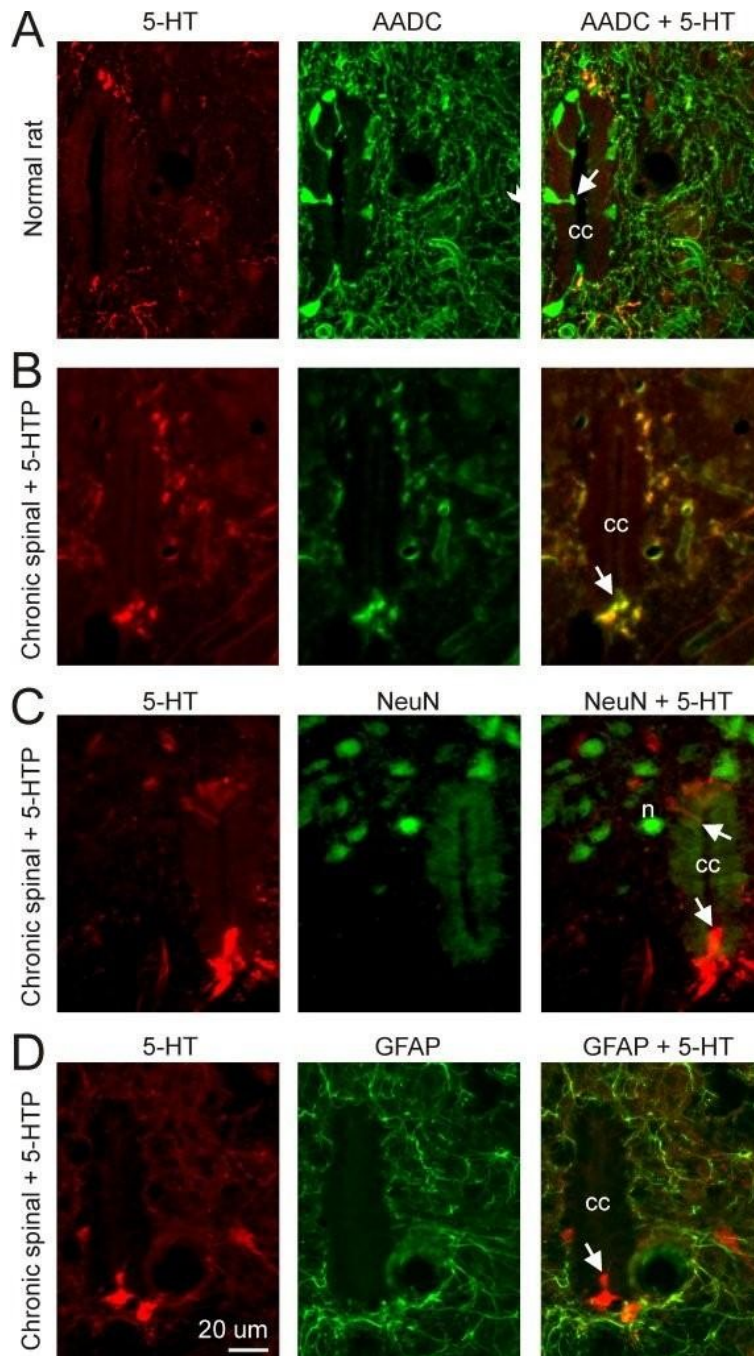


Figure 2-5. Characterization of AADC containing D-cells that line the central canal.

A: double immunofluorescence for 5-HT (red) and AADC (green) in normal rat, showing that many AADC-containing cells line the central canal (CC) and have end feet that project into the canal (arrow). These D cells do not endogenously synthesize 5-HT (not red). In contrast, numerous fibers contain AADC and 5-HT (descending 5-HT fibers). Transverse sections shown, with dorsal at *top*, as also in B–D. **B:** double labeling in chronic spinal rat treated with 5-HTP, showing a relative lack of D cells labeled with AADC and that the few remaining cells are always located on the ventral aspect of the central canal (arrow). These cells make 5-HT when treated with 5-HTP but not without (latter not shown). **C and D:** D cells are NeuN negative (not neurons) and GFAP negative (not astrocytes) in both chronic spinal (shown) and normal (not shown) rats. Same rats as in Fig. 2-4.

AADC-neurons and microvessels both increase spasms in 5-HTP treated rats

Next we tested whether 5-HTP influenced the muscle spasms in chronic spinal rats, and examined how AADC-containing microvessels and neurons individually contributed to spasms. In chronic spinal rats, tail spasms were evoked by brief electrical stimulation of the tip of the tail, and recorded by EMG wires implanted in the segmental tail muscles (Fig. 2-6A). These spasms were typically composed of a large short latency response, followed by a long lasting reflex (LLR, many seconds long), the latter which we quantified (Fig. 2-6B). Application of 5-HTP dose-dependently increased the LLR up to doses of 3 mg/kg, with about 1 mg/kg producing 50% of maximal effect (EC_{50} ; Fig. 2-6B, D, G). Higher doses than 3mg/kg decreased the reflex, similar to what has been demonstrated for the action on 5-HT on spasms (Fig. 2-6D-E, with excitation and inhibition depending on 5-HT₂ and 5-HT₁ receptors respectively) (Murray et al. 2011b). The excitatory effect of 5-HTP lasted for over an hour for a single dose.

Prior application of carbidopa (50 mg/kg, 30 mins before 5-HTP) to block vessel and peripheral AADC did not inhibit the action of 5-HTP (Fig. 2-6C, E): neither the peak effect of 5-HTP (Fig. 2-6F, 4-fold increase in LLR) nor the EC_{50} (Fig. 2-6G) were significantly altered by carbidopa, even though we know that this dose of carbidopa dramatically reduces vessel AADC synthesis of 5-HT. This demonstrates that the AADC neurons can alone affect spinal cord function, as these neurons remain the sole source of 5-HT synthesis in carbidopa-treated rats (Fig. 2-4). In contrast, a complete blockade of all AADC, with the centrally acting blocker NSD1015 significantly reduced the efficacy of 5-HTP and increased the EC_{50} (by > 10-fold, to > 30 mg/kg, data not shown, $n = 5$), demonstrating that conversion to 5-HT is necessary for the action of 5-HTP.

Carbidopa itself produced only a small transient increase in the LLR, in the first 10 to 15 mins after injection (Fig. 2-6F), unlike the long duration and large effects of 5-HTP, suggesting that there is little endogenous AADC activity directly affecting motor function. Saline control injections had no significant long term effect on the LLR ($n = 8$), although in some rats, it increased the reflex for a few minutes ($n = 2$), likely due to stress, which we know can transiently increase the LLR (unpublished observations).

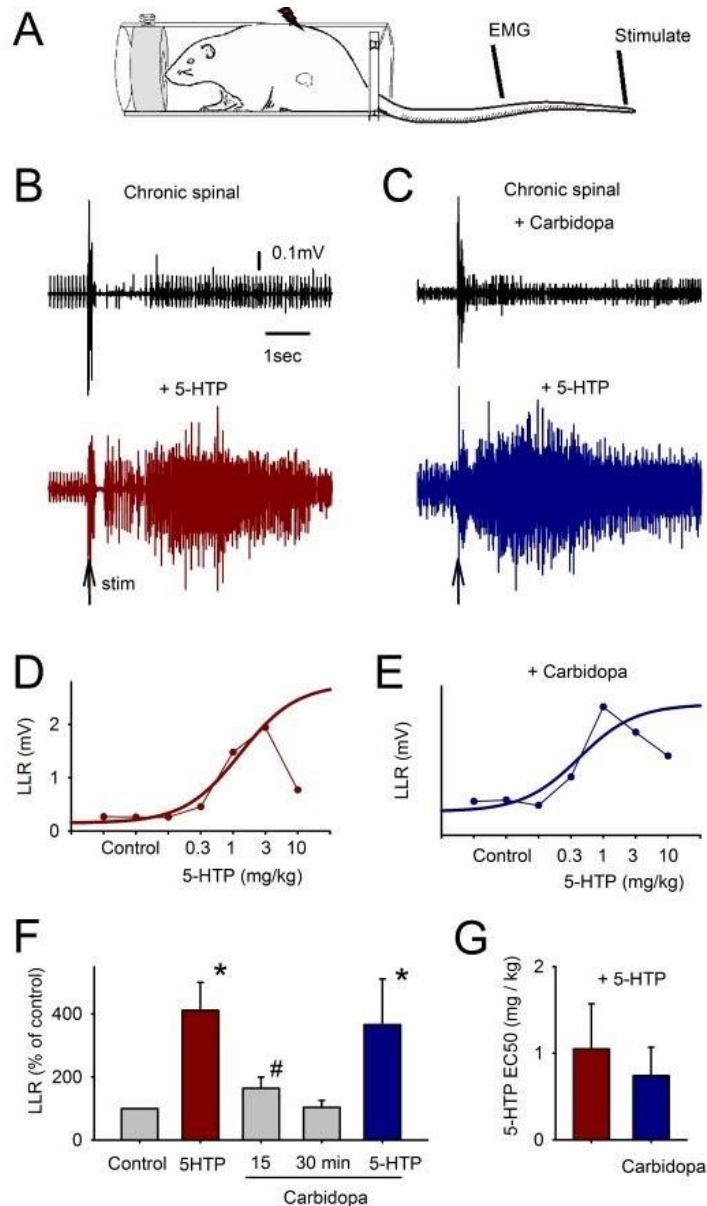


Figure 2-6. AADC-neurons and vessels both increase spasms in 5-HTP-treated rats.

A: schematic of awake chronic spinal rat in holding tube while tail muscle spasms are recorded with EMG and spasms are evoked with electrical stimulation of the tip of the tail (0.2 ms, 10 mA, single pulse). **B:** EMG response to stimulation, showing moderate long-lasting reflex (LLR) prior to 5-HTP and very large LLR with 5-HTP injection (1 mg/kg). **C:** a block of peripheral and vessel AADC with carbidopa prior to 5-HTP (50 mg/kg 30 min prior; see Fig. 2-4) does not prevent 5-HTP from similarly increasing spasms/LLRs (blue), showing that AADC neurons alone can produce enough 5-HT to augment spasms. **D and E:** typical cumulative dose-response relations for LLR in a chronic spinal rat without and with carbidopa. Increasing doses were given at 15 min intervals, and recording was made just prior to each new dose (at 15 min after drug). **F and G:** quantification of the peak effect of 5-HTP (peak of dose response) and dose to produce 50% of peak effect (EC_{50}), showing that 5-HTP has similar effects on amplitude (efficacy) and potency in rats without and with carbidopa ($n = 5$ and 6 rats, respectively). *Significantly different from control, #significantly different from control but also significantly less than 5-HTP treated, $P < 0.05$, $n > 5$ rats/condition.

Mechanisms of action of 5-HTP, including roles of AADC, 5-HT₂ receptors and MAO

We further examined the action of AADC and 5-HTP in chronic spinal rats by recording ventral root activity in cords that were isolated and maintained in vitro (Fig. 2-7A), which among other things, eliminated the interference of 5-HT synthesized in the peripheral system. We recorded long-lasting reflexes (LLRs) from the ventral roots in response to a low-threshold stimulation ($3 \times T$) on dorsal roots (Fig. 2-7B). These in vitro LLRs are the counterpart of the LLRs recorded in vivo, and thus are an indirect measure of muscle spasms (Murray et al. 2010). Application of 5-HTP dose-dependently increased the amplitude of LLRs, with a maximal response (efficacy) 3-times higher than in pre-drug conditions (Fig. 2-7B, D, F; significantly increase), and with an EC_{50} of about 10 μ M (Fig. 2-7G). Again, as previously reported for 5-HT (Murray et al. 2011b), there was always an initial increase in LLR with 5-HTP (over about one order of magnitude in dose), after which further 5-HTP decreased the reflex, in accordance with the dual action of 5-HT₂ and 5-HT₁ receptors (Fig. 2-7D). We only quantified the 5-HT₂ receptor-mediated increase in the LLR.

The AADC blocker NSD1015 completely inhibited 5-HTP's effect, so that the LLR was not significantly different than in pre-5-HTP control conditions (in NSD1015, Fig. 2-7C, D). These data again verify that 5-HTP needs to be converted to 5-HT via AADC to enhance motor output, and this must be occurring centrally (in vitro). Importantly, in the presence of leucine to selectively block 5-HT synthesis in just AADC neurons (see Fig. 2-4C), 5-HTP application still significantly increased the LLR (Fig. 2-7F), with an EC_{50} again of about 10uM, not significantly different than without leucine (Fig. 2-7G). This demonstrates the vessel AADC is sufficient alone to increase spasms, because only vessel AADC makes 5-HT in the presence of leucine, as

described earlier (Fig. 2-4C). Together with our carbidopa in vivo data, we can conclude that both vessels and AADC neurons produce functional 5-HT that increases spasms upon 5-HTP application.

The increase in LLRs with 5-HTP was completely blocked by the highly selective 5-HT_{2B/2C} receptor blocker SB206553 (10 μ M, Fig. 2-7E, F), which demonstrates that 5-HTP must be converted to 5-HT that in turn leaves the AADC-cells and acts on 5-HT_{2B/2C} receptors. These are known to be the main receptors that increase the LLR with 5-HT, and in particular the 5-HT₂ receptors on motoneurons increase the LLR by increasing persistent inward currents (Murray et al. 2010; Murray et al. 2011a). The less selective 5-HT₂ receptor antagonist methysergide (10 μ M) likewise blocked the action of 5-HTP (not shown, $n = 5/5$).

Considering that we have previously reported 5-HT itself to increase the LLR at a very low nanomolar EC₅₀ dose of about 10 nM (Murray et al. 2011a), our present finding that 5-HTP acts at an EC₅₀ dose 1000 times higher (10 μ M), indicates that there is a 1000 fold loss of functional 5-HT during synthesis of 5-HT by AADC. We suspected that this could be partly due to metabolism of 5-HT in AADC cells, and thus tested this by blocking metabolism of 5-HT. Monoamine oxidase A (MAO-A) is the key enzyme that metabolises 5-HT into 5-HIAA and is located intracellularly on the mitochondrial membrane (Kalaria et al. 1987; Wang et al. 2013). When we applied clorgyline, a MAO-A inhibitor (Lena et al. 1995), 5-HTP still increased LLRs with a similar efficacy (peak response) to 5-HTP alone (Fig. 2-7F), but the EC₅₀ of 5-HTP was markedly decreased to about 1 μ M, and thus there is indeed a 10-fold metabolism (loss) of 5-HT after it is synthesized (Fig. 2-7E, G). Application of 5-HT itself increased the LLR similarly to 5-

HTP, and again the MAO inhibitor did not affect the efficacy of this increase (peak amplitude, Fig. 2-7F), but did produce a significant reduction in the EC_{50} of exogenously applied 5-HT (by a factor of 2; Fig. 2-7G), although this effect was significantly smaller than that of 5-HTP. Thus, roughly speaking, in AADC cells (vessels and neurons) MAO causes an 8-fold loss in 5-HT made from applied 5-HTP, and after the 5-HT leaves these cells there is an additional 2-fold loss to MAO metabolism before the 5-HT diffuses to 5-HT receptors where it increases the LLR (see Discussion for mechanism).

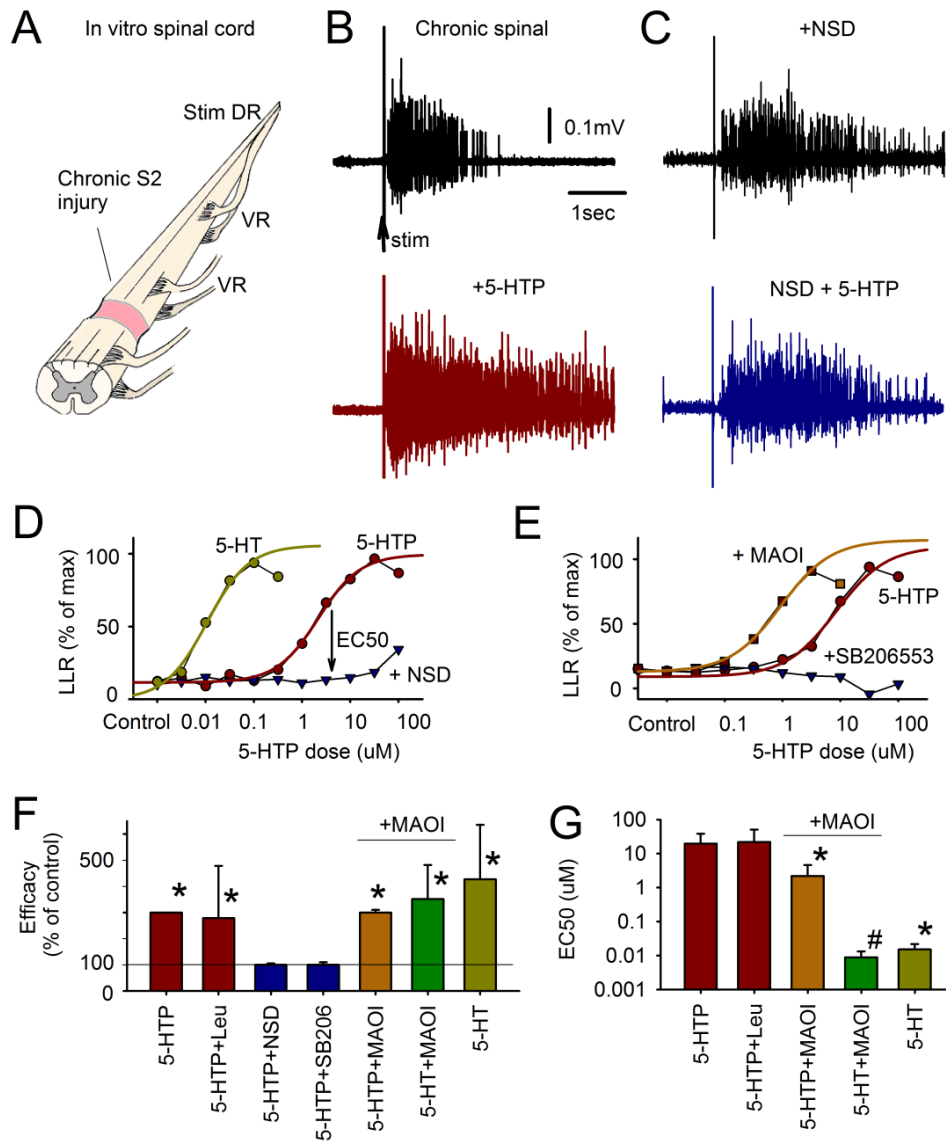


Figure 2-7. 5-HTP increases spasms in the isolated spinal cord of chronic spinal rats, via synthesis of 5-HT with AADC and activation of 5-HT₂ receptors, although much of this 5-HT is metabolized by MAO.

A: schematic of spinal cord caudal to an injury maintained in vitro, with stimulation of dorsal roots (DR) and recording from ventral roots (VR). **B:** LLR recorded from VR after stimulation of DR [0.1 ms pulse, 3 × afferent threshold (T)]. 5-HTP application (10 μM) increases the LLR (red). **C:** block of AADC with NSD1015 (NSD, 300 μM 30 min prior) eliminates the response to subsequently applied 5-HTP (10 μM, blue). **D:** representative dose-response relations for 5-HTP application at increasing doses, with an EC₅₀ of about 3 μM (red line). For comparison, application of 5-HT (green) increased the reflexes at much lower doses than 5-HTP. **E:** blocking MAO with clorgyline (1 μM) lowered the doses at which 5-HTP increased the reflex 10-fold (orange). Blocking the 5-HT₂ receptor with SB206553 (10 μM) eliminated the response to 5-HTP (blue). **F:** summary of efficacy (peak effect) of 5-HTP and 5-HT on the LLR for all rats with the following conditions: control normal ACSF (red, left), leucine (3 mM, Leu), NSD1015, SB206553 (SB206), and clorgyline (MAOI). Efficacy is normalized to control, so 100% indicates no change (SB206553 and NSD1015). **G:** summary of EC₅₀ doses of 5-HTP or 5-HT for increasing the LLR, with the following conditions: ACSF, leucine, and clorgyline (MAOI). Note the logarithmic scale. *Significantly different from control 5-HTP effect, #significantly different from control 5-HT effect, $P < 0.05$, $n > 7$ rats/condition.

5-HT produced by AADC activates receptors on motoneurons

Next we wanted to confirm that 5-HT produced from 5-HTP acted directly on motoneurons. To do this, we conducted intracellular recordings in motoneurons that were isolated from synaptic input by applying TTX (2 μ M) (Fig. 2-8A). Consistent with 5-HT's excitatory action on motoneurons (Li et al. 2007; Murray et al. 2010), when 5-HTP was applied, in all cases the motoneurons' input conductance was decreased (slope of thin leak-line in Fig. 2-8B, C), and resting membrane potential was depolarized (Fig. 2-8B, C, voltage at 0 nA, $n = 3/3$ rats tested). Furthermore, the persistent inward current (Ca PIC) onset voltage was decreased (zero slope region in current at Ca PIC label in Fig. 2-8B, C) and the magnitude of Ca PIC was increased (at arrow in Fig. 2-8C, $n = 3/3$). All these effects are qualitatively similar to the effects of 5-HT (Li et al. 2007; Murray et al. 2010), and together suggest that applied 5-HTP is converted to 5-HT via AADC, and then diffuses out of the AADC-containing cells to the motoneurons, where it acts on 5-HT_{2B/2C} receptors. To confirm these results, we also recorded overall spontaneous motoneuron pool activity on ventral roots in the presence of synaptic blockers (50 μ M APV, 50 μ M bicuculline, 10 μ M CNQX, 5 μ M strychnine) to block indirect synaptic inputs to the motoneurons. Indeed, in this synaptic blockade, 5-HTP significantly increased spontaneous ventral root activity (264 ± 76 % increase, $n = 8$, $P < 0.05$), though with a somewhat higher EC₅₀ (53.7 ± 38.9 μ M), compared to without synaptic blockade (15.1 ± 15.4 μ M).

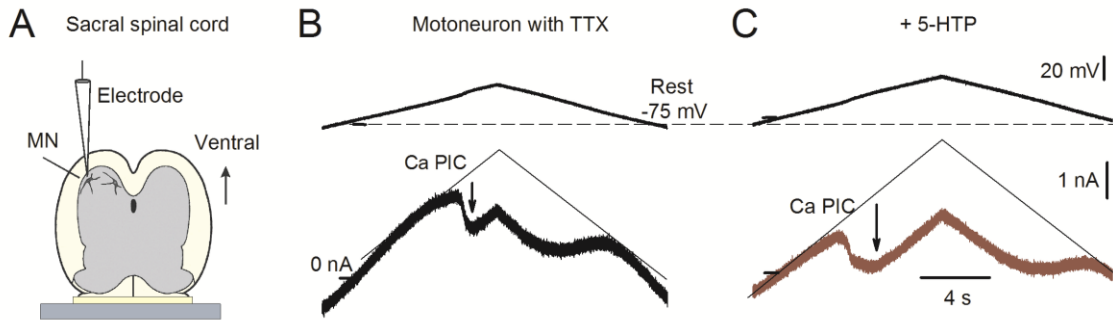


Figure 2-8. 5-HTP directly increases motoneuron excitability in chronic spinal rats.

A: schematic of setup for intracellular recording from motoneurons (MN) in spinal cords from chronic spinal rats in vitro. **B:** motoneuron current response (thick line, bottom) to slow voltage ramp (triangular plot, top) recorded in the presence of TTX to block synaptic inputs and thus isolate the motoneuron. At about -55 mV a persistent inward calcium current (Ca PIC) was activated that caused the current to deviate downward (at arrow), relative to the extrapolated leak current (thin line). **C:** application of 5-HTP (100 μ M) lowered the onset voltage of the Ca PIC (to near -70 mV), and increased the size of the Ca PIC (arrow). Also, the input conductance was decreased (leak current slope), as was the resting potential (at 0 nA, ticks).

Discussion

Spinal cord injury or neurodegenerative diseases like Parkinson's disease (PD) result in a loss of monoamines, like 5-HT and DA, which are critical for motor function. One long-standing therapeutic strategy has thus been to replace monoamines by giving their precursors, such as 5-HTP or L-DOPA (Barbeau et al. 1990; Bedard et al. 1979; Goldstein et al. 1982; Guertin 2009; Hayashi et al. 2010; Ikemoto 2004; Ikemoto et al. 1997; Lidbrink et al. 1974). However, the mechanism by which precursors are converted to monoamines has remained uncertain, especially with spinal cord injury, considering that the enzymes for synthesis of monoamines, including AADC, are normally mostly confined to monoamine fibres, and these fibres are almost entirely lost with a complete spinal transection (Murray et al. 2010; Newton et al. 1988). Our results demonstrate that an upregulation of AADC in spinal cord blood vessels, pericytes and neurons after spinal cord injury compensates for a loss of AADC in descending monoamines fibres after spinal cord injury. AADC in both spinal vessels and neurons are capable of generating 5-HT when the precursor 5-HTP is exogenously applied, thus explaining the therapeutic action of precursors like 5-HTP. In the brain of normal rats, AADC activity has previously been seen in vessel endothelial cells and pericytes, though in this case the monoamines produced from precursors by AADC are quickly metabolized by MAO (within minutes) (Wade et al. 1975), and thus do not accumulate substantially unless MAO is blocked (Hardebo et al. 1979a; Hardebo et al. 1979b), unlike what we see after injury.

Our results specifically demonstrate that exogenously applied 5-HTP acts by the following steps (also shown in the schematic in Fig. 2-9): 1) 5-HTP (and other amino acids like tryptophan) is taken up by the L-transport system (leucine-sensitive) and other amino acid carrier systems into

AADC containing cells (vessels and neurons), 2) AADC synthesizes 5-HT (and likely tryptamine) inside the AADC-containing cells, 3) much of this synthesized 5-HT is then metabolized by MAO (MAO blockers enhance 5-HTP potency 10 fold), 4) the remaining 5-HT somehow leaves the cells, which likely occurs by either simple diffusion or facilitated diffusion using the plasma membrane monoamine transporter (PMAT) (Berry et al. 2013; Engel et al. 2005), though likely only a few percent of the 5-HT diffuses out of the cells in this way (100-fold less than applied 5-HTP, as occurs at the BBB) (Oldendorf 1971), 5) about half of this extracellular 5-HT is diffusely taken up by other cells and further metabolized by MAO (thus 2-fold loss), and 6) the remaining 5-HT reaches 5-HT₂ receptors (SB206553-sensitive) on motoneurons (TTX-resistant) and increases the motoneuron excitability and LLRs, as previously reported for 5-HT (Murray et al. 2010). Overall, there are 1,000-fold losses in 5-HT, compared to applied 5-HTP, before 5-HT reaches the motoneuron receptors, and thus about 15 μM 5-HTP must be present in the spinal cord (in vitro) to affect motoneurons to produce the amount of 5-HT that affects motor function (about 15 nM EC₅₀).

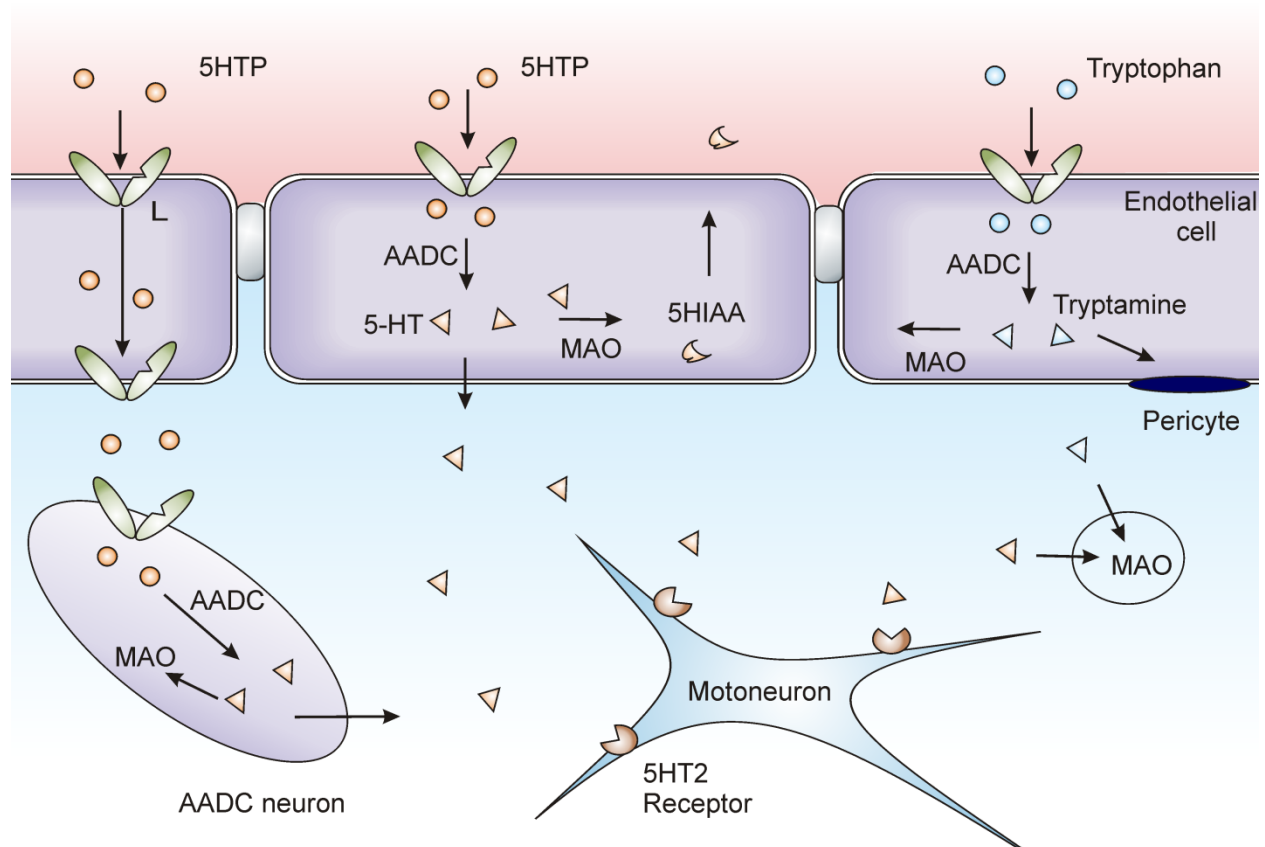


Figure 2-9. Schematic of the action of AADC and MAO after spinal cord injury

Exogenously applied 5-HTP (orange) is transported from the blood (top, red) into endothelial cells and eventually AADC neurons in the spinal cord (bottom, blue) by facilitated diffusion of the L-transport system (L, green). AADC then converts 5-HTP to 5-HT (yellow triangles), although a large part is metabolized by MAO to 5-hydroxyindole-3-acetic acid (5-HIAA) (in AADC-containing cells). The remaining 5-HT diffuses (with difficulty) out of the cells, but at least half of this is transported (perhaps by SERT) into cells diffusely located throughout the spinal cord and further consumed by MAO (small circular cell). The remaining 5-HT eventually reaches motoneurons, and activates 5-HT₂ receptors that increase motoneuron excitability (PICs and spasms). See details in text. AADC also converts endogenous tryptophan to the trace amine tryptamine, which may play a role after injury, possibly with local effects on endothelial cells or pericytes, although tryptamine is also an excellent substrate for MAO

Given these considerations of how 5-HT is synthesized from 5-HTP after spinal cord injury, it is very unlikely that functional amounts of 5-HT can be endogenously produced by the spinal cord after injury. For useful 5-HT to be produced in the spinal cord, according to our in vitro data, circulating endogenous 5-HTP would have to exceed 15 μ M, and this never occurs, as 5-HTP is generally not detected in serum, or at best detected in trace nanomolar quantities (Coppi et al. 1989; Engbaek et al. 1978; Kema et al. 2000; Tyce et al. 1981). Furthermore, our in vivo data show that we must apply about 1 mg/kg 5-HTP systemically to affect motor function, which would raise systemic 5-HTP concentrations to approximately 5 μ M (0.001/ 220 MW, assuming uniform distribution), consistent with our in vitro data (15 μ M EC₅₀), but again this is much higher than the trace nanomolar amounts of 5-HTP endogenously present in serum. These pharmacological data are consistent with our immunolabelling showing a complete absence of 5-HT in the injured spinal cord, even though the same immunolabelling methods can detect 5-HT produced by exogenously applied 5-HTP at near minimal functional doses (as discussed further below).

While AADC is abundant outside of the spinal cord, especially in the liver, kidney and gut (Berry 2004), this peripheral AADC is unlikely to produce 5-HT that affects spinal motor function, because only a very small fraction of serum 5-HT can cross the BBB (1 – 2%) (Oldendorf 1971), serum 5-HT concentrations are kept at low nanomolar levels by avid uptake into platelets (Kema et al. 2000; Paasonen 1965) and very little 5-HT is released into circulation by peripheral AADC sources. Again, this is consistent with the lack of functional endogenous 5-HT that we see after injury.

Finally, our data demonstrate that even if there is a small amount of endogenous 5-HT in the cord after injury that our methods did not detect, this 5-HT is likely to be taken up diffusely by many structures in the spinal cord, as occurs when we artificially raise 5-HT. We do not know the nature of this transport system, but do know that the majority of the 5-HT transported by this system is metabolized by MAO, as discussed further below.

AADC plasticity

Previous studies have shown that expression of AADC is very labile in other brain regions, and in particular AADC is known to increase as monoamine levels decrease, as a compensatory mechanism (Berry 2004; Berry et al. 1996). This would allow more production of trace amines like tryptamine, phenylethylamine or tyramine from readily available dietary amino acids, which in turn activate trace amine-associated receptors (TAARs) that augment the residual action of monoamines at their terminals, by for example modulating monoamine transporters (Xie et al. 2009a; b). Our observed increase in AADC with spinal cord injury is thus broadly consistent with the loss of 5-HT after injury, though again the function of this AADC remains uncertain. Possibly trace amines produced by AADC play a role after spinal cord injury, and we are investigating this in a companion paper (Li and Bennett, in preparation).

Novel emergence of AADC in neurons with spinal cord injury

For decades we have known that AADC-containing D-cells line the central canal (Jaeger et al. 1984; Jaeger et al. 1983), but unexpectedly, we find that these cells largely disappear (or at least down regulate AADC) after spinal cord injury and thus do not likely contribute to much 5-HT synthesis. Instead, we find that a novel class of mediolateral neurons (NeuN-positive and GFAP-

negative) newly express AADC after spinal cord injury and can alone produce enough 5-HT to affect motoneuron function (Fig. 2-9) when exogenous 5-HTP is applied, even in the presence of carbidopa to block vessel AADC. We find that these AADC neurons do not arise from D-cells migrating from the central canal, but instead appear to emerge by an upregulation of AADC in existing neurons, which starts early after injury, and remains for as long as we have examined (months). Low level AADC has been previously reported in spinal neurons, especially in neonates (Gozal 2010), so it is not unexpected that neurons can produce AADC. Interestingly, after DA neuron destruction (like in Parkinson's diseases) a novel population of AADC-neurons also emerge in the striatum (Mura et al. 1995), like with what we see with spinal cord injury.

The normal function of these AADC neurons is unknown. We find that these neurons often have processes that wrap blood vessels, and thus they may play a role in regulating vessel constriction and blood flow, together with the AADC in the vessel endothelial cells. Alternatively, in the striatum AADC neurons have been shown to be GABAergic (Mura et al. 2000), and also suggested to be pluripotent, eventually making dopamine after nigral destruction in PD (Ikemoto 2004).

Vessels contribute to 5-HT synthesis from exogenous 5-HTP after spinal cord injury

It has likewise been known for decades that vessels contain AADC, but this was thought to not normally directly affect spinal function, but on the contrary to act as part of the enzymatic BBB, converting excess precursors to monoamines, so that MAO can metabolize them and remove them from the brain (Hardebo et al. 1979a; Hardebo et al. 1979b; Hardebo et al. 1980b; Kalaria et al. 1987; Spatz et al. 1998). However, our findings demonstrate that, at least after spinal cord

injury, AADC in vessels and associated pericytes contributes to synthesis of 5-HT that affects the spinal cord and specifically motoneuron function (as summarized in Fig. 2-9), thus completely reversing the role of this BBB enzyme from expelling 5-HT and its precursors to providing 5-HT to the spinal cord. The pericytes are especially interesting, in that they often contain relatively more 5-HT than AADC, suggesting that 5-HT synthesized from 5-HTP is somehow accumulated in these cells.

Over 90% of systemically injected 5-HTP is metabolized by AADC and MAO in the liver or more directly removed by kidney AADC, converting it to 5-HT and 5-HIAA that is expelled in the urine (Warsh et al. 1976). Carbidopa or other similar peripheral AADC blockers (that do not cross the BBB) thus dramatically increase circulating 5-HTP. This ultimately allows much more 5-HTP (or L-DOPA) to enter the spinal cord or brain (Hardebo et al. 1979b; Hardebo et al. 1980b; Warsh et al. 1976), where it can be acted on by AADC neurons (and not vessels blocked by carbidopa). However, despite carbidopa markedly increasing the availability of 5-HTP in the spinal cord, the spinal cord LLR reflex is not made more sensitive to 5-HTP by carbidopa (EC_{50} unchanged), indicating that spinal AADC neurons alone cannot account for 5-HT synthesis without carbidopa. Instead, AADC in vessels must produce at least as much 5-HT as the AADC neurons. Thus, when carbidopa blocks vessel AADC, the loss of 5-HT synthesis is roughly offset by the increased synthesis of 5-HT by AADC neurons from increased 5-HTP delivery into the spinal cord. The importance of vessel AADC, is confirmed by our leucine data, where reflexes remain influenced by 5-HTP, even though leucine blocks uptake of 5-HT into AADC neurons. Our results raise the possibility that vessel AADC may also play a function in precursor treatment, like L-DOPA medication, in other neurological disorders like Parkinson's disease.

5-HT is not endogenously synthesized in the spinal cord after injury

Spinal microvessel and neuronal synthesis of 5-HT in the spinal cord only occurs when exogenous 5-HTP is applied. In microvessels, 5-HT is synthesized by AADC when 5-HTP is made available either from the inside (luminal) or outside (abluminal) of the vessel, as occurs when we systemically inject 5-HTP in vivo or bathe the cord in 5-HTP in vitro, respectively. However, with spinal cord transection there is no chance of the vessel getting endogenous 5-HTP from the spinal cord (abluminal), because 5-HTP and its synthesis enzyme (TPH) are largely eliminated together with the brainstem-derived 5-HT fibres after spinal transection (Carlsson et al. 1964; Clineschmidt et al. 1971), and no endogenous spinal synthesis of 5-HT from endogenous tryptophan occurs in the chronic spinal rats (Fig. 2-2), which would require TPH, as well as AADC. There is much confusion in the literature about the availability of 5-HTP in the blood, because of technical difficulties, but it appears that there is little to no detectable 5-HTP that normally circulates in the blood (Coppi et al. 1989; Engbaek et al. 1978; Kema et al. 2000; Tyce et al. 1981). Thus, the vessels are also unlikely to be able to obtain endogenous 5-HTP from the blood (luminal absorption), and this fits with our finding that vessels and other spinal cord structures are completely devoid of endogenous 5-HT after spinal cord injury.

We are confident that our immunolabelling method can detect even small functional amounts of 5-HT made endogenously by AADC in the spinal cord, because when we applied a very low dose of 5-HTP in vivo, near the minimum needed to see a functional increase in reflexes (and 10 - 30 times lower than standard doses used by us and others) (Bedard et al. 1979), we were still able to detect 5-HT synthesis in vessels and neurons. Thus, our finding of a complete lack of

detectable 5-HT in the cord caudal to a spinal transection indicates that there are not functional amounts of endogenous 5-HT made in the spinal cord, consistent with a lack of endogenous circulating 5-HTP (Engbaek et al. 1978). Our lack of observed effect of carbidopa, the AADC blocker, provides additional support that endogenous 5-HTP has no functional effects, even though exogenous 5-HTP dramatically increases motoneuron function (and LLRs).

Unlike our present study and others (Carlsson et al. 1964), some previous immunolabelling studies have detected small numbers of 5-HT fibres and even occasionally 5-HT-containing cell bodies below a chronic transection (Newton et al. 1989; 1988; Takeoka et al. 2009). We suggest that this was due to either: 1) non-selectivity of the antibodies detecting something other than 5-HT, or 2) fibres associated with the autonomic system that have taken up 5-HT (Lincoln 1995). An interesting possibility related to *point 1* is that some 5-HT antibodies may cross-react with tryptamine made by AADC from endogenous tryptophan. Regardless of the explanation for this discrepancy, there appears to be no endogenous 5-HT below a spinal transection that affects motor function, as our methods can detect minimal functional amounts of 5-HT, and 5-HT receptor antagonists have no effect on motor function (Murray et al. 2010).

Previous HPLC studies have suggested that some 5-HT remains below a spinal transection (Hadjiconstantinou et al. 1984), but at least in our rats, this 5-HT seems not to be functional. Also, careful examination of earlier HPLC studies of spinal cord injury (Hadjiconstantinou et al. 1984) reveals that in processing these spinal cords the authors did not clear the blood from the vessels, and so there must be substantial 5-HT remaining in the platelets, which are a major store of 5-HT in the body (Paasonen 1965), and thus would have contaminated the results. In our

experiments, we found it necessary to take extra precautions to dilate the vessels (with nitrite) and prevent coagulation (with heparin) during tissue perfusion and fixation, to clear the blood from vessels. Without these precautions, blood products were present that produced 5-HT immunolabelling and 5-HT detected in our HPLC studies (see Results), though with the immunolabelling these were clearly distinguishable as being inside vessels, as opposed to in vessel walls (endothelial cells). Thus, we are sure that 5-HT can only be made by AADC in endothelial cells when 5-HTP is exogenously applied and the labelling of 5-HT on vessels is not an artifact of 5-HT in blood products. Our data from the vessel AADC blocker carbidopa confirms this, because rats treated with prior carbidopa produce no vessel 5-HT from exogenously injected 5-HTP, unlike without carbidopa, and thus our observed vessel 5-HT is related only to AADC synthesis from exogenous 5-HTP and not to contamination from blood products (platelets).

MAO plays a major role in metabolizing 5-HT after injury

Monoamine oxidase (MAO) is the major enzyme that metabolizes biogenic amines like 5-HT and tryptamine (Berry 2004). While MAO is classically considered to function in monoamine terminals, there is plenty of evidence that MAO is diffusely located in the spinal cord (and throughout the body), including in non-neuronal structures such as glia and blood vessel endothelial cells (Hardebo et al. 1980a; Hardebo et al. 1979b; Lang et al. 2004; Lena et al. 1995; Vitalis et al. 2002; Wang et al. 2013). Indeed, our data showing that MAO blockers have major influences on the actions of 5-HT and 5-HTP on spinal cord function (LLR) verifies that MAO is functional after spinal cord injury. MAO acts entirely on intracellular substrates, and specifically is tightly bound to the outer membrane of the mitochondria (Broadley 2010; Wang et al. 2013).

Thus, any observed action of MAO blockers must be on monoamines that are inside cells. Our finding that MAO blockers change the sensitivity (EC_{50}) of the LLR to bath-applied 5-HT indicates that this 5-HT must be taken up by cells and metabolized by MAO, likely by MAO-A (Miller 2011), as summarized in Fig. 2-9.

Importantly, our results demonstrate that MAO inside AADC neurons and vessels must metabolize the majority of 5-HT made from 5-HTP, and it is partly this loss of 5-HT that makes endogenous 5-HTP unlikely to affect motoneuron function, as we have discussed. Specifically, we found that MAO blockers increase the sensitivity of the LLR to 5-HTP by over 10-fold, whereas they increase the sensitivity to exogenously applied 5-HT by 2-fold, indicating that much of the 5-HT manufactured by AADC is lost to MAO inside the AADC cells or vessel, before the AADC can even escape the cells. The remaining 5-HT must diffuse (with difficulty) out of the cells (Berry et al. 1996), and half of this is then lost to MAO in other cells, and only the remaining acts on 5-HT₂ receptors to increase the LLR.

Diffuse amine transport after spinal cord injury.

Our finding that the majority of exogenously applied 5-HT (or synthesized 5-HT, from 5-HTP) is metabolized by MAO, also indicates that 5-HT is somehow taken up by cells in the spinal cord, in order for MAO to be able to metabolize it (MAO is intracellular). This indicates that there is a widespread transport system that takes up 5-HT, even after spinal cord injury. This transport idea is broadly consistent with our observations that in spinal cords from both normal rats and 5-HTP-treated chronic spinal rats there is a diffuse staining for 5-HT in almost all spinal structures, especially near sources of 5-HT (gray matter and specifically motor nucleus; extracellular 5-HT

is washed away in tissue processing, and staining thus only represents intracellular 5-HT). This staining is much weaker than the staining of 5-HT fibres in normal rats or vessels in 5-HTP treated injured rats, but is, nevertheless, widespread and clearly exceeding 5-HT in untreated chronic spinal rats (no detectable staining, as in control sections without 5-HT antibody applied). Thus, even if there is an endogenous source of 5-HT or 5-HTP for the spinal cord after injury, which is undetectable to our immunolabelling, most of this 5-HT will not reach motoneurons, but instead get taken up by this diffuse uptake systems. This may well further explain why very small, but detectable, amounts of 5-HT are sometimes reported after spinal transection, when measured with HPLC or other biochemical methods (see above) (Hadjiconstantinou et al. 1984), and yet this endogenous 5-HT does not seem to affect motoneuron function (not sensitive to neutral antagonists) (Murray et al. 2010), as also discussed above. Furthermore, such a diffuse 5-HT uptake system that prevents 5-HT from affecting motoneurons may well explain why we have repeatedly found that after spinal cord injury exogenous 5-HT must be applied at about 10 times the dose expected from the known binding affinity of 5-HT to the relevant 5-HT receptors (Murray et al. 2011a; Murray et al. 2011b). Indeed, this is consistent with our HPLC data that demonstrates that 10 times more 5-HT accumulates in a spinal cord that is incubated in 5-HT than would be predicted if the applied 5-HT just stayed in the extracellular space (which is only 10% of the cord volume) (Vargova et al. 2008). The nature of the uptake system is unknown, though it may include PMAT (Engel et al. 2005). Furthermore, while some studies indicate that the high affinity serotonin transporter, SERT, is eliminated with injury (Hayashi et al. 2010; Kong et al. 2011), one study suggests a weak but diffuse SERT remaining in the spinal cord after injury (Husch et al. 2012) and this could contribute to 5-HT uptake.

Summary and possible roles of AADC

In summary, after spinal cord injury AADC and MAO enzymes in vessels and neurons maintain the spinal cord's ability to synthesize and metabolize 5-HT from exogenously applied 5-HTP, despite the loss of monoamine fibres that normally provide the traditional role in amine synthesis and metabolism. However, the balance of evidence indicates that endogenous 5-HTP is not available at adequate levels to have any effect on motor function. Thus, AADC does not endogenously produce 5-HT that activates 5-HT₂ receptors on motoneurons. In any case, the 5HT₂ receptors become constitutively active after spinal cord injury (Murray et al. 2010), and thus no longer need 5-HT for their function. The AADC and MAO enzymes must at least serve to synthesize trace amines like tryptamine from dietary amino acids (Fig. 2-9) and subsequently metabolize them respectively (Berry 2004), but we do not know the effects of these trace amines on motor function. Vessel MAO is thought to play a special function in preventing ingested tryptamine from entering the spinal cord, as tryptamine can be a component in certain foods (Broadley 2010). Given the high density of AADC in vessels and pericytes, we speculate that after injury AADC and associated trace amines help regulate blood vessel function, rather than motor function, and the changes in AADC with injury reflects a compensation for the loss of monoamines (Fig. 2-9), which normally regulate CNS vessel function (Broadley 2010; Lincoln 1995; Peppiatt et al. 2006; Rennels et al. 1975).

References

- Acerbo MJ, Hellmann B, and Gunturkun O.** Catecholaminergic and dopamine-containing neurons in the spinal cord of pigeons: an immunohistochemical study. *J Chem Neuroanat* 25: 19-27, 2003.
- Barbeau H, and Rossignol S.** The effects of serotonergic drugs on the locomotor pattern and on cutaneous reflexes of the adult chronic spinal cat. *Brain Res* 514: 55-67, 1990.
- Bedard P, Barbeau H, Barbeau G, and Fillion M.** Progressive increase of motor activity induced by 5-HTP in the rat below a complete section of the spinal cord. *Brain Res* 169: 393-397, 1979.
- Bennett DJ, Gorassini M, Fouad K, Sanelli L, Han Y, and Cheng J.** Spasticity in rats with sacral spinal cord injury. *J Neurotrauma* 16: 69-84, 1999.
- Bennett DJ, Sanelli L, Cooke C, Harvey PJ, and Gorassini MA.** Spastic long-lasting reflexes in the awake rat after sacral spinal cord injury. *J Neurophysiol* 91: 2247-2258, 2004.
- Berry MD.** Mammalian central nervous system trace amines. Pharmacologic amphetamines, physiologic neuromodulators. *J Neurochem* 90: 257-271, 2004.
- Berry MD, Juorio AV, Li XM, and Boulton AA.** Aromatic L-amino acid decarboxylase: a neglected and misunderstood enzyme. *Neurochem Res* 21: 1075-1087, 1996.
- Berry MD, Shitut MR, Almousa A, Alcorn J, and Tomberli B.** Membrane permeability of trace amines: Evidence for a regulated, activity-dependent, nonexocytotic, synaptic release. *Synapse* 10: 656-667 2013.
- Best J, Nijhout HF, and Reed M.** Serotonin synthesis, release and reuptake in terminals: a mathematical model. *Theor Biol Med Model* 7: 34, 2010.
- Broadley KJ.** The vascular effects of trace amines and amphetamines. *Pharmacol Ther* 125: 363-375, 2010.
- Carlsson A, Falck B, Fuxe K, and Hillarp NA.** Cellular localization of monoamines in the spinal cord. *Acta Physiol Scand* 60: 112-119, 1964.
- Chandler SH, Baker LL, and Goldberg LJ.** Characterization of synaptic potentials in hindlimb extensor motoneurons during L-DOPA-induced fictive locomotion in acute and chronic spinal cats. *Brain Res* 303: 91-100, 1984.
- Clineschmidt BV, Pierce JE, and Lovenberg W.** Tryptophan hydroxylase and serotonin in spinal cord and brain stem before and after chronic transection. *J Neurochem* 18: 1593-1596, 1971.
- Coppi G, and Barchielli M.** Simple method for the determination of L-5-hydroxytryptophan in plasma by high-performance liquid chromatography. *J Chromatogr* 495: 245-248, 1989.
- Engbaek F, and Magnusson I.** Determination of 5-Hydroxytryptophan in plasma by high-performance liquid chromatography and fluorometric detection after phthaldialdehyde reaction. *Clin Chem* 24: 376-378, 1978.
- Engel K, and Wang J.** Interaction of organic cations with a newly identified plasma membrane monoamine transporter. *Mol Pharmacol* 68: 1397-1407, 2005.
- Ershov PV, Ugrumov MV, Calas A, Krieger M, and Thibault J.** Degeneration of dopaminergic neurons triggers an expression of individual enzymes of dopamine synthesis in non-dopaminergic neurons of the arcuate nucleus in adult rats. *J Chem Neuroanat* 30: 27-33, 2005.

Goldstein M, Lieberman A, and Pearson J. Relatively high levels of dopamine in nucleus accumbens of levodopa treated patients with Parkinson's disease. *J Neural Transm* 54: 129-134, 1982.

Gomes P, and Soares-da-Silva P. L-DOPA transport properties in an immortalised cell line of rat capillary cerebral endothelial cells, RBE 4. *Brain Res* 829: 143-150, 1999.

Gozal EA. Trace amines as novel modulators of spinal motor function. In: *Biomedical Engineering*, Georgia Inst. of Tech., 2010, p. 262.

Grandy DK. Trace amine-associated receptor 1-Family archetype or iconoclast? *Pharmacol Ther* 116: 355-390, 2007.

Guertin PA. Recovery of locomotor function with combinatory drug treatments designed to synergistically activate specific neuronal networks. *Curr Med Chem* 16: 1366-1371, 2009.

Hadjiconstantinou M, Panula P, Lackovic Z, and Neff NH. Spinal cord serotonin: a biochemical and immunohistochemical study following transection. *Brain Res* 322: 245-254, 1984.

Hardebo JE, Emson PC, Falck B, Owman C, and Rosengren E. Enzymes related to monoamine transmitter metabolism in brain microvessels. *J Neurochem* 35: 1388-1393, 1980a.

Hardebo JE, Falck B, and Owman C. A comparative study on the uptake and subsequent decarboxylation of monoamine precursors in cerebral microvessels. *Acta Physiol Scand* 107: 161-167, 1979a.

Hardebo JE, Falck B, Owman C, and Rosengren E. Studies on the enzymatic blood-brain barrier: quantitative measurements of DOPA decarboxylase in the wall of microvessels as related to the parenchyma in various CNS regions. *Acta Physiol Scand* 105: 453-460, 1979b.

Hardebo JE, and Owman C. Barrier mechanisms for neurotransmitter monoamines and their precursors at the blood-brain interface. *Ann Neurol* 8: 1-31, 1980b.

Harvey PJ, Li X, Li Y, and Bennett DJ. 5-HT₂ receptor activation facilitates a persistent sodium current and repetitive firing in spinal motoneurons of rats with and without chronic spinal cord injury. *J Neurophysiol* 96: 1158-1170, 2006.

Hawkins RA, O'Kane RL, Simpson IA, and Vina JR. Structure of the blood-brain barrier and its role in the transport of amino acids. *J Nutr* 136: 218S-226S, 2006.

Hayashi Y, Jacob-Vadakot S, Dugan EA, McBride S, Olexa R, Simansky K, Murray M, and Shumsky JS. 5-HT precursor loading, but not 5-HT receptor agonists, increases motor function after spinal cord contusion in adult rats. *Exp Neurol* 221: 68-78, 2010.

Heckman CJ, Gorassini MA, and Bennett DJ. Persistent inward currents in motoneuron dendrites: implications for motor output. *Muscle Nerve* 31: 135-156, 2005.

Hochman S, Garraway SM, Machacek DW, and Shay BL. 5-HT receptors and the neuromodulatory control of spinal cord function. In: *Neurobiology of the Spinal Cord*, edited by Cope T. Washington, DC: CRC Press, 2001, p. 47-87.

Husch A, Van Patten GN, Hong DN, Scaperotti MM, Cramer N, and Harris-Warrick RM. Spinal cord injury induces serotonin supersensitivity without increasing intrinsic excitability of mouse V2a interneurons. *J Neurosci* 32: 13145-13154, 2012.

Ikemoto K. Significance of human striatal D-neurons: implications in neuropsychiatric functions. *Prog Neuropsychopharmacol Biol Psychiatry* 28: 429-434, 2004.

Ikemoto K, Kitahama K, Jouvet A, Arai R, Nishimura A, Nishi K, and Nagatsu I. Demonstration of L-dopa decarboxylating neurons specific to human striatum. *Neurosci Lett* 232: 111-114, 1997.

- Jacobs BL, and Azmitia EC.** Structure and function of the brain serotonin system. *Physiol Rev* 72: 165-229, 1992.
- Jaeger CB, Ruggiero DA, Albert VR, Joh TH, and Reis DJ.** Immunocytochemical localization of aromatic-L-aminoacid decarboxylase. In: *Handbook of Chemical Neuroanatomy: Classical Transmitters in the CNS, Part 1* edited by Bjorklund A, and Hokfelt T. New York: Elsevier SC Pub. , 1984, p. 387 - 408.
- Jaeger CB, Teitelman G, Joh TH, Albert VR, Park DH, and Reis DJ.** Some neurons of the rat central nervous system contain aromatic-L-amino-acid decarboxylase but not monoamines. *Science* 219: 1233-1235, 1983.
- Jonkers N, Sarre S, Ebinger G, and Michotte Y.** Benserazide decreases central AADC activity, extracellular dopamine levels and levodopa decarboxylation in striatum of the rat. *J Neural Transm* 108: 559-570, 2001.
- Kalaria RN, and Harik SI.** Blood-brain barrier monoamine oxidase: enzyme characterization in cerebral microvessels and other tissues from six mammalian species, including human. *J Neurochem* 49: 856-864, 1987.
- Karasawa N, Arai R, Isomura G, Nagatsu T, and Nagatsu I.** Chemical features of monoaminergic and non-monoaminergic neurons in the brain of laboratory shrew (*Suncus murinus*) are changed by systemic administration of monoamine precursors. *Neurosci Res* 24: 67-74, 1995.
- Kema IP, de Vries EG, and Muskiet FA.** Clinical chemistry of serotonin and metabolites. *J Chromatogr B Biomed Sci Appl* 747: 33-48, 2000.
- Kitahama K, Geffard M, Araneda S, Arai R, Ogawa K, Nagatsu I, and Pequignot JM.** Localization of L-DOPA uptake and decarboxylating neuronal structures in the cat brain using dopamine immunohistochemistry. *Brain Res* 1167: 56-70, 2007.
- Kong XY, Wienecke J, Chen M, Hultborn H, and Zhang M.** The time course of serotonin 2A receptor expression after spinal transection of rats: an immunohistochemical study. *Neurosci* 177: 114-126, 2011.
- Lang W, Masucci JA, Caldwell GW, Hageman W, Hall J, Jones WJ, and Rafferty BM.** Liquid chromatographic and tandem mass spectrometric assay for evaluation of in vivo inhibition of rat brain monoamine oxidases (MAO) A and B following a single dose of MAO inhibitors: application of biomarkers in drug discovery. *Anal Biochem* 333: 79-87, 2004.
- Lena I, Ombetta JE, Chalon S, Dognon AM, Baulieu JL, Frangin Y, Garreau L, Besnard JC, and Guilloteau D.** Iododerivative of pargyline: a potential tracer for the exploration of monoamine oxidase sites by SPECT. *Nucl Med Biol* 22: 727-736, 1995.
- Li X, Murray K, Harvey PJ, Ballou EW, and Bennett DJ.** Serotonin facilitates a persistent calcium current in motoneurons of rats with and without chronic spinal cord injury. *J Neurophysiol* 97: 1236-1246, 2007.
- Lidbrink P, Jonsson G, and Fuxe K.** Selective reserpine-resistant accumulation of catecholamines in central dopamine neurones after DOPA administration. *Brain Res* 67: 439-456, 1974.
- Lincoln J.** Innervation of cerebral arteries by nerves containing 5-hydroxytryptamine and noradrenaline. *Pharmacol Ther* 68: 473-501, 1995.
- Magnusson T.** Effect of chronic transection on dopamine, noradrenaline and 5-hydroxytryptamine in the rat spinal cord. *Naunyn Schmiedebergs Arch Pharmacol* 278: 13-22, 1973.

Miller GM. The emerging role of trace amine-associated receptor 1 in the functional regulation of monoamine transporters and dopaminergic activity. *J Neurochem* 116: 164-176, 2011.

Mura A, Jackson D, Manley MS, Young SJ, and Groves PM. Aromatic L-amino acid decarboxylase immunoreactive cells in the rat striatum: a possible site for the conversion of exogenous L-DOPA to dopamine. *Brain Res* 704: 51-60, 1995.

Mura A, Linder JC, Young SJ, and Groves PM. Striatal cells containing aromatic L-amino acid decarboxylase: an immunohistochemical comparison with other classes of striatal neurons. *Neurosci* 98: 501-511, 2000.

Murray KC, Nakae A, Stephens MJ, Rank M, D'Amico J, Harvey PJ, Li X, Harris RL, Ballou EW, Anelli R, Heckman CJ, Mashimo T, Vavrek R, Sanelli L, Gorassini MA, Bennett DJ, and Fouad K. Recovery of motoneuron and locomotor function after spinal cord injury depends on constitutive activity in 5-HT_{2C} receptors. *Nat Med* 16: 694-700, 2010.

Murray KC, Stephens MJ, Ballou EW, Heckman CJ, and Bennett DJ. Motoneuron excitability and muscle spasms are regulated by 5-HT_{2B} and 5-HT_{2C} receptor activity. *J Neurophysiol* 105: 731-748, 2011a.

Murray KC, Stephens MJ, Rank M, D'Amico J, Gorassini MA, and Bennett DJ. Polysynaptic excitatory postsynaptic potentials that trigger spasms after spinal cord injury in rats are inhibited by 5-HT_{1B} and 5-HT_{1F} receptors. *J Neurophysiol* 106: 925-943, 2011b.

Newton BW, and Hamill RW. Immunohistochemical distribution of serotonin in spinal autonomic nuclei: I. Fiber patterns in the adult rat. *J Comp Neurol* 279: 68-81, 1989.

Newton BW, and Hamill RW. The morphology and distribution of rat serotonergic intraspinal neurons: an immunohistochemical study. *Brain Res Bull* 20: 349-360, 1988.

Oldendorf WH. Brain uptake of radiolabeled amino acids, amines, and hexoses after arterial injection. *Am J Physiol* 221: 1629-1639, 1971.

Paasonen MK. Release of 5-hydroxytryptamine from blood platelets. *J Pharm Pharmacol* 17: 681-697, 1965.

Peppiatt CM, Howarth C, Mobbs P, and Attwell D. Bidirectional control of CNS capillary diameter by pericytes. *Nature* 443: 700-704, 2006.

Perrier JF, and Delgado-Lezama R. Synaptic release of serotonin induced by stimulation of the raphe nucleus promotes plateau potentials in spinal motoneurons of the adult turtle. *J Neurosci* 25: 7993-7999, 2005.

Rennels ML, and Nelson E. Capillary innervation in the mammalian central nervous system: an electron microscopic demonstration. *Am J Anat* 144: 233-241, 1975.

Schmidt BJ, and Jordan LM. The role of serotonin in reflex modulation and locomotor rhythm production in the mammalian spinal cord. *Brain Res Bull* 53: 689-710, 2000.

Spatz M, and McCarron RM. Blood-brain barrier and monoamines, revisited. In: *Introduction to the Blood-Brain Barrier*, edited by Pardridge WM. Los Angeles: Cambridge University Press, 1998, p. 362-376.

Takeoka A, Kubasak MD, Zhong H, Kaplan J, Roy RR, and Phelps PE. Noradrenergic innervation of the rat spinal cord caudal to a complete spinal cord transection: effects of olfactory ensheathing glia. *Exp Neurol* 222: 59-69, 2010.

Takeoka A, Kubasak MD, Zhong H, Roy RR, and Phelps PE. Serotonergic innervation of the caudal spinal stump in rats after complete spinal transection: effect of olfactory ensheathing glia. *J Comp Neurol* 515: 664-676, 2009.

Tremblay LE, Bedard PJ, Maheux R, and Di Paolo T. Denervation supersensitivity to 5-hydroxytryptamine in the rat spinal cord is not due to the absence of 5-hydroxytryptamine. *Brain Res* 330: 174-177, 1985.

Tyce GM, and Creagan ET. Measurement of free and bound 5-hydroxytryptophan in plasma by liquid chromatography with electrochemical detection. *Anal Biochem* 112: 143-150, 1981.

Ugrumov MV. Non-dopaminergic neurons partly expressing dopaminergic phenotype: distribution in the brain, development and functional significance. *J Chem Neuroanat* 38: 241-256, 2009.

Vargova L, and Sykova E. Extracellular space diffusion and extrasynaptic transmission. *Physiol Res Suppl* 3: S89-99, 2008.

Viala D, and Buser P. [Methods of obtaining locomotor rhythms in the spinal rabbit by pharmacological treatments (DOPA, 5-HTP, D-amphetamine)]. *Brain Res* 35: 151-165, 1971.

Vitalis T, Fouquet C, Alvarez C, Seif I, Price D, Gaspar P, and Cases O. Developmental expression of monoamine oxidases A and B in the central and peripheral nervous systems of the mouse. *J Comp Neurol* 442: 331-347, 2002.

Wade LA, and Katzman R. Rat brain regional uptake and decarboxylation of L-DOPA following carotid injection. *Am J Physiol* 228: 352-359, 1975.

Wang CC, Billett E, Borchert A, Kuhn H, and Ufer C. Monoamine oxidases in development. *Cell Mol Life Sci* 70: 599-630, 2013.

Warsh JJ, and Stancer HC. Brain and peripheral metabolism of 5-hydroxytryptophan-14C following peripheral decarboxylase inhibition. *J Pharmacol Exp Ther* 197: 545-555, 1976.

Xie Z, and Miller GM. A receptor mechanism for methamphetamine action in dopamine transporter regulation in brain. *J Pharmacol Exp Ther* 330: 316-325, 2009a.

Xie Z, and Miller GM. Trace amine-associated receptor 1 as a monoaminergic modulator in brain. *Biochem Pharmacol* 78: 1095-1104, 2009b.

Chapter 3: Chronic hypoxia mediated by trace amines after spinal cord injury

Introduction

The mammalian central nervous system (CNS) is uniquely susceptible to damage when its blood supply is compromised even for very short periods (Acker et al. 2004; Martirosyan et al. 2011; Pena et al. 2005). Accordingly, the CNS has numerous control systems to ensure adequate blood supply, including: 1) *neurovascular coupling* whereby neuronal activity locally dilates blood vessels to increase blood flow in an active area (via glutamate and nitric oxide signalling), 2) *metabolic coupling*, where energy systems (ATP, O₂, etc) regulate neuronal activity and vessel diameter, 3) *basal vascular tone*, where CNS derived neuromodulators such as NA, 5-HT and dopamine produce widespread vasoconstriction (along with myogenic tone), which effectively conserves blood for locally active areas dilated by neurovascular coupling (Attwell et al. 2002; Hamilton et al. 2010; Itoh et al. 2012; Krimer et al. 1998; Peppiatt et al. 2006; Reber et al. 2003). The latter is analogous to the sympathetic control system in the periphery, where NA causes widespread vessel tone (Barcroft et al. 1943; Westcott et al. 2013), though in the CNS neurons in the brainstem provide most of the NA and 5-HT, except for sympathetic innervation of large cerebral arteries above the pia (pial arteries) (Attwell et al. 2002; Bonvento et al. 1991; Cohen et al. 1996; Cohen et al. 1997; Lincoln 1995).

With severe spinal cord injury (SCI) vessels and neurons caudal to the injury survive, but lose contact with brain-derived axons, including losing monoamine innervation that normally arises mostly from the brainstem (Alvarez et al. 1998; Attwell et al. 2002; Björklund et al. 1982; Carlsson et al. 1964; Cohen et al. 1996; Cohen et al. 1997; Jacobs et al. 1992; Schroder et al. 1985). While vessels directly damaged by a traumatic SCI undergo well documented plasticity (Brown et al. 2014; Dolan et al. 1982; Fried et al. 1971; Kang et al. 2010; Kobrine et al. 1975;

Krassioukov 2009; Ohashi et al. 1996; Popa et al. 2010; Sinescu et al. 2010; Smith et al. 1978), including angiogenesis (Kundi et al. 2013; Xiaowei et al. 2006), little is known about these uninjured vessels caudal to the SCI, especially long after injury (Martirosyan et al. 2011). Some uninjured spinal neurons undergo remarkable adaptations that compensate for loss of supraspinal innervation after SCI, including adaptations in monoamine receptors, and this contributes both to recovery of motor function (locomotion) and pathological activity in the form of muscle spasms (Murray et al. 2010; Murray et al. 2011a; Murray et al. 2011b; Rank et al. 2011). Perhaps vessels undergo similar adaptations.

Normally, spinal sources of 5-HT and other monoamines are produced in *brainstem-derived* neurons via enzymatic pathways such as tryptophan hydroxylase (TPH) converting tryptophan to 5-hydroxytryptophan (5-HTP) and then AADC converting 5-HTP to 5-HT (Best et al. 2010; Hardebo et al. 1980; Ikemoto 2004). Thus, spinal transection severs the axons of these brainstem neurons, leaving the cord *without* classic monoamines (Carlsson et al. 1964; Murray et al. 2010). Spinal cord capillaries normally contain small amounts of AADC, even though they lack other enzymes like TPH for monoamine synthesis; however, we have recently confirmed that this capillary AADC is markedly upregulated caudal to a SCI (Hardebo et al. 1979a; Hardebo et al. 1979b; Hardebo et al. 1980; Li et al. 2014; Spatz et al. 1998). AADC alone can directly convert amino acids, like tryptophan, to unconventional monoamines, like tryptamine, collectively termed trace amines (TAs), though the functions of TAs in the spinal cord are obscure (Berry 2004; Berry et al. 1996; Burchett et al. 2006). Tryptamine and other TAs have an affinity to monoamine receptors (Boess et al. 1994; U'Prichard et al. 1977), but are not packaged or released in vesicles, lack a high affinity transporter, and are accordingly rapidly metabolized by

monoamine oxidase (MAO), leaving only trace (nanomolar) quantities (Berry 2004; Burchett et al. 2006; Murray et al. 2011a). However, TAs are synthesized by AADC at the same high rate as classic monoamines, and their precursors, dietary amino acids, are readily available to all cells at micromolar concentrations (Berry 2004; Ekstrom-Jodal et al. 1974; Glaeser et al. 1983; Nasset et al. 1979; Wurtman et al. 1980). Thus, with the dramatic upregulation of AADC in vessels after SCI (Li et al. 2014), TAs like tryptamine are likely to reach micromolar concentrations *locally* within the vessels, prior to being metabolized by MAO (Murray et al. 2011b). At these micromolar concentrations, tryptamine binds to 5-HT₁, alpha₂ receptors (Boess et al. 1994; Murray et al. 2011a; U'Prichard et al. 1977) and specialized trace amine associated receptors (TAARs) (Bunzow et al. 2001), and has known effects on heart and mesentery vasculature (Anwar et al. 2012; Broadley et al. 2013). Thus, we explore here whether trace amines replace the monoaminergic control of vessel tone after SCI.

Classically, CNS blood flow is thought to be mostly controlled by smooth muscle cells (SMCs) that uniformly wrap arteries and arterioles in distinctive bands, and constrict with vasoactive substances, including centrally derived 5-HT and NA acting on 5-HT₁ and alpha₂ adrenergic receptors (Attwell et al. 2010; Bonvento et al. 1991; Busija et al. 1987; Cohen et al. 1996; Cohen et al. 1999; Cohen et al. 1997; Edvinsson et al. 1983; Hamilton et al. 2010; Rennels et al. 1975; Winkler et al. 2011; Xiong et al. 1995), via similar mechanisms to those in the periphery (Westcott et al. 2013; Xiong et al. 1995). When these larger vessels branch to form small capillaries SMCs disappear, but are replaced by sparsely spaced *pericytes* that tightly wrap the capillaries (Winkler et al. 2011) (Fig. 3-1a). While pericytes have many functions (Dalkara et al. 2011; Hamilton et al. 2010; Krueger et al. 2010; Winkler et al. 2011), including angiogenesis

(Ribatti et al. 2011), a subclass of the pericytes contain actin, are known to be contractile, and have recently been shown to play a primary role in controlling CNS blood flow under normal and pathological conditions (Dalkara et al. 2011; Fernandez-Klett et al. 2010; Hall et al. 2014; Peppiatt et al. 2006; Yemisci et al. 2009), (though controversy still exists over pericytes not containing actin (Hill et al. 2015)). Coincidentally, we find that after SCI the pericytes of the capillaries most intensely upregulate AADC and accumulate monoamines (Li et al. 2014). Interestingly, we find that endogenous TAs are so effective in constricting capillary pericytes after SCI that the cord caudal to the injury remains in a chronic state of hypoxia, and thus clinically relevant improvements can be gained by simply inhaling oxygen-enriched air.

Results

Endogenously produced trace amines constrict capillaries at pericytes.

In the spinal cord of normal and injured rats, immunolabelling with the pericyte marker NG2 (Fig. 3-1b) revealed pericytes spaced about every 50 μm along the length of capillaries, with fine processes extending around vessels, as described elsewhere in the brain (Peppiatt et al. 2006). These pericytes have characteristic hemispherical soma and round nuclei, different from other cells like astrocytes, endothelial cells or smooth muscle (Fig. 3-1a, b), allowing us to identify them morphologically with Differential interference contrast (DIC) microscopy in situ, in live whole spinal cords (Fig. 3-1c, d) (Peppiatt et al. 2006).

To assess whether AADC regulates pericytes and capillary diameter, we bath applied AADC substrates (tryptophan, etc.) and blockers onto live cords from rats with chronic spinal cord injury (2 months post injury). Physiological concentrations of tryptophan, tyrosine or phenylalanine (10 - 100 μM) (Ekstrom-Jodal et al. 1974; Glaeser et al. 1983; Nasset et al. 1979; Wurtman et al. 1980) induced pronounced local constrictions of capillaries adjacent to pericytes (Fig. 3-1d, i). Other regions of the capillary without pericytes lacked constrictions, consistent with pericytes producing the vasoconstrictions (Fig. 3-1d, black arrows), as previously reported (Hall et al. 2014; Peppiatt et al. 2006). Pericytes were divided roughly into two classes: those on straight sections of capillaries associated with contractions (quantified in Fig. 3-1i), and those at vessel junctions that were not associated with contractions (Peppiatt et al. 2006). Tryptophan was the most potent amino acid, inducing widespread displacement of red blood cells (RBCs; displaced into large veins), changes in vessel morphology (which altered focal plane), and increases in overall cord opacity. About 65% of pericytes induced tonic contractions lasting as

long as tryptophan was present, whereas the remainder (35%) underwent rhythmic, rather than tonic, contractions, repeatedly constricting and partially re-dilating every few minutes (with peak overall constriction quantified; Supplementary Fig. 3-1 and video). Overall capillary diameter decreased by about 25%, corresponding to ~50% reduction in cross-sectional area (Fig. 3-1i). Blocking AADC with NSD1015 eliminated the tryptophan-induced vasoconstrictions (Fig. 3-1e, i), indicating that these are mediated by AADC producing tryptamine from tryptophan. Indeed, exogenously applied TAs (tryptamine or tyramine) mimicked the vasoconstrictions induced by tryptophan or tyrosine, and this action was resistant to NSD1015 (Fig. 3-1f, i). Neither veins nor arteries constricted with tryptophan, but application of tryptamine did produce rhythmic vasoconstrictions of arteries (not shown). In contrast to the situation in chronic spinal rats, tryptophan had no effect in normal rats (Fig. 3-1h,i), consistent with the relative scarcity of vessel AADC (Li et al. 2014).

Trace amines activate 5-HT_{1B} and alpha₂ adrenergic receptors to constrict capillaries.

To determine the receptors involved in these TA-mediated vasoconstrictions, we screened numerous receptor antagonists and agonists. Tryptamine- and tryptophan-induced capillary vasoconstrictions were both blocked by the selective 5-HT_{1B/D} receptor antagonist GR127935 (Fig. 3-1g,i), and mimicked by the 5-HT_{1B/D} agonist zolmitriptan (Fig. 3-1i), which constricted capillaries at doses consistent with its moderate affinity to 5-HT_{1B} receptors, and not its high affinity to 5-HT_{1D} receptors (Murray et al. 2011b). Tyrosine- and tyramine-induced vasoconstrictions were blocked by the alpha₂ receptor antagonist RX821002 (Fig. 3-1i). In spinal cords from normal rats 5-HT induced capillary constrictions at pericytes (Fig. 3-1i). 5-HT or its precursor 5-HTP had mixed effects on capillaries in chronic spinal rats (unlike tryptophan),

constricting them at low doses, consistent with the 5-HT_{1B} receptor action, but dilating them at higher doses (Fig. 3-1i, Supplementary Fig. 3-2). The latter dilation was mimicked by the 5-HT_{2B/C} receptor agonist alpha-methyl-5-HT (0.3 μM, 37.1 ± 4.2% diameter increase, *n* = 5).

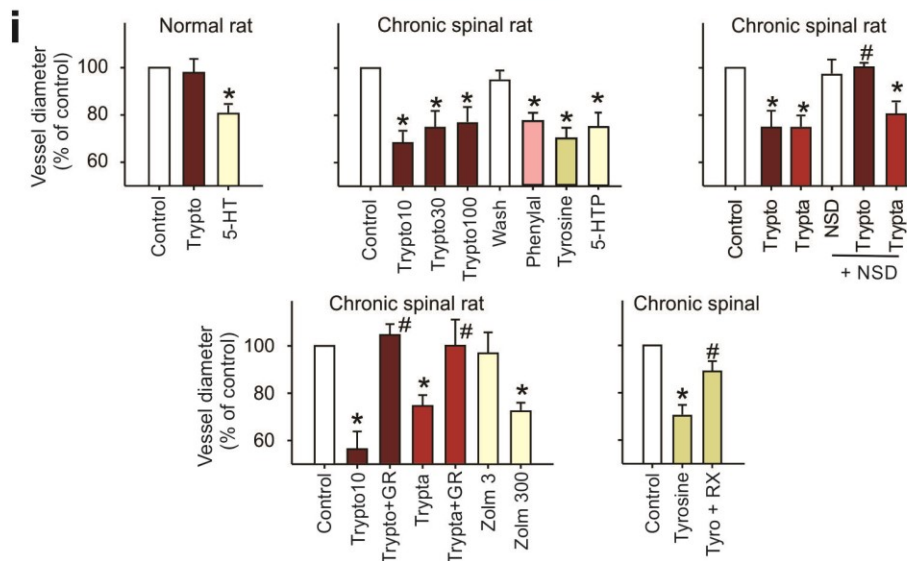
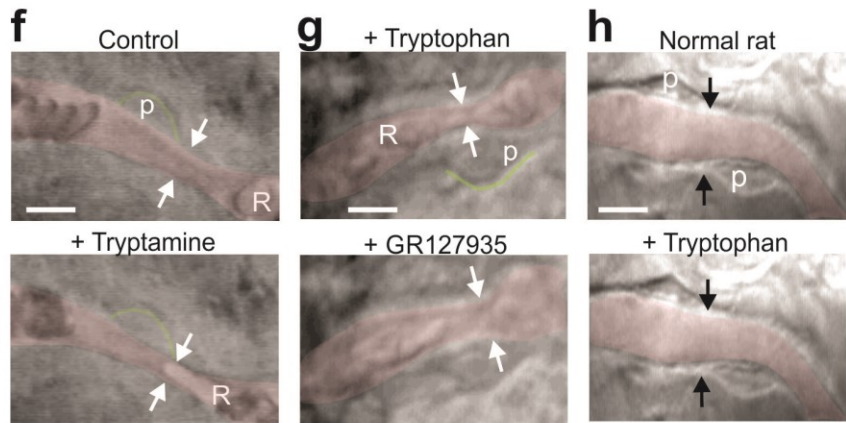
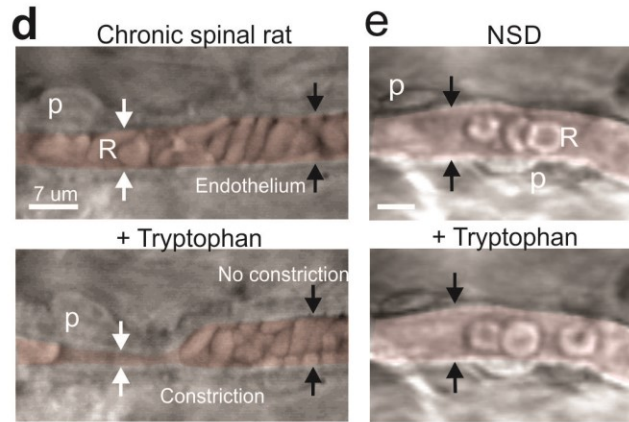
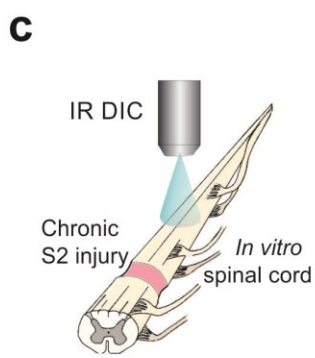
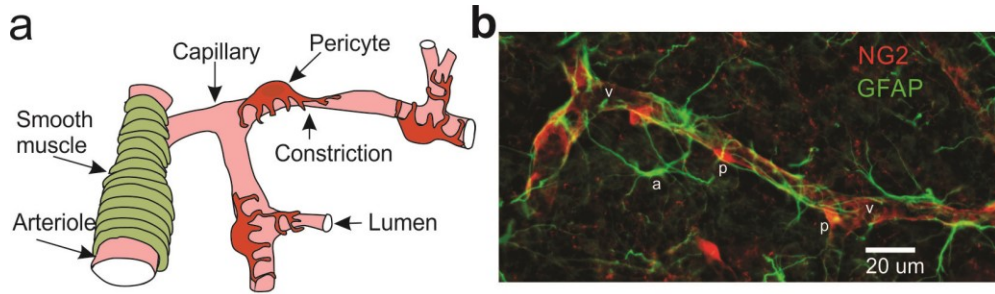


Figure 3-1. Trace amines produced in spinal microvasculature of chronic spinal rats constrict capillaries at pericytes.

(a) Schematic of spinal cord vasculature, showing pericytes and SMCs that regulate the diameter of capillaries and arterioles, respectively. (b) Immunolabelling for pericytes (with NG2 proteoglycan, red, p) and astrocytes (GFAP, green). Image from cord below transection. (c) Schematic of live spinal cord preparation for in situ imaging of capillaries with IR DIC microscopy. (d) DIC image of capillary in the spinal cord caudal to a chronic sacral transection (2 months prior), with red blood cells (RBC) and the region within endothelium (thin white band) pseudo-colored red for clarity. Application of tryptophan (lower panel) induced a local vasoconstriction (white arrows; starting at 2 min and maintained tonically) adjacent to a pericyte (left, p), but not in regions lacking pericytes (right, black arrows). (e) Blocking tryptamine production by AADC (with NSD1015) prevented tryptophan's action. (f) Tryptamine application mimicked tryptophan vasoconstrictions, adjacent to pericytes (outlined in green for clarity). (g) Antagonizing 5-HT_{1B} receptors with GR127935 prevented tryptophan action. (h) Lack of effect of tryptophan in normal rat. (i) Group means of capillary constrictions (normalized to pre-drug control) induced by bath application of: amino acids [10 - 100 μ M tryptophan (trypto10, etc), 30 μ M tyrosine (tyro), 50 μ M phenylalanine, and 0.1 μ M 5-HTP, abbreviated in figure, with dose indicated], AADC products (10-100 μ M tryptamine, 0.3 μ M 5-HT) and zolmitriptan (3 and 300 nM, abbreviated zolm 3 and 300), with and without blocking AADC (with NSD, 300 μ M) or antagonizing 5-HT_{1B} and α_2 receptors (with 3 μ M GR127935 and 0.5 - 1 μ M RX821002, respectively), with $n > 8$ per drug. * $P < 0.05$: significant change relative to pre-drug control, 100%. # significant change with blocker or antagonist. Error bars, s.e.m.

AADC, trace amines and 5-HT_{1B} receptors are co-localized in capillary pericytes.

To localize AADC function we used antibodies to AADC and its products tryptamine and 5-HT. Unlike in normal rats where AADC is predominantly in monoamine axons (Li et al. 2014), caudal to a SCI the AADC and its products (tryptamine) were mostly confined to the microvasculature, with highest density where pericytes adhered to the endothelium (Fig. 3-2a, b, d). While immunolabelling for 5-HT was completely absent after SCI (Fig. 3-2f) (Li et al. 2014), pre-treatment of the rat with the precursor 5-HTP led to pronounced 5-HT immunolabelling in microvasculature, especially at NG2 labelled pericytes, making it a useful surrogate marker of AADC enzyme activity after SCI (Fig. 3-2c, d; AADC produces 5-HT from 5-HTP). Interestingly, while the AADC-product (5-HT) densely filled the round pericyte cell bodies (NG2 labelled, Fig. 3-2c, d), it was not equally dense in neighboring endothelial cells along the vessel wall (Fig. 3-2c, d) and AADC itself was only co-localized with its product in a strip at the endothelial-pericyte interface (yellow in right image of Fig. 3-1d, adjacent to red pericyte), suggesting again that AADC is confined mostly to the pericyte (at flat endothelium interface region) from where AADC products freely diffuse (Fig. 3-2e). Likewise, the 5-HT_{1B} receptor labelling was found to be most densely expressed in pericytes compared to other regions of the capillary, though especially concentrated in the pericyte processes (Fig. 3-2g), and equally dense to the classic localization of 5-HT_{1B} receptors on afferents in the superficial dorsal horn (Supplemental Fig. 3-3).

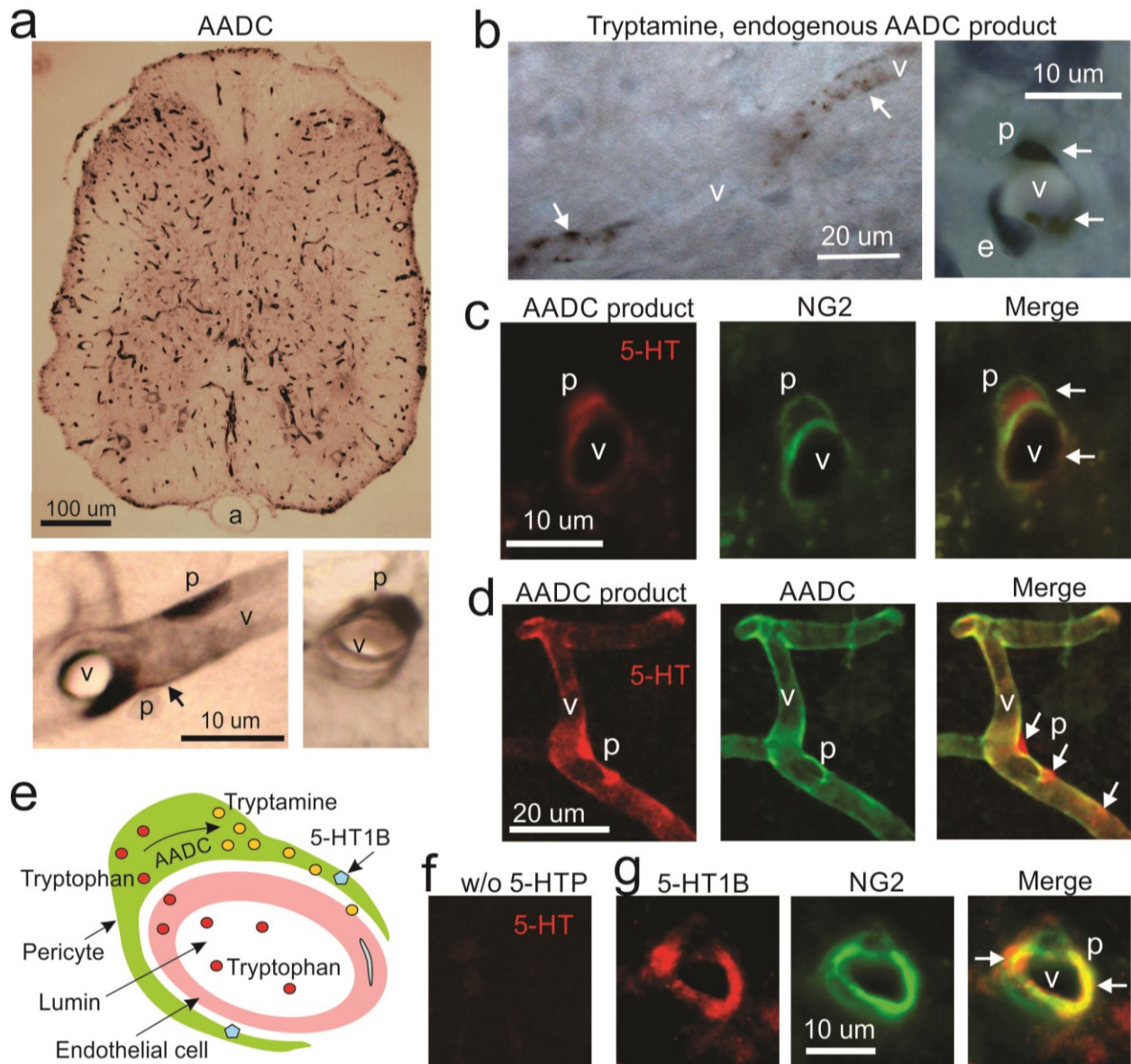


Figure 3-2. AADC, trace amines and 5-HT_{1B} receptors are co-expressed in pericytes after SCI.

(a) Immunolabeling with AADC antibody (black, DAB) in transverse section of spinal cord below a chronic spinal transection, with AADC widely expressed on microvasculature (v) throughout the cord, and especially dense in patches at the interface between pericytes (p) and endothelial cells of capillaries (lower panels expanded scale). **(b)** Immunolabeling for the endogenous AADC product tryptamine (black, DAB) in same rats with SCI, again expressed most densely in pericytes (arrows and p). Cresyl-violet counterstain (blue) showing nuclei of pericytes (p, hemispherical) and endothelial cells (e, flat) in expanded image (right). **(c)** Immunolabeling for 5-HT (red) caudal to a chronic transection injury in rat pre-treated with the precursor 5-HTP, which serves as surrogate label of AADC enzyme activity, because 5-HT is absent in untreated rats (f, below). This AADC activity (red, AADC product) is confined to vessels, and especially accumulates within NG2 labelled pericytes (green). **(d)** AADC products (5-HT) are especially dense in pericyte cell bodies and processes (arrows), whereas AADC is confined to dense strips at the pericyte endothelial interface. **(e)** Schematic of probable pericyte action on capillaries after SCI, showing tryptophan (red) diffusing from blood to pericytes, and AADC then synthesizing tryptamine (yellow), which acts on 5HT_{1B}

receptors to constrict the capillary. **(f)** Lack of 5-HT in untreated rat with SCI. **(g)** Immunolabeling with a 5-HT_{1B} receptor antibody, with 5-HT_{1B} co-expressed with NG2-labelled pericytes throughout the spinal cord after SCI .

Endogenous trace amines reduce blood flow and induce hypoxia after SCI.

Considering that after SCI physiological doses of tryptophan and associated TA production locally constrict capillary at pericytes, we next examined how this affected general blood flow in *vivo*. Interestingly, without any treatment, below a chronic transection injury, the spinal cord vasculature perfused at rates half that of normal or half that of the cord above the injury, as quantified by the time taken to fill all vessels with the vital dye methylene blue (with intracardial injection; Fig. 3-3a, b). Furthermore, after injecting a fluorescent dextran into the blood, two-photon fluorescence microscopy revealed that after SCI the flow rates in spinal capillaries were very low compared to normal CNS flow throughout the capillary (RBC velocity; Fig. 3-3c; 1-2 mm/s normal (Unekawa et al. 2010)). Blocking trace amine production (with AADC blocker NSD1015; Fig. 3-3c) or action (with 5-HT_{1B} receptors antagonist GR127935; Fig. 3-3b) restored blood flow to near normal (doubling RBC velocity along length of capillary without diameter changes, Fig. 3c), consistent with *endogenous* tryptophan acting via AADC to excessively restrict capillary flow. The reduced flow rate after SCI was not due to anatomical plasticity constricting flow after injury, because application of the nitric oxide (NO) donor sodium nitrite to dilate all vessels sped up flow by an order of magnitude, and made normal and injured cords perfuse equally rapidly (Fig. 3-3b).

Consistent with the reduced blood flow after SCI, we found that oxygenation of the cord was significantly impaired in *vivo*, with the partial pressure of O₂ (pO₂) about 15 mmHg in the cord below the injury (Fig. 3-3d, e), consistent with a chronic state of severe hypoxia (< 25 - 35 mmHg is considered hypoxic (Carreau et al. 2011)). In contrast, above the injury or in normal rats, the pO₂ was over twice that below the injury (Fig. 3-3e). Treatments that dilated the

capillaries (Fig. 3-3e, f) restored normal pO₂, including blocking AADC (with NSD1015), and blocking 5-HT_{1B} or alpha₂ receptors (with GR127935 or RX821002, respectively). Tryptophan application itself did not decrease pO₂, likely because circulating endogenous tryptophan levels (~50 μM (Ekstrom-Jodal et al. 1974; Glaeser et al. 1983; Nasset et al. 1979; Wurtman et al. 1980)) were already well above the concentration we found produces peak effects (10 μM) in isolated spinal cord (in vitro, Fig. 3-1i).

Increasing inhaled O₂ to 95 - 100 % (from usual 21% in air) rapidly increased the pO₂ throughout the rat, both above and below the injury, as expected (Fig. 3-3e, blue bar). However, the cord pO₂ caudal to the SCI remained elevated for 20 min *after* a brief period of O₂ breathing (1 min), even though rostral to the injury the cord pO₂ returned rapidly to normal (within 1 min; Fig. 3-3e), as did the breathing rate and exhaled CO₂ (4.5%, not shown). Even more interesting was the finding that transient hypoxia (10% O₂ for 1.5 min) or hypercapnia (10% CO₂ in air) likewise led to prolonged (20 min) elevated pO₂ caudal to the injury, while elsewhere pO₂ returned rapidly to normal (Supplemental Fig. 3-4).

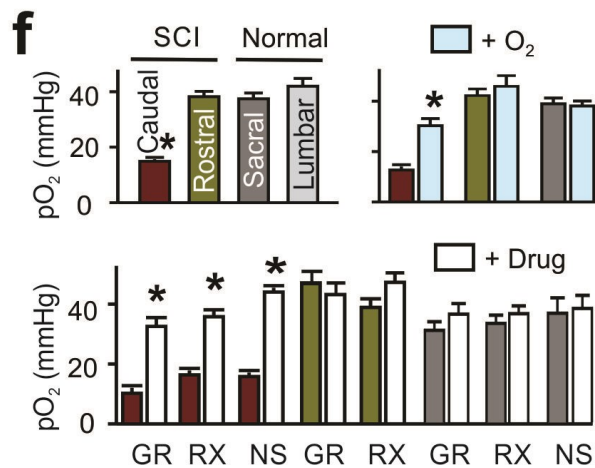
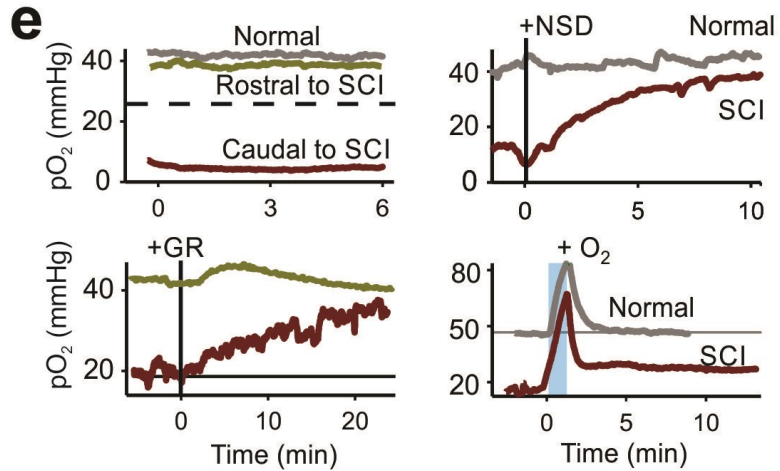
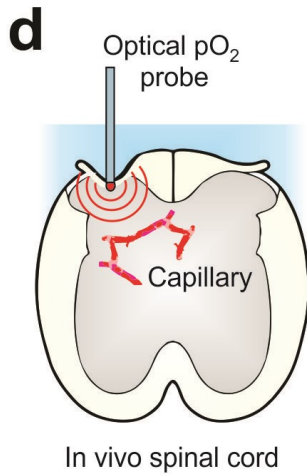
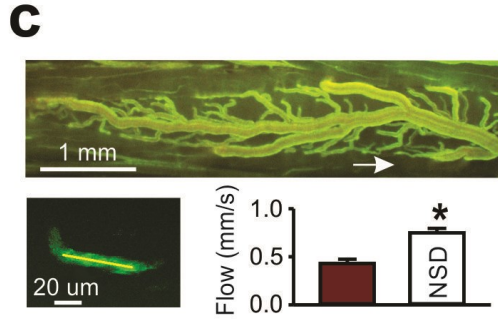
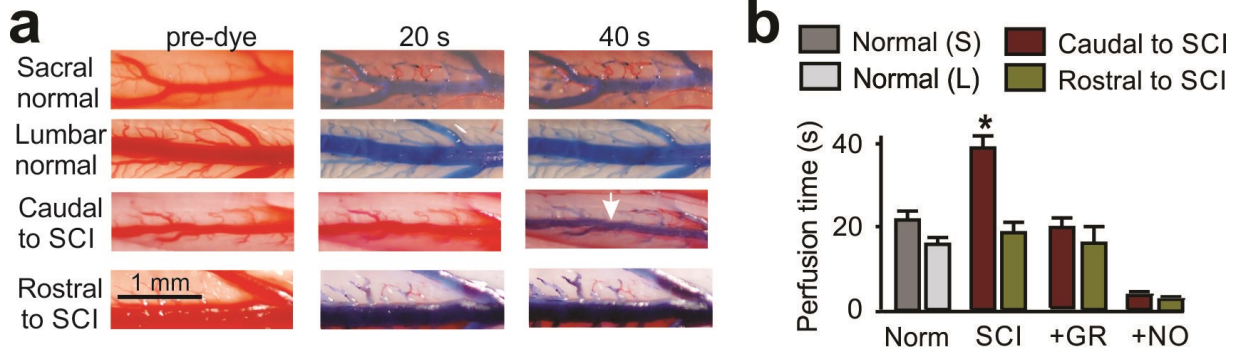


Figure 3-3. Poor spinal cord blood flow and hypoxia after chronic SCI, due to trace amine.

(a) *In vivo* images of sacral and lumbar spinal cord vasculature in normal rats and rats with sacral spinal transection (large vessel: dorsal vein), before and after (20 and 40 sec) intracardial injection of methylene blue dye (5% in saline), with dye slowest to perfuse the sacral cord caudal to the chronic SCI (40 sec to first appear, at arrow). **(b)** Summary of perfusion times of sacral and lumbar cord in normal and injured rats, without and with treatments with the 5-HT_{1B} antagonist GR127935 (GR, to block actions of trace amines; 3 μM topically applied to cord) or sodium nitrate (NO donor; in oxygenated CSF). **(c)** Two-photon microscopy image of sacral vasculature caudal to a SCI *in vivo*, after fluorescent FITC-dextran injection into circulation (*i.v.*). A region where surface vessels dive below pia to connect to capillaries (at arrow) is expanded and brightened (bottom left) to show a spinal capillary where RBC flow rate was determined (at yellow line). Mean capillary RBC flow rate is shown caudal to the SCI (red), and after blocking AADC (with topical 3 mM NSD1015, NSD). **(d)** Schematic of *in vivo* oxygen (pO₂) measurement in the spinal cord with an optical electrode (optode). **(e)** Caudal to a chronic SCI (red) the pO₂ is hypoxic (below dashed-line), and less than rostral to the injury, or in normal cords (top left). Treatments that block TA synthesis via AADC (topical NSD1015), block TA action via 5-HT_{1B} receptors (topical 30 μM GR127935, GR) or transiently (1 min) increase inhaled O₂ eliminates hypoxia after SCI. **(f)** Group means of pO₂ in normal and injured rats before and 10 - 20 min after treatments with transient oxygen (1 min), GR127935, RX821002 (RX; 5 μM topical), and NSD1015 (NS), with *n* > 8 per drug. **P* < 0.05: significant difference relative to pre-treatment control (f) or normal tissue (b; f, top left). Error bars, s.e.m.

Motoneuron function is enhanced by blocking trace amine action and preventing hypoxia.

To evaluate the functional effects of the impaired circulation and chronic hypoxia after SCI we recorded EMG in the awake chronic spinal rat. The muscles innervated by cord below the injury were paralysed with little spontaneous activity (EMG), and yet brief innocuous sensory stimulation (tip of tail) evoked long lasting muscle activity (EMG), associated with tonic uncontrolled muscle spasms (Murray et al. 2010) (Fig. 3-4a). Pharmaceutical treatments that we know improve pO_2 consistently increased spontaneous EMG, including antagonizing monoamine receptors with GR127935 or RX821002 (Fig. 3-4b, EMG to left of stim.). Transient hyperoxia (95% O_2) or hypercapnia (10% CO_2 , not shown) likewise increased spontaneous EMG activity (Fig. 3-4d), with effects lasting 20 mins beyond the treatments (Fig. 3-4e), consistent with our pO_2 measures. All these treatments (GR127935, RX821002 and transient hyperoxia) also increased the sensory evoked EMG responses (long-lasting reflexes, LLR in Fig. 3-4b, c), and interestingly increased the incidence of rhythmic bursting (Fig. 3-4d, blue thin line), suggesting a potential in treating locomotor deficits.

Similar sensory evoked responses (LLRs) were also tested in the isolated spinal cords (in vitro) from chronic spinal rats, maintained in vitro in oxygenated artificial CSF, where vessels have no influence. In this case, when the sensory afferents on the dorsal roots were stimulated motoneuron activity was recorded from the ventral roots, with similar long lasting responses (LLRs) to the spasms seen in vivo (Supplementary Fig. 3-5a, b). Altering the pO_2 of the in vitro CSF transiently altered the motoneuron activity (LLRs; Fig. 3-4e,f), with increasing pO_2 producing increasing neuronal activity, consistent with previous reports (Wilson et al. 2003). However, this increase in activity only occurred during and a few minutes after a transient

increase in pO_2 , unlike the EMG activity that outlasted the O_2 application by 20 mins (Fig. 3-4e, f). Unlike in vivo, spontaneous motoneuron activity and reflexes (LLRs on ventral roots) were not significantly altered by NSD1015, GR127935 or RX821002 (Fig. 3-4c), consistent with the primary action of these drugs being on vessels and blood flow (via AADC and trace amine mechanisms), rather than neurons. Furthermore, tryptophan had no significant effect on neuronal activity in vitro (unless MAO was blocked), unlike its potent effect on vessels, though tryptamine itself could activate neurons (Supplemental Fig. 3-5).

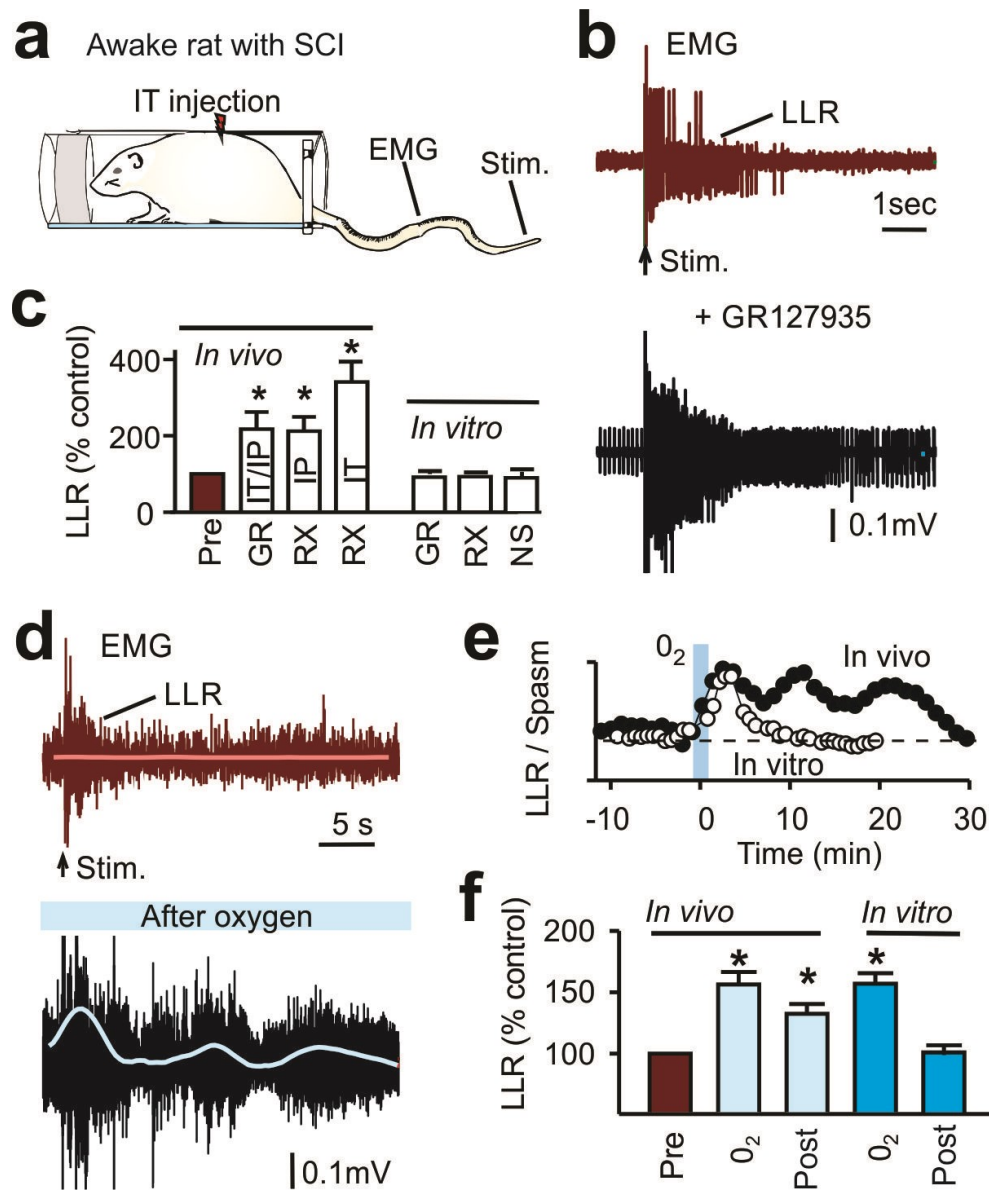


Figure 3-4. Increased motoneuron activity after SCI induced by treatments that improve perfusion and oxygenation.

(a) Schematic of awake (*in vivo*) chronic spinal rat in plexiglass bottle for tail EMG recording and electrical stimulation to evoke reflexes. (b) Motoneuron activity (EMG) in chronic spinal rat, before (red) and after GR127935 treatment (black; i.t., 30 μ l, 10 mM), with treatment increasing baseline EMG (left) and post-stimulus EMG (long-lasting reflex; LLR). (c) Group means of increased LLR activity induced *in vivo* by blocking the TA-mediated vasoconstriction of capillary flow with either GR127935 (application 8 mg/kg IP or I.T. 10 mM in 30 μ l; combined) or RX821002 (i.p. 1 mg/kg or i.t. 3 mM in 30 μ l), and lack of effects of same drugs in the *in vitro* isolated spinal cord, where vessels have no function (see methods in Supplementary Fig. 3-5). LLR normalized to pre-drug (red) levels; $n > 8$ per drug, and $* P < 0.05$ significant difference relative to pre-drug. Error bars, s.e.m. (d) EMG in chronic spinal rat before (red) and 15 min after (black) transient breathing of 95% O₂ (1 min). (e) Time course of LLR response to transiently increased O₂ (1 min), with long-lasting response *in vivo* (as in d) and only transient response *in vitro*. (f) Group means of LLR in injured rats before, during and 10 - 20 min after treatment with transient oxygen (1 min), both *in vivo* and *in vitro*, as in c (normalized to pre-drug control LLR; 100%).

Locomotor function after SCI is improved by treatments that improve capillary blood flow.

To evaluate locomotion after SCI, we studied rats with a major thoracic SCI, either from a contusion or a staggered hemisection injury (Fig. 3-5a), which transects most or all descending axons, respectively, including removing monoamines (Murray et al. 2010). Three weeks after these injuries, rats regained some voluntary hindlimb locomotor ability, though weight support was impaired, plantar foot placement poor and step timing slow, in part because of leg extensor spasms (Fig. 3-5b). In the lumbar region caudal to the injury pO_2 was hypoxic, significantly lower than normal or rostral to the SCI (Fig. 3-5e). Transient O_2 breathing (95%) or blocking trace amine action on receptors (with GR127935) restored near normal pO_2 , and accordingly significantly improved walking ability (Fig. 3-5c-e; walking tested just prior to pO_2 measures).

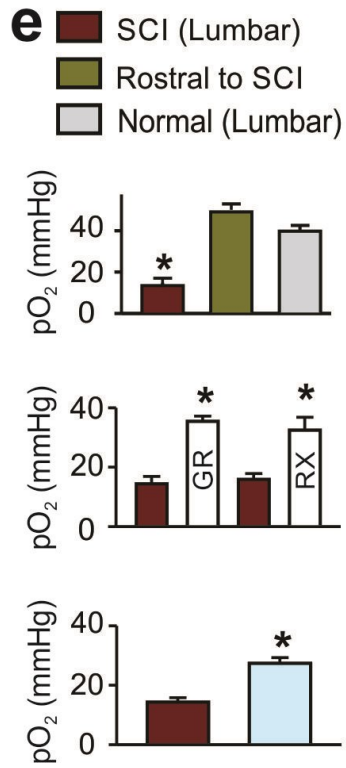
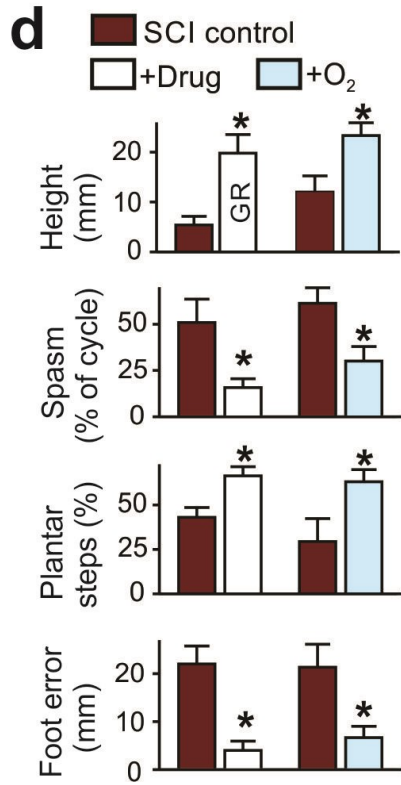
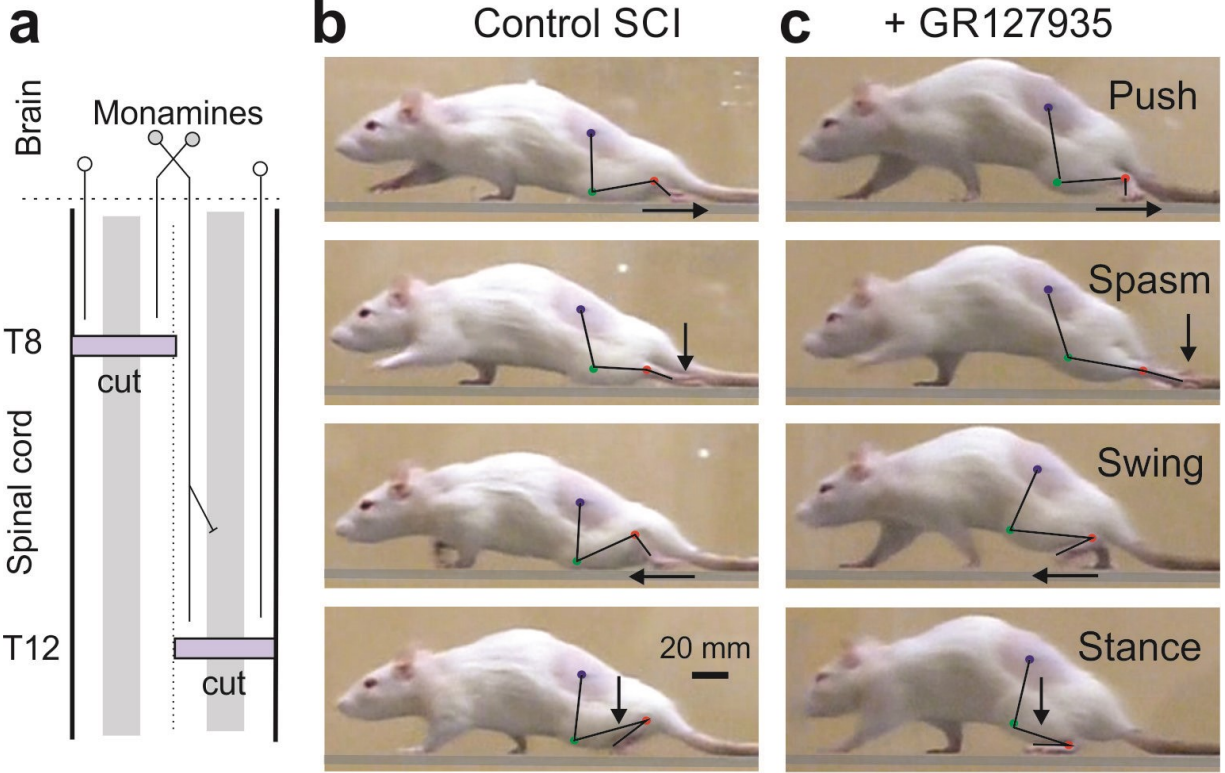


Figure 3-5. Thoracic SCI induces chronic hypoxia that impairs locomotion.

(a) Schematic of thoracic staggered-hemisection SCI, which transects all descending axons from brain, including 5-HT neurons (white circles), but leaves local propriospinal neurons (black) that transverse the injury and help relay descending signals for initiation of locomotion (gray neurons). (b) Rat with staggered hemisection, 3 weeks post injury, walking with impaired hindlimb function, including: poor weight support (measured as hip height minus torso width: clearance above ground), leg extensor spasms lasting up to half a step cycle (quantified as time the foot over-extends and drags immobile on its dorsal surface, relative to step cycle duration), slow poorly timed steps not always on plantar foot surface (no. plantar steps counted relative to no. of front steps) and poor foot placement in stance (measured as deviation behind hip). Hip (iliac crest), knee and ankle are marked with blue, green and red dots. Scale bar 2 cm. (c) Intrathecal application of GR127935 (10 mM in 30 μ l) improves locomotion. (d) Group means of body height, extensor spasms time, number of hindlimb plantar steps per front foot step, and foot placement error before and after application of GR127935 or transient breathing of 95% O₂ (90 sec; peak effect at 10 - 15 min). * $P < 0.05$: significant difference with treatment. Error bars, s.e.m. (e) Group means of pO₂ in normal (lumbar cord) and SCI rats [caudal (lumbar) and rostral (thoracic) to injury], before and 10 - 15 min after treatments with transient oxygen (95%, 90 s), GR127935 (GR, topically applied 30 μ M, and RX821002 (RX, topical 5 μ M), with $n = 5$ per treatment. Contusion and staggered hemisection rat results similar and combined. * $P < 0.05$: significant difference relative to normal or rostral tissue or change with treatment.

Discussion

Our results demonstrate important new concepts that significantly alter how we view spinal cord physiology, pathology and rehabilitation, including: 1) capillaries and associated *pericytes* play a major role in regulating vessel tone and blood flow in the spinal cord, 2) spinal cord injury leads to a *chronic* state of excess capillary tone, poor blood flow and hypoxia, 3) the monoamine receptors 5-HT_{1B} and alpha₂ regulate this capillary tone, even in the *absence* of the monoamines 5-HT and NA, 4) the *trace amines* (tryptamine), produced endogenously from dietary amino acids (tryptophan) by AADC in capillaries, activate these monoamine receptors, replacing the function of brainstem-derived monoamines (5-HT) lost with SCI, and 5) antagonizing monoamine receptors, blocking AADC enzyme function, or augmenting inhaled O₂ produces lasting improvements in blood flow, normalizing oxygenation, and ultimately improving recovery of motor function after SCI, including locomotion. Especially impressive is how transient O₂ breathing leads to long-lasting improvements in function, a simple treatment that could readily be translated into clinical practice, for example, to help initiate walking during treadmill training therapy in humans after SCI (Gorassini et al. 2009; Wirz et al. 2005).

The concept that pericytes play a major role in controlling blood flow in the spinal cord is new, and only recently been examined in the brain (cerebellum and retina) (Hall et al. 2014; Peppiatt et al. 2006; Yemisci et al. 2009). While both smooth muscle cells (SMCs) on arterioles and pericytes on capillaries can regulate CNS blood flow, controversy exists as to whether SMCs or pericytes play the primary role, particularly because the functions of pericytes are so diverse, with some not containing actin or constricting at all (Hall et al. 2014; Hill et al. 2015). Compared to SMCs, pericytes and associated capillaries have been argued to be closer to neurons that

control blood flow, respond first to changes in neuronal activity, and ideally positioned to locally change flow of active brain areas (Hall et al. 2014). Indeed, our data clearly demonstrate that capillaries and associated pericytes can play a primary role in regulating blood flow, because after SCI tryptophan induces widespread capillary constrictions at or near pericytes, but not in non-pericyte regions of the capillary. Furthermore, these capillary constrictions are mediated by AADC that is exclusively expressed in the region of the capillary pericytes, which in turn endogenously produce trace amines that activate monoamine receptors, and blocking these receptors or AADC in vivo, dramatically changes blood flow. In contrast, arterioles and associated SMCs are not constricted by endogenously produced tryptamine (with tryptophan application). Even though SMCs and arterioles have appropriate receptors and respond to exogenously applied monoamines (5-HT and tryptamine) (Cohen et al. 1996; Cohen et al. 1999), they do not express significant AADC after SCI (Li et al. 2014), and as we discuss below, the actions of trace amines are highly localized to AADC-containing cells.

Intriguingly, some capillaries undergo rhythmic tryptophan-induced contractions, a phenomenon described previously in the capillaries of the finger (Crawford et al. 1926), but not in the CNS. These rhythmic contractions would presumably allow intermittent flow, with the possibility of an average flow below the minimum rate possible with a tonic contraction.

We had not anticipated the marked hypoxia that exists chronically (months) in the cord caudal to a SCI, as previous studies have focused exclusively on the acute stage of injury and the epicentre of the injury, where there are well documented disruptions in blood flow that are resolved within days (Dolan et al. 1982; Fried et al. 1971; Kobrine et al. 1975; Kundi et al. 2013; Martirosyan et

al. 2011; Ohashi et al. 1996; Smith et al. 1978). The chronic hypoxia results entirely from excess capillary tone mediated by AADC (NSD1015-sensitive). The finding of chronic hypoxia importantly changes how we study and treat SCI, as any treatment that increases systemic arterial pO₂, including exercise (Barbeau et al. 1987; de Leon et al. 1998; Girgis et al. 2007; Gorassini et al. 2009; Rossignol 2006; Wirz et al. 2005), will increase cord neuronal function, because typically neurons become less excitable in hypoxia (in vitro data, though there are exceptions) (Pena et al. 2005; Takahashi et al. 2011; Wilson et al. 2003). Indeed, we find that increasing pO₂ (with NSD1015, GR127935, or inhaled O₂) dramatically increases motoneuron and locomotor function, in vivo. The mechanism that after SCI mediates the sustained restoration of pO₂ and motor function after only a transient 1 min period of inhaling O₂ is uncertain, though it may involve an exaggerated form of normal neurovascular coupling (Peppiatt et al. 2006), where transient increased O₂ causes increased neuronal activity, which in turn dilates capillaries. Paradoxically, transient hypoxic breathing produces a rebound increase in spinal pO₂ that lasts for > 20 mins, which might help explain why intermittent hypoxia improves rehabilitation after SCI (Navarrete-Opazo et al. 2014). The long-term implications of chronic spinal cord hypoxia are less certain, though likely it contributes to metabolic plasticity (Kundi et al. 2013; Xiaowei et al. 2006), chronic spinal cord inflammation (Beck et al. 2010; Narzo et al. 2015), long-term deterioration and loss of neurons (Kapitza et al. 2012), and exhaustion during locomotor activity in rats and humans with SCI (Beauparlant et al. 2013; Dietz et al. 2009).

Our finding that TAs control capillary tone, arguably represents the first time that endogenous TAs have been shown to have a major stand-alone CNS function, in the complete absence of

classical monoamines. Previously, only secondary functions have been ascribed to TAs in the CNS, involving modulating classical monoamine functions (Berry 2004; Burchett et al. 2006), including TAs modulating the dopamine transporter, to compensate for reductions in dopamine (Bunzow et al. 2001; Lindemann et al. 2008; Miller 2012; 2011; Xie et al. 2009a; b).

Interestingly, the latter dopamine mechanism involves trace amines acting *within* the cell where they are produced (dopamine neuron). Recent studies (Gozal et al. 2014) have shown that *exogenously* applied trace amines can affect motor function in neonatal rats, but TAs produced from endogenous amino acids have no direct neuronal function because of heavy use of the precursor amino acids in protein synthesis, as well as metabolism of TAs by MAO (Li et al. 2014). We were surprised to find that the endogenous actions of TAs in pericytes was mediated mostly by conventional monoamine receptors (sensitive to antagonists), and not apparently related to TAARs (GR127935-sensitive) (Borowsky et al. 2001; Bunzow et al. 2001).

Our results indicate that the AADC acts locally to the pericyte, likely producing TAs within the pericyte that immediately induce vasoconstrictions of the same pericyte, analogous to the local action of TAs in dopamine cells. We reach this conclusion from several lines of evidence: 1) AADC is localized mostly at the pericytes, sandwiched in a thin layer along the pericyte-endothelial interface, ideally situated to produce trace amines in response to blood-borne amino acids. 2) AADC products (amines) densely accumulate in NG2-positive pericytes, and not in immediately adjacent endothelial cells, suggesting that the thin layer of AADC is within the pericyte itself. 3) Amino acids are readily transported across the BBB and into all cells (L-transport) (Gomes et al. 1999; Hawkins et al. 2006), and are specifically available at high micromolar concentrations (Ekstrom-Jodal et al. 1974; Glaeser et al. 1983; Nasset et al. 1979;

Wurtman et al. 1980), and thus pericyte AADC can produce trace amines at the micromolar concentrations needed to activate the 5-HT₁ receptors (Boess et al. 1994) on the pericytes. 4) In contrast, trace amines do not readily diffuse out of cells and are not packaged in vesicles for release, unlike neurotransmitters, and concentrations outside of cells are likely to be low (trace, nanomolar) (Burchett et al. 2006). 5) Spinal cord pericytes express monoamine receptors (e.g. 5HT_{1B}) that likely mediate the TA vasoconstrictions (Fig. 3-2), as in other CNS pericytes (Dalkara et al. 2011; Hamilton et al. 2010).

Other intermediary cells, like astrocytes, expressing monoamine receptors could contribute to TA-mediated pericyte constrictions, though this seems less likely, with the high micromolar TA concentrations needed to activate these receptors (Boess et al. 1994) and widespread MAO that metabolizes TAs before they can reach nearby cells (e.g. motoneurons) (Li et al. 2014). Outside of capillaries, the only other spinal source of TAs are sparsely spaced neurons that upregulate AADC after SCI (Li et al. 2014; Wienecke et al. 2014), but these appear to have no direct endogenous influence on neuronal function (Li et al. 2014). However, these AADC neurons do have axons/dendrites that sometimes contact capillaries or the central canal (Li et al. 2014) and thus may well act to complement pericyte function in regulating vessel tone.

The remarkable adaptation of capillary pericytes to SCI is functionally similar to the adaptation of motoneurons to SCI, where motoneurons become hyperactive as a result of paradoxical monoamine receptor activity, and ultimately lead to muscle spasms, analogous to the excessive vessel tone (Murray et al. 2010; Rank et al. 2011). However, the mechanisms are very different, with motoneurons upregulating isoforms of 5-HT_{2C} receptors that are constitutively active (in

absence of 5-HT) (Murray et al. 2010; Murray et al. 2011a), whereas pericytes upregulate AADC that leads to TA production and 5-HT_{1B} receptor activation. These 5-HT_{1B} receptors may additionally exhibit constitutive activity, though this seems unlikely, because the 5-HT_{1B} receptor activity is eliminated by blocking AADC, and 5-HT₁ receptors appear to generally exhibit less constitutive activity than 5-HT₂ receptors after SCI (Murray et al. 2011b).

Methods

All rat use was approved by the University of Alberta Animal Care and Use Committee: Health Sciences. Most of studies were performed in the sacrocaudal transected injury model, except locomotion related studies. The S2 sacral spinal cord was transected in rats as described previously (Bennett et al. 2004; Li et al. 2014; Murray et al. 2010). Briefly, under general anesthetic (sodium pentobarbital, 58.5 mg/kg) and sterile conditions, a laminectomy was performed on the L2 vertebrae to expose the S2 spinal cord. The dura was slit transversely, and 0.1–0.3 ml Xylocaine (1%) was applied topically. Under a surgical microscope, the spinal cord was transected by holding the pia with forceps and sucking under the pia with a fine suction tip. Caution was needed to avoid damaging the anterior artery or posterior/dorsal vein, since the sacrocaudal spinal cord dies without this midline vasculature. The dura was closed with two 8-0 silk sutures, and the muscle layers and skin were tightly sutured over the cord, and the rat allowed to recover. We evaluated capillary vasoconstrictions and oxygenation of the spinal cord ~2 months post-injury (chronic spinal rats), and in uninjured tissue. Also, electrical recordings were made from muscle, motoneurons, and associated ventral roots of the sacrocaudal spinal cord of spastic adult rats.

Contusion and staggered hemisection injury models were used for locomotion studies (Murray et al. 2010). Under fentanyl (Hypnorm 120 µl/200g; Janssen, Canada) and midazolam (0.75 mg/200g; Sabex, Belgium) anesthesia, 12 adult female Sprague-Dawley rats were injured at ~6 weeks of age. Four rats received a severe contused injury at spinal T8 vertebrae (impact force 200kDyn) and 8 rats underwent a staggered hemisection. The latter rats were first hemisected on the right at the T10 spinal vertebrae (T10 -T11 cord level). Then two weeks later, rats received

an over-hemisection on the left at spinal T5 - T7 vertebrae (T5-T8 cord). In this staggered hemisection model all direct descending supraspinal inputs, including 5-HT, are cut (Fig. 3-5a), whereas spared local propriospinal neurons (Fig. 3-5a) relay descending signals (originating from supraspinal neurons; Fig. 3-5a) around the lesion site. This allows some spontaneous recovery of voluntary locomotion (unlike in transected animals) in the absence of most 5-HT. Bladders were expressed 3 times daily for at least 3 days, until bladder function recovered. Locomotion was evaluated 2 - 3 weeks after contusion or the second hemisection using parameters of plantar foot placement, step frequency and iliac crest height (see below).

In vitro preparation. Under urethane anesthesia (1.8 g/kg, with a maximum dose of 0.45 g), the whole spinal cord caudal to the S2 injury level was removed from chronic spinal rats and immersed in oxygenated modified artificial cerebrospinal fluid (mACSF). For ventral root reflexes testing, spinal roots were removed, except the sacral S4 and caudal Ca1 ventral roots and the Ca1 dorsal roots, but no roots were kept for DIC microscopy. After 0.5 - 1.5 h in the mACSF (at 20°C), the cord was transferred to a recording chamber containing normal ACSF (nACSF) saturated with carbogen (95% O₂ - 5% CO₂), and maintained near 21°C, with a flow rate of 5 ml/min. A 45-min period in nACSF was given to wash out the residual anesthetic and mACSF before recording, at which time the nACSF was recycled in a closed system. In some cords pO₂ was measured using that same sensor as used in vivo (Optode, see below), and adjusted to a desired level (10 - 50 mmHg) by mixing small amounts of N₂ with the carbogen.

In vitro ventral root reflex recording and averaging. Dorsal and ventral roots were mounted on silver-silver chloride wires above the nACSF of the recording chamber and covered with a

5:1 mixture of petroleum jelly and mineral oil for monopolar stimulation and recording. The dorsal root was stimulated with a single pulse (0.1 ms, 0.02 mA, $3 \times T$; repeated 5 times at 10 s intervals for one trial, trials repeated every 12 mins), and the long-lasting reflex (LLR) response was recorded on the ventral roots, and then analyzed as for the ENG. The ventral root recordings were amplified (2,000), high-pass filtered at 100 Hz, low-pass filtered at 3 kHz, and recorded with a data acquisition system sampling at 6.7 kHz (Axonscope 8, Axon Instruments, Burlingame, CA). We quantified the LLR with custom-written software (MATLAB, MathWorks, Natick, MA) by averaging the rectified ventral root activity over a time-window 500 – 4,000 ms post stimulus, a period previously shown to reflect the motoneuron Ca PIC activity in isolation. Because of slow diffusion in whole spinal cord preparations, drugs required $10 \times$ higher concentrations than in thin slice preparations, and peak effects require a 10 – 15 mins. To assure selectivity of drugs, they were titrated to a minimal dose that produced peak effect, and results were reported after 25 – 45 min of drug application. Cumulative dose-response relations were computed by increasing agonist doses at these 12 min intervals (0.003, 0.01, 0.03, 0.1 M, etc. doses used). The effects of agonists on the reflexes were reversible on washout of the agonist, but full recovery to baseline only occurred after several hours, likely because of the large size of the whole cord preparation. Thus washout of agonists was not feasible between doses of the agonists used in the construction of dose-response relations.

IR-DIC microscopy of vessels, *in vitro*. The sacrocaudal spinal cord was removed from rats and put in a recording chamber under IR-DIC microscope (Leica Axioskop2 FC plus) as mentioned in *in vitro* preparation. Spinal capillaries were imaged both through the dorsal surface of the whole cord preparations (sub pial dorsal horn capillaries) and throughout the cord in transverse

sections (the latter, 0.5 mm and cut on vibratome). Similar results were found for all capillaries, in gray and white matter, and so data were combined. Capillaries were chosen mostly in S4-Co segments with the following criteria: 1) diameter was $< 11 \mu\text{m}$, 2) clearly under axons, so they were not pial vessels, 3) lacking continuous smooth muscle seen on arterioles, 4) wrapped with sparsely spaced oval shape pericytes. We analyzed pericytes on straight stretches of capillaries (Peppiatt et al. 2006), rather than at vessel branch points, where drug-induced constrictions were maximal. Drug application was the same as in vitro root reflex recording methods, including applying tryptophan and tryptamine. Video was taken of vessels with an infrared camera and streamed to a computer via a HD video H.264 recorder (Blackmagic Design), and vessel diameter computed offline at common focal planes, before and after drug application effects reached steady state (5 - 10 mins).

Spasms in awake chronic spinal rat. Tail muscle activity and spasms were evoked with brief electrical stimulation of the skin of the tail tip and recorded with tail muscle EMG. Percutaneous EMG wires (50 μm stainless steel, Cooner Wires) were inserted in segmental tail muscles at the midpoint of the tail, and recordings were made while the rat was in a Plexiglas tube, as detailed previously. Muscle spasms were evoked with low-threshold electrical stimulation of the skin at the distal tip of the tail [cutaneous stimulation; 0.2 ms, 10 mA pulse; 50 reflex threshold ($50 \times T$); spasms evoked continuously during experiments with 40 s intervals], and the tail was partly restrained from moving with a piece of masking tape connecting the midpoint of the tail to a rigid stand. EMG was sampled at 5 kHz, rectified and averaged over a 500 to 4,000 ms interval to quantify spasms [LLR; using Axoscope (Axon Instruments) and MATLAB (MathWorks)]. EMG over 300 ms prior to stimulation was also averaged (background). Drugs were applied in

vivo with both intraperitoneal (i.p.) and intrathecal (i.t.) injections and were dissolved in sterile saline. Carbogen (95% O₂-5% CO₂) was given for 60 secs for each trial and 10% CO₂ in air was given for 30 secs to mimic hypercapnia.

Spinal vascular imaging and blood flow, *in vivo*. To evaluate blood flow rate in capillaries, *in vivo* two-photon laser scanning microscopy (TPLSM) was performed in chronic sacrocaudal transected rats. Briefly, rats were anesthetized with urethane (1.8 g/Kg, with a maximum dose of 0.45 g), and then a laminectomy was performed over spinal T10-L4 vertebrae to expose the injured sacrocaudal spinal cord and the uninjured lumbar spinal cord. The exposed spinal segments were bathed in 0.9% saline and the rat positioned under the microscope with stereotaxic stabilizing vertebrae. Fluorescein isocyanate-dextran (FITC-dextran; 70,000 MW, Sigma-Aldrich) was injected via the lateral tail vein (0.3 ml, 5% (w/v) in saline). *In vivo* 2-photon fluorescence microscopy was performed to track RBC velocity in capillaries (8 - 11 μm diameter), using a Leica SP5 MP TPLSM and Coherent Chameleon Vision II pulse laser tuned to 800 nm. Z-stacks and line scans through the first 200-400 μm of spinal tissue were acquired through the spinal preparation using a 20X 1.0 N.A. water dipping objective. Velocity of RBC measurements were made from line scans using Leica MM AF software, with a high frame rate adequate to accurately estimate velocity (~ 500 fps)(Unekawa et al. 2010). Velocity was estimated before and after NSD was topically applied to the spinal cord (dissolved in saline). Velocity was measured in long section of capillary between pericytes, chosen to be without obvious overall vessel diameter changes, so that velocity corresponds to overall capillary flow rate (volume).

We also measured global blood flow rates in the cord below the injury compared to above the injury and in normal rats. Rats were anesthetized and laminectomy performed as in the *in vivo* two photon imaging experiments to expose the lumbar and sacrocaudal spinal cord, which was filmed with a digital camera (Panasonic G3 digital camera with Leica macro-lens). Then rats were perfused intracardially with the vital dye methylene blue (5% methylene blue solution, 1 g/ml, Sigma) in saline at room temperature using gravity fed perfusion (at 1.05 m height to mimic a common blood pressure for all rats; ~100 mmHg). Global flow above and below the SCI was estimated by the time taken for the methylene blue to completely turn major dorsal surface vessels blue (including dorsal vein), thus assuring the dye fully traversed spinal capillary beds and filled the venous return. GR127935 (30 μ M in saline absorbed into a piece of gel-foam, Tocris) was applied locally onto the sacrocaudal spinal cord 5 mins before perfusion (by putting the gelfoam on the cord). For nitric oxide (NO) control experiments, rats were perfused for 2 min (via a pump) with oxygenated ACSF containing sodium nitrite (1 g/l; NO donor; Fisher) and heparin (300 IU/l, from 1,000 U/ml stock; Leo Pharma) to pre-dilate the vessels (via NO). Then the perfusion solution was switched to the 5% methylene blue solution (gravity fed) and the time taken to for cord perfusion was again measured. For many years, we had anecdotally noticed that after SCI the cord caudal to the injury perfused poorly with PFA during preparation for histology, and thus these methylene blue experiments were used to quantify this poor flow. Oxygenated ACSF and NO reversed this poor flow (see Results) and was thus used in some rats to clear the cord prior to PFA fixation to improve immunolabelling (see below).

Oxygen concentration measurement, *in vivo*. Anesthesia, laminectomy and stereotactic stabilizing was similar to the setup for spinal vascular imaging. The partial pressure of oxygen

(pO₂) in the spinal cord was measured with an optical sensor (MicroOptode; Unisense) with a 50 μm tip coated with a fluorophore that when excited with 610 nm red light pulses emitted 780nm infrared light that varied in intensity proportional to the quenching of this light by nearby O₂. The sensor was mounted on a micromanipulator to advance the probe vertically to the dorsal cord surface. Either the probe penetrated the pia or dimpled the pia (by > 200 μm) to measure pO₂ in the dorsal horn, with similar pO₂ measures with either method, likely because the infrared light penetrates deep into the cord through the pia (300 μm, as in our IR-DIC setup). The pia dimple method (Fig. 3-3d) caused less local damage and was thus preferred. Oxygen concentration was measured in the chronic injured cord, and compared with that rostral to the lesion cord and in uninjured rats. Drugs were dissolved in saline and applied topically onto the cord.

Locomotion analysis and i.t. drug injections. The iliac crest (near hip) and fifth metatarsal of the foot were marked on the left and right sides of both contused and stagger hemisectioned rats with a black permanent spot. Rats were filmed with a high speed digital camera (Panasonic, 120 frames/s) while walking across a 1.5 m long Plexiglas runway with a mirror underneath, with markers on their hindlimbs to estimate hip (iliac crest), knee, ankle, and foot (fifth metatarsal) position. The following parameters are used to evaluate locomotion: 1) weight support (measured as hip height minus torso width: clearance above ground), 2) leg extensor spasms (quantified as time the foot over-extends and drags immobile on its dorsal surface, relative to step cycle duration), 3) plantar steps (no. plantar steps counted relative to no. of front steps) and 4) foot placement in stance (measured as foot deviation behind hip at onset of stance). To inhale oxygen, rats were put into a chamber filled with 95% O₂ for 90 secs. GR127935 (GR) was given

intrathecally (i.t., with one exception given i.p. at 8 mg/kg). The i.t. injection was done under very brief isoflurane anesthesia as previously described (Rank et al. 2011). That is, a standard 26 gauge injection needle connected to a Hamilton-syringe was inserted by sliding the needle down the caudal aspect of the L5 vertical process to a small opening between the L5 and L6 vertebrae (at cauda equine) obtained by lifting the hips 5 - 10 cm with one hand while injecting with the other. Rats received a control saline IT injection (30 μ l) and 1 h later a drug i.t. injection (GR, dissolved in sterile saline, 10 mM, 30 μ l) in one experiment session. We quantified the walking in control and drug-treated rats at about 5 - 15 mins after the i.t. injection, long enough for the rat to be fully alert (rats woke and walked in < 2 mins), but prior to i.t. drugs washing away. Interestingly, even in control injections the forelimb function returned within 2 mins, but hindlimb function returned more slowly (4 mins), consistent with poorer circulation caudal to the injury to wash out anesthesia. For this reason, we were careful to compare control and drug-treated animals at a fixed time for each rat post i.t. injections (typically about 8 mins).

Drugs and solutions. Two kinds of ACSF were used in in vitro experiments: mACSF in the dissection dish before recording and nACSF in the recording chamber. mACSF was composed of (in mM) 118 NaCl, 24 NaHCO₃, 1.5 CaCl₂, 3 KCl, 5 MgCl₂, 1.4 NaH₂PO₄, 1.3 MgSO₄, 25 D-glucose, and 1 kynurenic acid. nACSF was composed of (in mM) 122 NaCl, 25 NaHCO₃, 2.5 CaCl₂, 3 KCl, 1 MgCl₂, 0.5 NaH₂PO₄, and 12 D-glucose. Both types of ACSF were saturated with carbogen (95% O₂ - 5% CO₂) and maintained at pH 7.4. The drugs added to the ACSF were 5-HTP, clorgyline, pargyline, tryptamine, L-tryptophan, tyramine, L-tyrosine, 2-phenylethylamine, L-phenylalanine, NSD1015 (Sigma-Aldrich), alpha-methyl 5-HTP, octopamine, SB206553, RX821002, GR127935 (Tocris) and zolmitriptan (AstraZenica). All

drugs were first dissolved as a 10–50 mM stock in water before final dilution in ACSF for *in vitro* ventral root reflexes recording and DIC microscopy or in saline for *in vivo* oxygen measurements and two photon microscopy, with the exception of zolmitriptan, which was dissolved in minimal amounts of DMSO (final concentration in ACSF 0.04%; by itself, DMSO had no effect on *in vitro* LLR in vehicle controls).

Immunolabeling. Rats were euthanized with Euthanyl (BimedaMTC; 700 mg/kg) and perfused intracardially with 100 ml of saline containing sodium nitrite (1 g/l; Fisher) and heparin (300 IU/l, from 1,000 U/ml stock; Leo Pharma) for 3– 4 min, followed by 400 ml of 4% paraformaldehyde (PFA; in phosphate buffer at room temperature), over 15 min. Spinal cords were postfixed in PFA overnight at 4°C, cryoprotected in 30% sucrose in phosphate buffer, frozen, and cut on a cryostat NX70 (Fisher Scientific) in horizontal or transverse 20 µm sections. We mounted spinal cord sections on slides and rinsed in Tris-buffered saline containing 0.3% Triton X-100 (PBS-TX). Sections were incubated overnight at 4°C with the following primary antibodies: rabbit anti-5-HT (1:5,000; Sigma S5545), mouse anti-glial fibrillary acidic protein (GFAP) (1:500; Millipore MAB360), mouse (1:200; Millipore MAB5384) and rabbit (1:200, Millipore; AB5320) anti-NG2 Chondroitin Sulfate Proteoglycan, rabbit anti-Tryptamine conjugated to glutaraldehyde (1:1000; Advanced Targeting Systems AB-T04), rabbit anti-5-HT_{1B} (1:100; Abcam AB13896), and sheep anti-AADC (1:200; Millipore AB119) in TBS-TX. The slides were rinsed in PBS-TX. For staining of AADC, antigen retrieval was performed by incubating slides in 10 mM citrate buffer (pH 8.5) at 80°C for 30 min prior to primary antibody incubation. For staining of 5-HT_{1B}, antigen retrieval was performed by immersion in 50 mM TBS with 0.05% tween 20 (pH 9) at 80°C for 40 min, then after 20 min at room temperature the

blocking procedure was performed. For staining of tryptamine, rats were instead perfused with 0.1 % glutaraldehyde and 2 % PFA, rather than 4% PFA and the fixed spinal sections were incubated in 1% sodium borohydride for 10 minutes. Then the slides underwent 1 h blocking in 10% normal goat serum (NGS) (vector, S-1000) in PBS-TX at room temperature. Sections were incubated overnight in PBS-TX with 1% NGS at room temperature. To visualize the labeling of 5-HT, GFAP, 5-HT1B and NG2, fluorescent secondary antibodies were used, including goat anti-rabbit Texas red (1:200-1:500; Vector T-1000) and goat anti-mouse Alexa Fluor 488 (1:200-1:500; Invitrogen A11029) in PBS-TX, applied on slides for 2 h at room temperature. To visualize the AADC with fluorescent labels, tyramide amplification was additionally performed (Invitrogen TSA Kit no. 12), which included an Alexa Fluor 488 tyramide following ABC amplification (Vector PK-6101). Alternatively, to view DAB labeling of AADC or tryptamine, biotinylated donkey anti-sheep antibody (1:2,000; Millipore AP184B) or goat anti-rabbit antibody (1:200; Vector ABC kit) was applied at room temperature for 2 h in PBS-TX, followed by DAB-ABC amplification according to manufacturer guidelines (ABC, Vector PK-6101; DAB, Vector SK-4100). 0.1% cresyl-violet counterstain was applied with tryptamine DAB staining. After washing steps, the slides were serially dehydrated with alcohol, cleared with xylene, and coverslipped in Permount (Sakura Finetek USA, Torrance, CA, USA). Image acquisition was by both conventional microscopy (for DAB) and confocal microscopy with a Leica TCS SP2 II Spectral Confocal System (for fluorescence). The latter used 1.3 μ m optical sections that were collected into a z-stack over 5–20 μ m and subsequently projected into a single image with maximum-intensity sorting (with ImageJ).

In general, antibody binding and labelling was found to be reduced in over-fixed tissue, especially in vasculature that necessarily received the most direct fixative during perfusion. Thus, vessel labelling with some antibodies (NG2, tryptamine, 5-HT) was confirmed and improved using emersion fixation in 4 % FA, rather than perfusion fixation with 4% PFA perfusion (or perfusion with lower PFA, 2%), after rinsing out blood with perfusion with ASCF with nitric oxide (2 min; see above). Standard controls in which the primary antibody was omitted or quenched with its antigen were used to confirm the selectivity of the antibody staining. Also, clear labeling of monoamine fibers in normal rats was used as a positive control for AADC and 5-HT, and loss of these fibers in chronic spinal rats was a negative control.

References

- Acker T, and Acker H.** Cellular oxygen sensing need in CNS function: physiological and pathological implications. *J Exp Biol* 207: 3171-3188, 2004.
- Alvarez FJ, Pearson JC, Harrington D, Dewey D, Torbeck L, and Fyffe RE.** Distribution of 5-hydroxytryptamine-immunoreactive boutons on alpha- motoneurons in the lumbar spinal cord of adult cats. *J Comp Neurol* 393: 69-83, 1998.
- Anwar MA, Ford WR, Broadley KJ, and Herbert AA.** Vasoconstrictor and vasodilator responses to tryptamine of rat-isolated perfused mesentery: comparison with tyramine and beta-phenylethylamine. *Br J Pharmacol* 165: 2191-2202, 2012.
- Attwell D, Buchan AM, Charpak S, Lauritzen M, Macvicar BA, and Newman EA.** Glial and neuronal control of brain blood flow. *Nature* 468: 232-243, 2010.
- Attwell D, and Iadecola C.** The neural basis of functional brain imaging signals. *Trends Neurosci* 25: 621-625, 2002.
- Barbeau H, and Rossignol S.** Recovery of locomotion after chronic spinalization in the adult cat. *Brain Res* 412: 84-95, 1987.
- Barcroft H, Bonnar WM, Edholm OG, and Effron AS.** On sympathetic vasoconstrictor tone in human skeletal muscle. *J Physiol* 102: 21-31, 1943.
- Beauparlant J, van den Brand R, Barraud Q, Friedli L, Musienko P, Dietz V, and Courtine G.** Undirected compensatory plasticity contributes to neuronal dysfunction after severe spinal cord injury. *Brain* 136: 3347-3361, 2013.
- Beck KD, Nguyen HX, Galvan MD, Salazar DL, Woodruff TM, and Anderson AJ.** Quantitative analysis of cellular inflammation after traumatic spinal cord injury: evidence for a multiphasic inflammatory response in the acute to chronic environment. *Brain* 133: 433-447, 2010.
- Bennett DJ, Sanelli L, Cooke C, Harvey PJ, and Gorassini MA.** Spastic long-lasting reflexes in the awake rat after sacral spinal cord injury. *J Neurophysiol* 91: 2247-2258, 2004.
- Berry MD.** Mammalian central nervous system trace amines. Pharmacologic amphetamines, physiologic neuromodulators. *J Neurochem* 90: 257-271, 2004.
- Berry MD, Juorio AV, Li XM, and Boulton AA.** Aromatic L-amino acid decarboxylase: a neglected and misunderstood enzyme. *Neurochem Res* 21: 1075-1087, 1996.
- Best J, Nijhout HF, and Reed M.** Serotonin synthesis, release and reuptake in terminals: a mathematical model. *Theor Biol Med Model* 7: 34, 2010.
- Björklund A, and Skagerberg G.** Descending monoaminergic projections to the spinal cord. In: *Brain Stem Control of Spinal Mechanisms*, edited by Sjolund B, and Bjorklund A. Amsterdam: Elsevier Biomedical Press, 1982, p. 55-88.
- Boess FG, and Martin IL.** Molecular biology of 5-HT receptors. *Neuropharmacol* 33: 275-317, 1994.
- Bonvento G, Lacombe P, MacKenzie ET, Fage D, Benavides J, Rouquier L, and Scatton B.** Evidence for differing origins of the serotonergic innervation of major cerebral arteries and small pial vessels in the rat. *J Neurochem* 56: 681-689, 1991.
- Borowsky B, Adham N, Jones KA, Raddatz R, Artymyshyn R, Ogozalek KL, Durkin MM, Lakhiani PP, Bonini JA, Pathirana S, Boyle N, Pu X, Kouranova E, Lichtblau H, Ochoa FY, Branchek TA, and Gerald C.** Trace amines: identification of a family of mammalian G protein-coupled receptors. *Proc Natl Acad Sci U S A* 98: 8966-8971, 2001.

Broadley KJ, Fehler M, Ford WR, and Kidd EJ. Functional evaluation of the receptors mediating vasoconstriction of rat aorta by trace amines and amphetamines. *Eur J Pharmacol* 715: 370-380, 2013.

Brown A, Nabel A, Oh W, Etlinger JD, and Zeman RJ. Perfusion imaging of spinal cord contusion: injury-induced blockade and partial reversal by beta2-agonist treatment in rats. *J Neurosurg Spine* 20: 164-171, 2014.

Bunzow JR, Sonders MS, Arttamangkul S, Harrison LM, Zhang G, Quigley DI, Darland T, Suchland KL, Pasumamula S, Kennedy JL, Olson SB, Magenis RE, Amara SG, and Grandy DK. Amphetamine, 3,4-methylenedioxymethamphetamine, lysergic acid diethylamide, and metabolites of the catecholamine neurotransmitters are agonists of a rat trace amine receptor. *Mol Pharmacol* 60: 1181-1188, 2001.

Burchett SA, and Hicks TP. The mysterious trace amines: protean neuromodulators of synaptic transmission in mammalian brain. *Prog Neurobiol* 79: 223-246, 2006.

Busija DW, and Leffler CW. Postjunctional alpha 2-adrenoceptors in pial arteries of anesthetized newborn pigs. *Dev Pharmacol Ther* 10: 36-46, 1987.

Carlsson A, Falck B, Fuxe K, and Hillarp NA. Cellular localization of monoamines in the spinal cord. *Acta Physiol Scand* 60: 112-119, 1964.

Carreau A, El Hafny-Rahbi B, Matejuk A, Grillon C, and Kieda C. Why is the partial oxygen pressure of human tissues a crucial parameter? Small molecules and hypoxia. *J Cell Mol Med* 15: 1239-1253, 2011.

Cohen Z, Bonvento G, Lacombe P, and Hamel E. Serotonin in the regulation of brain microcirculation. *Prog Neurobiol* 50: 335-362, 1996.

Cohen Z, Bouchelet I, Olivier A, Villemure JG, Ball R, Stanimirovic DB, and Hamel E. Multiple microvascular and astroglial 5-hydroxytryptamine receptor subtypes in human brain: molecular and pharmacologic characterization. *J Cereb Blood Flow Metab* 19: 908-917, 1999.

Cohen Z, Molinatti G, and Hamel E. Astroglial and vascular interactions of noradrenaline terminals in the rat cerebral cortex. *J Cereb Blood Flow Metab* 17: 894-904, 1997.

Crawford JH, and Rosenberger H. Studies on human capillaries: II. Observations on the capillary circulation in normal subjects. *J Clin Invest* 2: 351-364, 1926.

Dalkara T, Gursoy-Ozdemir Y, and Yemisci M. Brain microvascular pericytes in health and disease. *Acta Neuropathol* 122: 1-9, 2011.

de Leon RD, Hodgson JA, Roy RR, and Edgerton VR. Locomotor capacity attributable to step training versus spontaneous recovery after spinalization in adult cats. *J Neurophysiol* 79: 1329-1340, 1998.

Dietz V, Grillner S, Trepp A, Hubli M, and Bolliger M. Changes in spinal reflex and locomotor activity after a complete spinal cord injury: a common mechanism? *Brain* 132: 2196-2205, 2009.

Dolan EJ, and Tator CH. The effect of blood transfusion, dopamine, and gamma-hydroxybutyrate on posttraumatic ischemia of the spinal cord. *J Neurosurg* 56: 350-358, 1982.

Edvinsson L, Degueurce A, Duverger D, MacKenzie ET, and Scatton B. Central serotonergic nerves project to the pial vessels of the brain. *Nature* 306: 55-57, 1983.

Ekstrom-Jodal B, von Essen C, Haggendal E, and Roos BE. Effects of L-dopa and L-tryptophan on the cerebral blood flow in the dog. *Acta Neurol Scand* 50: 3-10, 1974.

Fernandez-Klett F, Offenhauser N, Dirnagl U, Priller J, and Lindauer U. Pericytes in capillaries are contractile in vivo, but arterioles mediate functional hyperemia in the mouse brain. *Proc Natl Acad Sci U S A* 107: 22290-22295, 2010.

Fried LC, and Goodkin R. Microangiographic observations of the experimentally traumatized spinal cord. *J Neurosurg* 35: 709-714, 1971.

Girgis J, Merrett D, Kirkland S, Metz GA, Verge V, and Fouad K. Reaching training in rats with spinal cord injury promotes plasticity and task specific recovery. *Brain* 130: 2993-3003, 2007.

Glaeser BS, Maher TJ, and Wurtman RJ. Changes in brain levels of acidic, basic, and neutral amino acids after consumption of single meals containing various proportions of protein. *J Neurochem* 41: 1016-1021, 1983.

Gomes P, and Soares-da-Silva P. L-DOPA transport properties in an immortalised cell line of rat capillary cerebral endothelial cells, RBE 4. *Brain Res* 829: 143-150, 1999.

Gorassini MA, Norton JA, Nevett-Duchcherer J, Roy FD, and Yang JF. Changes in locomotor muscle activity after treadmill training in subjects with incomplete spinal cord injury. *J Neurophysiol* 101: 969-979, 2009.

Gozal EA, O'Neill BE, Sawchuk MA, Zhu H, Halder M, Chou CC, and Hochman S. Anatomical and functional evidence for trace amines as unique modulators of locomotor function in the mammalian spinal cord. *Front Neural Circuits* 8: 134, 2014.

Hall CN, Reynell C, Gesslein B, Hamilton NB, Mishra A, Sutherland BA, O'Farrell FM, Buchan AM, Lauritzen M, and Attwell D. Capillary pericytes regulate cerebral blood flow in health and disease. *Nature* 508: 55-60, 2014.

Hamilton NB, Attwell D, and Hall CN. Pericyte-mediated regulation of capillary diameter: a component of neurovascular coupling in health and disease. *Front Neuroenergetics* 2: 2010.

Hardebo JE, Falck B, and Owman C. A comparative study on the uptake and subsequent decarboxylation of monoamine precursors in cerebral microvessels. *Acta Physiol Scand* 107: 161-167, 1979a.

Hardebo JE, Falck B, Owman C, and Rosengren E. Studies on the enzymatic blood-brain barrier: quantitative measurements of DOPA decarboxylase in the wall of microvessels as related to the parenchyma in various CNS regions. *Acta Physiol Scand* 105: 453-460, 1979b.

Hardebo JE, and Owman C. Barrier mechanisms for neurotransmitter monoamines and their precursors at the blood-brain interface. *Ann Neurol* 8: 1-31, 1980.

Hawkins RA, O'Kane RL, Simpson IA, and Vina JR. Structure of the blood-brain barrier and its role in the transport of amino acids. *J Nutr* 136: 218S-226S, 2006.

Hill RA, Tong L, Yuan P, Murikinati S, Gupta S, and Grutzendler J. Regional blood flow in the normal and ischemic brain is controlled by arteriolar smooth muscle cell contractility and not by capillary pericytes. *Neuron* 87: 95-110, 2015.

Ikemoto K. Significance of human striatal D-neurons: implications in neuropsychiatric functions. *Prog Neuropsychopharmacol Biol Psychiatry* 28: 429-434, 2004.

Itoh Y, and Suzuki N. Control of brain capillary blood flow. *J Cereb Blood Flow Metab* 32: 1167-1176, 2012.

Jacobs BL, and Azmitia EC. Structure and function of the brain serotonin system. *Physiol Rev* 72: 165-229, 1992.

Kang CE, Clarkson R, Tator CH, Yeung IW, and Shoichet MS. Spinal cord blood flow and blood vessel permeability measured by dynamic computed tomography imaging in rats after localized delivery of fibroblast growth factor. *J Neurotrauma* 27: 2041-2053, 2010.

Kapitza S, Zorner B, Weinmann O, Bolliger M, Filli L, Dietz V, and Schwab ME. Tail spasms in rat spinal cord injury: changes in interneuronal connectivity. *Exp Neurol* 236: 179-189, 2012.

Kobrine AI, Doyle TF, and Martins AN. Local spinal cord blood flow in experimental traumatic myelopathy. *J Neurosurg* 42: 144-149, 1975.

Krassioukov A. Autonomic function following cervical spinal cord injury. *Respir Physiol Neurobiol* 169: 157-164, 2009.

Krimer LS, Muly EC, 3rd, Williams GV, and Goldman-Rakic PS. Dopaminergic regulation of cerebral cortical microcirculation. *Nat Neurosci* 1: 286-289, 1998.

Krueger M, and Bechmann I. CNS pericytes: concepts, misconceptions, and a way out. *Glia* 58: 1-10, 2010.

Kundi S, Bicknell R, and Ahmed Z. The role of angiogenic and wound-healing factors after spinal cord injury in mammals. *Neurosci Res* 76: 1-9, 2013.

Li Y, Li L, Stephens MJ, Zenner D, Murray KC, Winship IR, Vavrek R, Baker GB, Fouad K, and Bennett DJ. Synthesis, transport, and metabolism of serotonin formed from exogenously applied 5-HTP after spinal cord injury in rats. *J Neurophysiol* 111: 145-163, 2014.

Lincoln J. Innervation of cerebral arteries by nerves containing 5-hydroxytryptamine and noradrenaline. *Pharmacol Ther* 68: 473-501, 1995.

Lindemann L, Meyer CA, Jeanneau K, Bradaia A, Ozmen L, Bluethmann H, Bettler B, Wettstein JG, Borroni E, Moreau JL, and Hoener MC. Trace amine-associated receptor 1 modulates dopaminergic activity. *J Pharmacol Exp Ther* 324: 948-956, 2008.

Martirosyan NL, Feuerstein JS, Theodore N, Cavalcanti DD, Spetzler RF, and Preul MC. Blood supply and vascular reactivity of the spinal cord under normal and pathological conditions. *J Neurosurg Spine* 15: 238-251, 2011.

Miller GM. Avenues for the development of therapeutics that target trace amine associated receptor 1 (TAAR1). *J Med Chem* 55: 1809-1814, 2012.

Miller GM. The emerging role of trace amine-associated receptor 1 in the functional regulation of monoamine transporters and dopaminergic activity. *J Neurochem* 116: 164-176, 2011.

Murray KC, Nakae A, Stephens MJ, Rank M, D'Amico J, Harvey PJ, Li X, Harris RL, Ballou EW, Anelli R, Heckman CJ, Mashimo T, Vavrek R, Sanelli L, Gorassini MA, Bennett DJ, and Fouad K. Recovery of motoneuron and locomotor function after spinal cord injury depends on constitutive activity in 5-HT_{2C} receptors. *Nat Med* 16: 694-700, 2010.

Murray KC, Stephens MJ, Ballou EW, Heckman CJ, and Bennett DJ. Motoneuron excitability and muscle spasms are regulated by 5-HT_{2B} and 5-HT_{2C} receptor activity. *J Neurophysiol* 105: 731-748, 2011a.

Murray KC, Stephens MJ, Rank M, D'Amico J, Gorassini MA, and Bennett DJ. Polysynaptic excitatory postsynaptic potentials that trigger spasms after spinal cord injury in rats are inhibited by 5-HT_{1B} and 5-HT_{1F} receptors. *J Neurophysiol* 106: 925-943, 2011b.

Narzo AF, Kozlenkov A, Ge Y, Zhang B, Sanelli L, May Z, Li Y, Fouad K, Cardozo C, Koonin EV, Bennett DJ, and Dracheva S. Decrease of mRNA editing after spinal cord injury is caused by down-regulation of ADAR2 that is triggered by inflammatory response. *Sci Rep* 5: 12615, 2015.

Nasset ES, Heald FP, Calloway DH, Margen S, and Schneeman P. Amino acids in human blood plasma after single meals of meat, oil, sucrose and whiskey. *J Nutr* 109: 621-630, 1979.

Navarrete-Opazo A, and Mitchell GS. Therapeutic potential of intermittent hypoxia: a matter of dose. *Am J Physiol Regul Integr Comp Physiol* 307: R1181-1197, 2014.

Ohashi T, Morimoto T, Kawata K, Yamada T, and Sakaki T. Correlation between spinal cord blood flow and arterial diameter following acute spinal cord injury in rats. *Acta Neurochir (Wien)* 138: 322-329, 1996.

Pena F, and Ramirez JM. Hypoxia-induced changes in neuronal network properties. *Mol Neurobiol* 32: 251-283, 2005.

Peppiatt CM, Howarth C, Mobbs P, and Attwell D. Bidirectional control of CNS capillary diameter by pericytes. *Nature* 443: 700-704, 2006.

Popa C, Popa F, Grigorean VT, Onose G, Sandu AM, Popescu M, Burnei G, Strambu V, and Sinescu C. Vascular dysfunctions following spinal cord injury. *J Med Life* 3: 275-285, 2010.

Rank MM, Murray KC, Stephens MJ, D'Amico J, Gorassini MA, and Bennett DJ. Adrenergic receptors modulate motoneuron excitability, sensory synaptic transmission and muscle spasms after chronic spinal cord injury. *J Neurophysiol* 105: 410-422, 2011.

Reber F, Gersch U, and Funk RW. Blockers of carbonic anhydrase can cause increase of retinal capillary diameter, decrease of extracellular and increase of intracellular pH in rat retinal organ culture. *Graefes Arch Clin Exp Ophthalmol* 241: 140-148, 2003.

Rennels ML, and Nelson E. Capillary innervation in the mammalian central nervous system: an electron microscopic demonstration. *Am J Anat* 144: 233-241, 1975.

Ribatti D, Nico B, and Crivellato E. The role of pericytes in angiogenesis. *Int J Dev Biol* 55: 261-268, 2011.

Rossignol S. Plasticity of connections underlying locomotor recovery after central and/or peripheral lesions in the adult mammals. *Philos Trans R Soc Lond B Biol Sci* 361: 1647-1671, 2006.

Schroder HD, and Skagerberg G. Catecholamine innervation of the caudal spinal cord in the rat. *J Comp Neurol* 242: 358-368, 1985.

Sinescu C, Popa F, Grigorean VT, Onose G, Sandu AM, Popescu M, Burnei G, Strambu V, and Popa C. Molecular basis of vascular events following spinal cord injury. *J Med Life* 3: 254-261, 2010.

Smith AJ, McCreery DB, Bloedel JR, and Chou SN. Hyperemia, CO₂ responsiveness, and autoregulation in the white matter following experimental spinal cord injury. *J Neurosurg* 48: 239-251, 1978.

Spatz M, and McCarron RM. Blood-brain barrier and monoamines, revisited. In: *Introduction to the Blood-Brain Barrier*, edited by Pardridge WM. Los Angeles: Cambridge University Press, 1998, p. 362-376.

Takahashi N, Kuwaki T, Kiyonaka S, Numata T, Kozai D, Mizuno Y, Yamamoto S, Naito S, Knevels E, Carmeliet P, Oga T, Kaneko S, Suga S, Nokami T, Yoshida J, and Mori Y. TRPA1 underlies a sensing mechanism for O₂. *Nat Chem Biol* 7: 701-711, 2011.

U'Prichard DC, Greenberg DA, and Snyder SH. Binding characteristics of a radiolabeled agonist and antagonist at central nervous system alpha noradrenergic receptors. *Mol Pharmacol* 13: 454-473, 1977.

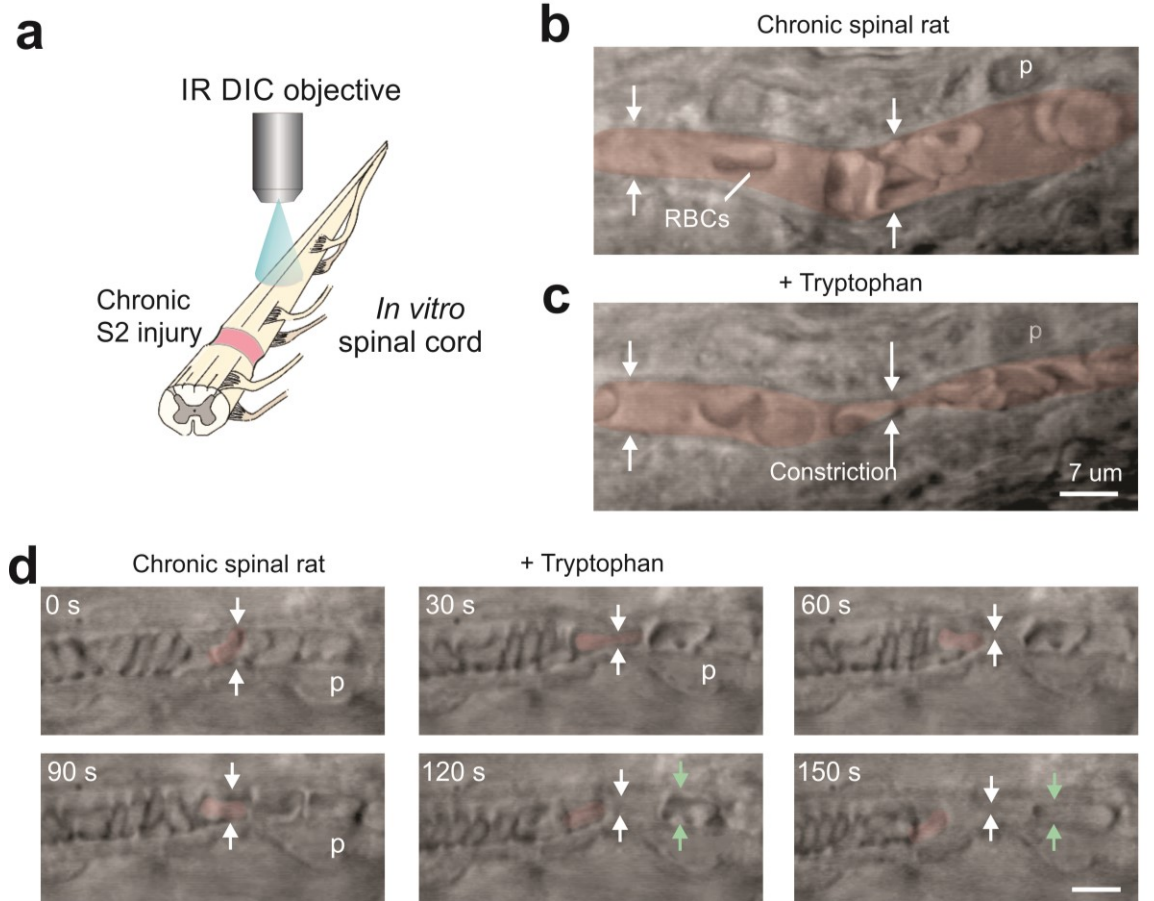
Unekawa M, Tomita M, Tomita Y, Toriumi H, Miyaki K, and Suzuki N. RBC velocities in single capillaries of mouse and rat brains are the same, despite 10-fold difference in body size. *Brain Res* 1320: 69-73, 2010.

Westcott EB, and Segal SS. Perivascular innervation: a multiplicity of roles in vasomotor control and myoendothelial signaling. *Microcirculation* 20: 217-238, 2013.

Wienecke J, Ren LQ, Hultborn H, Chen M, Moller M, Zhang Y, and Zhang M. Spinal cord injury enables aromatic L-amino acid decarboxylase cells to synthesize monoamines. *J Neurosci* 34: 11984-12000, 2014.

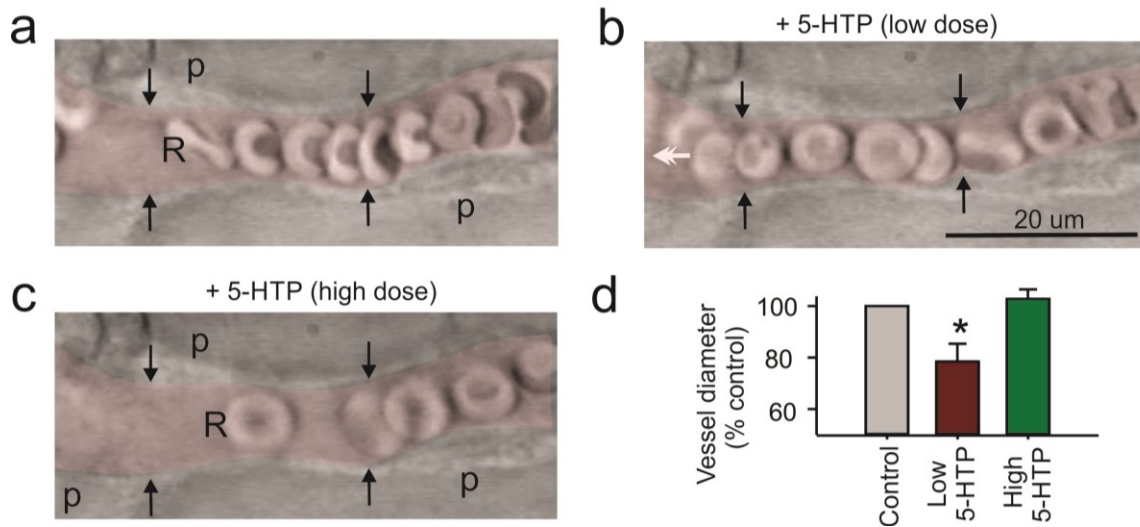
- Wilson RJ, Chersa T, and Whelan PJ.** Tissue PO₂ and the effects of hypoxia on the generation of locomotor-like activity in the in vitro spinal cord of the neonatal mouse. *Neuroscience* 117: 183-196, 2003.
- Winkler EA, Bell RD, and Zlokovic BV.** Central nervous system pericytes in health and disease. *Nat Neurosci* 14: 1398-1405, 2011.
- Wirz M, Zemon DH, Rupp R, Scheel A, Colombo G, Dietz V, and Hornby TG.** Effectiveness of automated locomotor training in patients with chronic incomplete spinal cord injury: a multicenter trial. *Arch Phys Med Rehabil* 86: 672-680, 2005.
- Wurtman RJ, Hefti F, and Melamed E.** Precursor control of neurotransmitter synthesis. *Pharmacol Rev* 32: 315-335, 1980.
- Xiaowei H, Ninghui Z, Wei X, Yiping T, and Linfeng X.** The experimental study of hypoxia-inducible factor-1alpha and its target genes in spinal cord injury. *Spinal Cord* 44: 35-43, 2006.
- Xie Z, and Miller GM.** A receptor mechanism for methamphetamine action in dopamine transporter regulation in brain. *J Pharmacol Exp Ther* 330: 316-325, 2009a.
- Xie Z, and Miller GM.** Trace amine-associated receptor 1 as a monoaminergic modulator in brain. *Biochem Pharmacol* 78: 1095-1104, 2009b.
- Xiong Z, and Sperelakis N.** Regulation of L-type calcium channels of vascular smooth muscle cells. *J Mol Cell Cardiol* 27: 75-91, 1995.
- Yemisci M, Gursoy-Ozdemir Y, Vural A, Can A, Topalkara K, and Dalkara T.** Pericyte contraction induced by oxidative-nitrative stress impairs capillary reflow despite successful opening of an occluded cerebral artery. *Nat Med* 15: 1031-1037, 2009.

Supplementary information



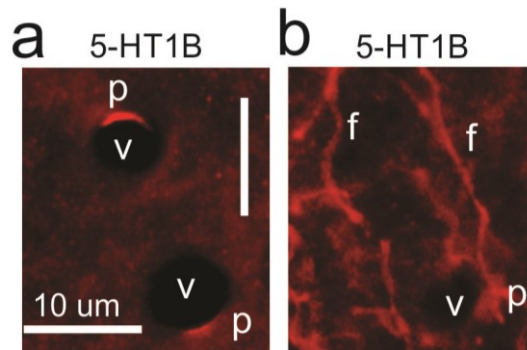
Supplementary Figure 3-1. Tryptophan induces both tonic and rhythmic contractions of capillaries.

(a) Schematic of live spinal cord preparation for in situ imaging of capillaries with IR-DIC microscopy in spinal cord from chronic spinal rat, maintained in vitro. (b) Image of spinal capillary in the cord caudal to a chronic sacral transection (2 months prior), with red blood cells (RBC) and the region within endothelium (thin white band) pseudo-colored red for clarity, and pericyte nucleus labelled p. (c) Application of tryptophan (30 μ M) tonically constricts this capillary adjacent to the pericyte (at 1 min post dose). (d) In other capillaries (28%), tryptophan produces a rhythmic capillary motion, with the capillary constricting at about 1 min after tryptophan application (at white arrows adjacent to pericyte, p), and then partially relaxing at 2 min, and then further constricting at about 3 min (with additional areas constricting, green arrows). This rhythmic contraction repeats throughout tryptophan application (1 hour). During the peak of the constriction it completely obstructs the capillary, displacing RBSs, but then it partial re-opens rhythmically, which would allow a very slow flow rate, below the minimum flow possible with tonic contractions. One RBC is pseudo colored red to show its motion. See Supplementary Video for motion of the same capillary (sped up 16 \times).



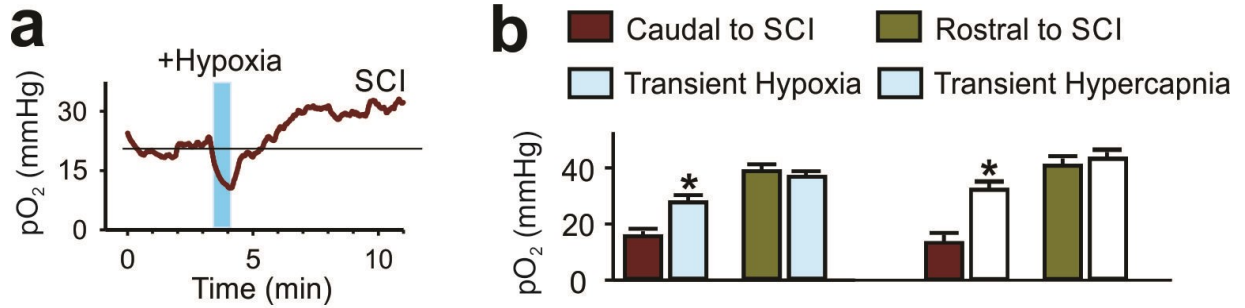
Supplementary Figure 3-2. Bimodal modal action of 5-HTP on capillary diameter.

(a) Image of spinal capillary (DIC image 200 μ m below pia) in the cord caudal to a chronic sacral transection (2 months prior), with red blood cells (RBC) and the region within endothelium (thin white band) pseudo-colored red for clarity. Image from a live whole sacral cord maintained in vitro. (b) Application of 5-HT precursor 5-HTP at a low dose (0.1 μ M) constricts capillary adjacent to pericytes (at 3 min post dose). (c) Application of a subsequent higher dose induces the opposite action, dilating the capillary. (d) Group means of vessel diameter measurements with 5HTP, compared to pre-drug control (100%). ** $P < 0.05$, relative to pre-treatment. $n > 8$ per condition. Error bars, s.e.m.



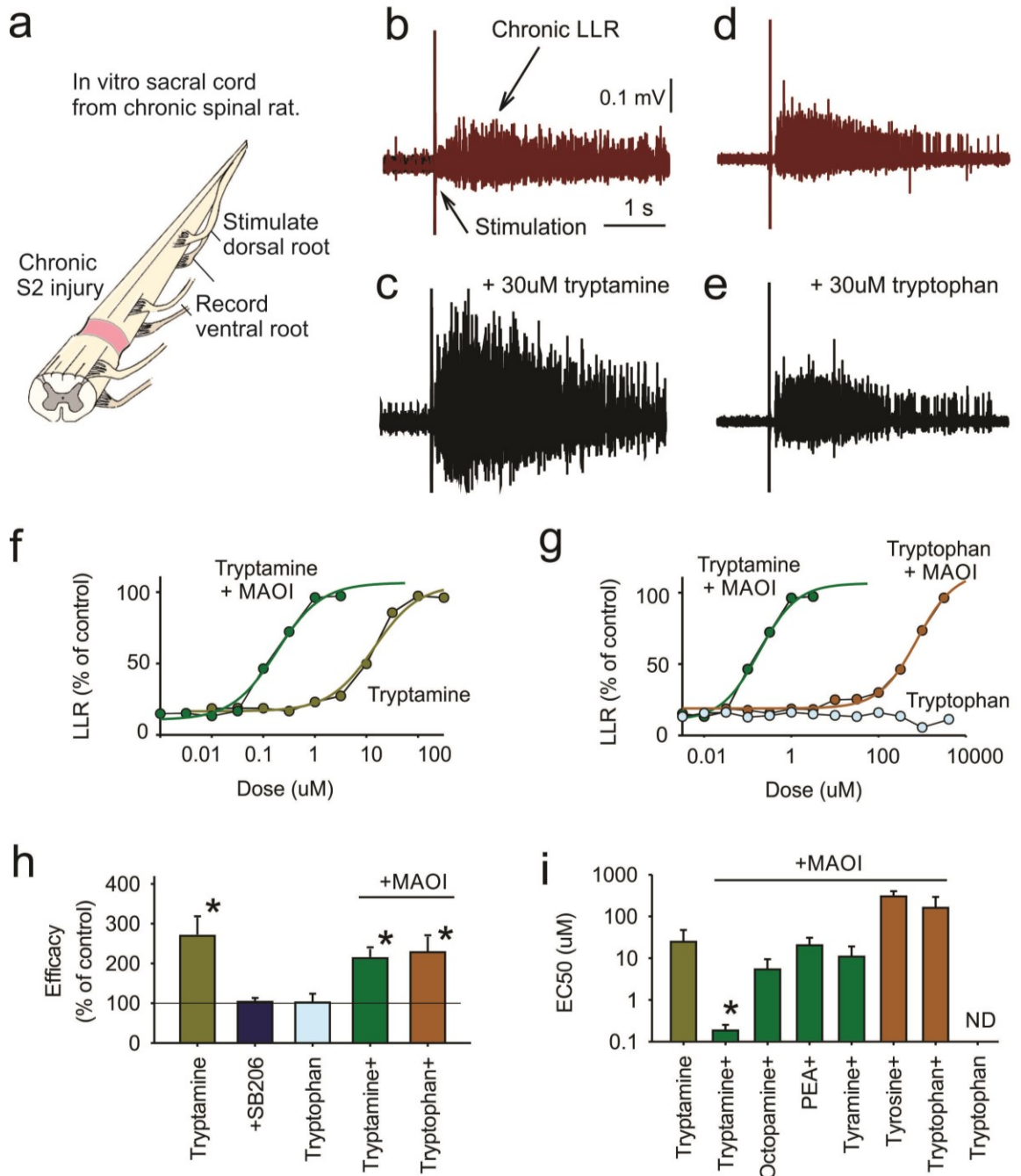
Supplementary Figure 3-3. 5-HT_{1b} on capillary pericytes and dorsal fibres.

(a) Immunolabelling for 5-HT_{1B} receptors with strong expression on pericytes (p) attached to a capillary (v) in ventral spinal cord caudal to a SCI (sacral). **(b)** Immunolabelling for 5-HT_{1B} receptors on fine fibres (f) on the superficial dorsal horn, some of which clearly entered the dorsal root (likely unmyelinated sensory afferents).



Supplementary Figure 3-4. Hypoxia is followed by a rebound increased oxygenation in the spinal cord in rats with SCI.

(a) Partial pressure of oxygen (pO₂) measured in the spinal cord with an optical electrode (optode), caudal to a spinal cord injury. Under baseline conditions the cord is anoxic (about 14 mm Hg). A brief episode of hypoxia (1 min breathing 10%, rather than usual 21%, air) induces an immediate decrease in pO₂, further increasing the hypoxia, but this is followed by a sustained increase in pO₂. **(b)** Group means of pO₂ prior, during and 15 min after hypoxia. **P* < 0.05: significant difference relative to pre-hypoxia conditions. Error bars, s. e.m.



Supplementary Figure 3-5. Endogenously produced trace amines do not affect motoneuron activity after SCI, even though exogenously applied trace amines do.

(a) Schematic of isolated sacral spinal cord from chronic spinal rat, maintained in vitro, with roots mounted stimulation and recording of motoneuron activity and reflexes. (b) Long lasting reflex (LLR) recorded from ventral root in response to dorsal root stimulation pulse (0.1 ms, 3×T). (c) Increased LLR in response to exogenous application of the trace amine tryptamine. (d - e) In contrast, motoneuron activity (LLR and spontaneous activity prior to stimulation) is *not* increased by tryptophan application, indicating that tryptamine endogenously produced by spinal sources of AADC (in vessels; Fig. 3-2) does not influence neurons. (f-g) Dose-response relations for LLR (amplitude) with increasing dose of tryptamine and

tryptophan. Inhibiting MAO (MAOI) with clorgyline and pargyline (2 μM each) increased the potency of tryptamine by 2 orders of magnitude (increasing doses needed to affect the LLR from 0.1 μM to 10 μM), suggesting that MAO normally metabolises most of the tryptamine in the spinal cord. In particular, even if physiological levels of tryptophan (30 μM) produced similar tryptamine levels (via AADC), these would be reduced by 2 orders of magnitude (to 0.3 μM), far too low to affect monoamine receptors (5-HT_{2C}, see below). Indeed, the same MAOI treatment enabled tryptophan to increase the LLR, but only at very high unphysiological doses (\gg 100 μM), indicating that tryptamine endogenously produced by AADC from tryptophan is largely metabolized by MAO before it can influence motoneurons. **(h)** Group means of efficacy (maximum response amplitude, as a percent of pre-drug) of tryptamine and tryptophan, with the 5-HT_{2C} receptor antagonist SB206553 blocking the action of tryptamine, and tryptophan only effective with MAOI. **(i)** Group means of potency (EC₅₀, effective concentration for 50% effect) of trace amines (tryptamine, tyramine, PEA and octopamine) and amino acids (tyrosine and tryptophan), in the presence of MAOI. Note that tryptamine is most potent (lowest EC₅₀), especially compared to PEA, consistent with 5-HT_{2C} receptors mediating the action of tryptamine on motoneurons, rather than TAARs (which are most sensitive to PEA) (Borowsky et al. 2001; Bunzow et al. 2001). Also note that tryptophan, tyrosine and associated trace amines only had substantial effects when MAO was blocked, suggesting that MAO metabolizes AADC products (trace amines) before they can directly affect neuronal activity. $**P < 0.05$, relative to pre-treatment. $n > 8$ per condition. Error bars, s.e.m.

Supplementary information references

Borowsky B, Adham N, Jones KA, Raddatz R, Artymyshyn R, Ogozalek KL, Durkin MM, Lakhani PP, Bonini JA, Pathirana S, Boyle N, Pu X, Kouranova E, Lichtblau H, Ochoa FY, Branchek TA, and Gerald C. Trace amines: identification of a family of mammalian G protein-coupled receptors. *Proc Natl Acad Sci U S A* 98: 8966-8971, 2001.

Bunzow JR, Sonders MS, Arttamangkul S, Harrison LM, Zhang G, Quigley DI, Darland T, Suchland KL, Pasumamula S, Kennedy JL, Olson SB, Magenis RE, Amara SG, and Grandy DK. Amphetamine, 3,4-methylenedioxymethamphetamine, lysergic acid diethylamide, and metabolites of the catecholamine neurotransmitters are agonists of a rat trace amine receptor. *Mol Pharmacol* 60: 1181-1188, 2001.

Chapter 4: Thesis discussion and future directions

Discussion

In this thesis, our results demonstrate that AADC is upregulated in ectopic locations after spinal cord transection, specifically in capillary pericytes, and certain AADC interneurons. Our results are consistent with previous studies that suggest that AADC is upregulated when monoamine levels are decreased (Berry et al. 1996), because monoamines are eliminated in our transected rats, and mostly eliminated in our staggered hemisection rats, as well as our contused rats.

Pursuing the physiological role of AADC after SCI, we find the upregulated AADC in pericytes produces trace amines (TAs) from endogenous amino acids, which function as substitutes for classical monoamines, setting up a basal microvascular tone. However, this TA action is excessive after SCI, constricting capillaries more than normal, increasing vascular resistance and thus leaving the injured spinal cord in a chronic hypoxia state. Excessive production of TAs results partly from over-expression of microvascular AADC, which is the sole rate limiting enzyme producing TAs. Additionally, previous work has shown that L-type transporters are upregulated after SCI, which would provide AADC increased access to amino acids (Toyooka et al. 2008). TAs' precursors, such as tryptophan, tyrosine and phenylalanine, are passively transported into endothelial cells by this L transporter (Na⁺-independent) on the luminal (blood) side, and then are transported into the spinal cord via both L transporters and Na⁺-dependent LNAA transporters on the abluminal (spinal cord) side of endothelial cells (Duelli et al. 2000; Gomes et al. 1999; Hawkins et al. 2006; Toyooka et al. 2008; Tsitsiou et al. 2009). Considering these precursor concentrations of TAs in plasma are around the 30-100 μ M range separately and pericytes make direct physical contact with endothelial cells, concentrations of amino acids reaching the pericytes are likely sustained in the tens of micro-molar range, leading to production of TAs in the micro-molar range, which is high enough to activate classical monoamine receptors.

However, this upregulated AADC is unlikely to endogenously produce functional classic monoamines, such as 5-HT and DA, that can affect the spinal cord after spinal transection, for several reasons. First, peripherally synthesized 5-HT is mostly transported, stored in vesicles, or metabolized before it gets into the circulation; what little 5-HT does enter the circulation (from the gut) is avidly transported into platelets, leaving serum 5-HT levels very low (Kema et al. 2000; Paasonen 1965). This remaining 5-HT does not easily cross the BBB (Oldendorf 1971). Second, while 5-HTP does easily cross the BBB (by the amino acid L-transport system) (Gomes et al. 1999; Hawkins et al. 2006), very little if any is normally detected in serum (Coppi et al. 1989; Kema et al. 2000; Tyce et al. 1981), and thus AADC-containing cells in the spinal cord (D cells and vessels) are unlikely to receive adequate endogenous 5-HTP to make 5-HT. Finally, there is not likely a significant source of 5-HTP intrinsic to the spinal cord after transection, considering that most TPH is lost with injury, along with the associated descending 5-HT fibers (Carlsson et al. 1964; Clineschmidt et al. 1971).

Other than producing TAs to regulate microcirculation, the role of vessel AADC (in endothelial cells and pericytes) could be also an enhancement of the endothelial trapping system. Under normal conditions, because monoamines are much denser in the CNS than in the peripheral system, as part of the BBB endothelial AADC normally disposes of excessive CNS monoamines and monoamine precursors into the peripheral system. But this role may well reverse with SCI, whereby endothelial cells may prevent excessive amines from going into the spinal cord. Considering plastic adaption of monoamine receptors after SCI, including receptor supersensitivity and the increase of constitutive activities (Kong et al. 2010; Murray et al. 2010), non-controlled excessive release of amines under pathological conditions or exogenous application of

amines' precursors could result in dramatic spinal disruption, such as spasticity or pain behavior (Murray et al. 2010; Murray et al. 2011; Viguier et al. 2013).

Unfortunately, the physiological function of the AADC interneurons and the occurrence of downregulation of AADC in D cells are still unknown. We find that some of the processes of these AADC neurons contact the capillaries, suggesting that they may participate in regulating the vessels, though there are no direct results to support this hypothesis yet. Also, though according to Gozal's study ventral D-cells serve a critical role in modulating locomotor-like activities in the normal spinal cord (Gozal et al. 2014), we still don't know how dorsal D-cells affect neuronal function or why AADC in dorsal D-cells is downregulated after SCI.

Future direction

We were surprised by the finding that the injured spinal cord suffers from chronic hypoxia and that simply restoring oxygen to the spinal cord enhances rat's motor output. For practical treatments, briefly inhaling oxygen may be easily transferred into human trials, which could potentially enhance subjects' weight support and locomotion. This also offers an opportunity to re-evaluate vessel dilation drugs as a treatment for SCI; these drugs are used to treat hypertension or erectile dysfunction (β -blockers for instance) (Ripley et al. 2014; Wong et al. 2014). Furthermore, we find that exogenously applied 5-HTP promotes motoneuron function via spinal AADC. Based on this and earlier animal studies (Barbeau et al. 1990; Bedard et al. 1979; Hayashi et al. 2010) and the use of 5-HTP in the clinic to treat depression or sleep disorder (Birdsall 1998; Shaw et al. 2002), it also potentially should be examined in human SCI studies.

Chronic hypoxia could contribute to many of the major consequences of SCI, and thus fundamental mechanisms are well worth pursuing: 1) Cell death. It has long been known that cell numbers are reduced after acute SCI, but most studies focused on excitotoxicity caused by primary injury (Beattie et al. 2010; Ferguson et al. 2008). We find AADC upregulation starts as early as two days after spinal cord transection (data not shown) in accordance with diminishing of monoamine fibres, suggesting that harmed microcirculation possibly has a very early onset. How soon hypoxia starts to present after SCI and whether it plays a critical role in cell death through secondary damage is still unknown. It would also be interesting to know if chronic hypoxia results in further neuron loss in the spinal cord caudal to the lesion. 2) Allodynia. A sensitization to non-harmful stimuli is a common syndrome after SCI. In our sacral transected rat model, a sensitization of tail skin to the von frey test is readily observed (Bennett et al. 1999). Our unpublished data suggest that briefly inhaling oxygen in transected rats dramatically

increases sensory threshold to von frey test back to normal level (data not shown). Also considering that exercise, which provides both cardiovascular output and fast breathing rates, reduces pain behavior in persons with SCI, chronic hypoxia could be a trigger for allodynia (Hicks et al. 2003). Mechanisms behind hypoxia and allodynia provide a new aspect to consider for treating allodynia after SCI. 3) Inflammation and monoamine receptor editing. Intermittent hypoxia (IH) has long been studied. More recently it shows beneficial effects in enhancing motor function in spinal injured rats and has been transferred into human trials (Astorino et al. 2015; Hayes et al. 2014; Lovett-Barr et al. 2012). These IH studies suggest that both acute and chronic IH induce inflammatory response in the spinal cord (Huxtable et al. 2015; Smith et al. 2013). Our oxygen concentration measurements show that briefly inhaling low concentrations of oxygen leads to acute hypoxia in the injured spinal cord. If IH induced-inflammation is due to low oxygen levels, chronic hypoxia that we find could play a crucial role in long-term elevation of inflammatory responses after SCI. Moreover, Dracheva's group recently showed a link between inflammatory response and constitutive 5-HT_{2C} receptor editing after SCI (Narzo et al. 2015). To find out the relationships among hypoxia, inflammatory response and monoamine receptor editing after SCI is a valuable project worth pursuing.

References

- Astorino TA, Harness ET, and White AC.** Efficacy of acute intermittent hypoxia on physical function and health status in humans with spinal cord injury: A brief review. *Neural Plast* 2015: 409625, 2015.
- Barbeau H, and Rossignol S.** The effects of serotonergic drugs on the locomotor pattern and on cutaneous reflexes of the adult chronic spinal cat. *Brain Res* 514: 55-67, 1990.
- Beattie MS, Ferguson AR, and Bresnahan JC.** AMPA-receptor trafficking and injury-induced cell death. *Eur J Neurosci* 32: 290-297, 2010.
- Bedard P, Barbeau H, Barbeau G, and Filion M.** Progressive increase of motor activity induced by 5-HTP in the rat below a complete section of the spinal cord. *Brain Res* 169: 393-397, 1979.
- Bennett D, Gorassini M, Fouad K, Sanelli L, Han Y, and Cheng J.** Spasticity in rats with sacral spinal cord injury. *J Neurotrauma* 16: 69-84, 1999.
- Berry M, Juorio A, Li X-M, and Boulton A.** Aromatic L-amino acid decarboxylase: A neglected and misunderstood enzyme. *Neurochem Res* 21: 1075-1087, 1996.
- Birdsall TC.** 5-Hydroxytryptophan: a clinically-effective serotonin precursor. *Altern Med Rev* 3: 271-280, 1998.
- Carlsson A, Falck B, Fuxe K, and Hillarp Nr.** Cellular localization of monoamines in the spinal cord. *Acta physiologica Scandinavica* 60: 112-119, 1964.
- Clineschmidt B, Pierce J, and Lovenberg W.** Tryptophan hydroxylase and serotonin in spinal cord and brain stem before and after chronic transection. *Journal of neurochemistry* 18: 1593-1596, 1971.
- Coppi G, and Barchielli M.** Simple method for the determination of L-5-hydroxytryptophan in plasma by high-performance liquid chromatography. *J Chromato B: Biomed Sci Appl* 495: 245-248, 1989.
- Duelli R, Enerson BE, Gerhart DZ, and Drewes LR.** Expression of large amino acid transporter LAT1 in rat brain endothelium. *J Cereb Blood Flow Metab* 20: 1557-1562, 2000.
- Ferguson AR, Christensen RN, Gensel JC, Miller BA, Sun F, Beattie EC, Bresnahan JC, and Beattie MS.** Cell death after spinal cord injury is exacerbated by rapid TNF alpha-induced trafficking of GluR2-lacking AMPARs to the plasma membrane. *J Neurosci* 28: 11391-11400, 2008.
- Gomes P, and Soares-da-Silva P.** L-DOPA transport properties in an immortalised cell line of rat capillary cerebral endothelial cells, RBE 4. *Brain Res* 829: 143-150, 1999.
- Gozal EA, O'Neill BE, Sawchuk MA, Zhu H, Halder M, Chou CC, and Hochman S.** Anatomical and functional evidence for trace amines as unique modulators of locomotor function in the mammalian spinal cord. *Front Neural Circuits* 8: 134, 2014.
- Hawkins RA, O'Kane RL, Simpson IA, and Via JR.** Structure of the blood-brain barrier and its role in the transport of amino acids. *J Nutr* 136: 218S-226S, 2006.
- Hayashi Y, Jacob-Vadakot S, Dugan E, McBride S, Olexa R, Simansky K, Murray M, and Shumsky J.** 5-HT precursor loading, but not 5-HT receptor agonists, increases motor function after spinal cord contusion in adult rats. *Exp Neurol* 221: 68-78, 2010.
- Hayes HB, Jayaraman A, Herrmann M, Mitchell GS, Rymer WZ, and Trumbower RD.** Daily intermittent hypoxia enhances walking after chronic spinal cord injury: a randomized trial. *Neurology* 82: 104-113, 2014.

Hicks AL, Martin KA, Ditor DS, Latimer AE, Craven C, Bugaresti J, and McCartney N. Long-term exercise training in persons with spinal cord injury: effects on strength, arm ergometry performance and psychological well-being. *Spinal Cord* 41: 34-43, 2003.

Huxtable AG, Smith SM, Peterson TJ, Watters JJ, and Mitchell GS. Intermittent hypoxia-induced spinal inflammation impairs respiratory motor plasticity by a spinal p38 MAP kinase-dependent mechanism. *J Neurosci* 35: 6871-6880, 2015.

Kema IP, de Vries EG, and Muskiet FA. Clinical chemistry of serotonin and metabolites. *J Chromato B: Biomed ScisAppl* 747: 33-48, 2000.

Kong XY, Wienecke J, Hultborn H, and Zhang M. Robust upregulation of serotonin 2A receptors after chronic spinal transection of rats: an immunohistochemical study. *Brain Res* 1320: 60-68, 2010.

Lovett-Barr MR, Satriotomo I, Muir GD, Wilkerson JE, Hoffman MS, Vinit S, and Mitchell GS. Repetitive intermittent hypoxia induces respiratory and somatic motor recovery after chronic cervical spinal injury. *J Neurosci* 32: 3591-3600, 2012.

Murray KC, Nakae A, Stephens MJ, Rank M, D'Amico J, Harvey PJ, Li X, Harris RLW, Ballou EW, and Anelli R. Recovery of motoneuron and locomotor function after spinal cord injury depends on constitutive activity in 5-HT_{2C} receptors. *Nat Med* 16: 694-700, 2010.

Murray KC, Stephens MJ, Ballou EW, Heckman CJ, and Bennett DJ. Motoneuron excitability and muscle spasms are regulated by 5-HT_{2B} and 5-HT_{2C} receptor activity. *J Neurophysiol* 105: 731-748, 2011.

Narzo AF, Kozlenkov A, Ge Y, Zhang B, Sanelli L, May Z, Li Y, Fouad K, Cardozo C, Koonin EV, Bennett DJ, and Dracheva S. Decrease of mRNA editing after spinal cord injury is caused by down-regulation of ADAR2 that is triggered by inflammatory response. *Sci Rep* 5: 12615, 2015.

Oldendorf WH. Brain uptake of radiolabeled amino acids, amines, and hexoses after arterial injection. *Am J Physiol* 221: 1629-1639, 1971.

Paasonen M. Release of 5-hydroxytryptamine from blood platelets. *J Pharma Pharmacol* 17: 681-697, 1965.

Ripley TL, and Saseen JJ. beta-blockers: a review of their pharmacological and physiological diversity in hypertension. *Ann Pharmacother* 48: 723-733, 2014.

Shaw K, Turner J, and Del Mar C. Tryptophan and 5-hydroxytryptophan for depression. *Cochrane Database Syst Rev* CD003198, 2002.

Smith SM, Friedle SA, and Watters JJ. Chronic intermittent hypoxia exerts CNS region-specific effects on rat microglial inflammatory and TLR4 gene expression. *PLoS One* 8: e81584, 2013.

Toyooka T, Nawashiro H, Shinomiya N, Yano A, Ooigawa H, Ohsumi A, Uozumi Y, Yanagawa Y, Matsuo H, and Shima K. Up-regulation of L type amino acid transporter 1 after spinal cord injury in rats. *Acta Neurochir Suppl* 102: 385-388, 2008.

Tsitsiou E, Sibley CP, D'Souza SW, Catanescu O, Jacobsen DW, and Glazier JD. Homocysteine transport by systems L, A and y⁺L across the microvillous plasma membrane of human placenta. *J Physiol* 587: 4001-4013, 2009.

Tyce GM, and Creagan ET. Measurement of free and bound 5-hydroxytryptophan in plasma by liquid chromatography with electrochemical detection. *Anal Biochem* 112: 143-150, 1981.

Viguiet F, Michot B, Hamon M, and Bourgoin S. Multiple roles of serotonin in pain control mechanisms--implications of 5-HT(7) and other 5-HT receptor types. *Eur J Pharmacol* 716: 8-16, 2013.

Wong GW, Boyda HN, and Wright JM. Blood pressure lowering efficacy of partial agonist beta blocker monotherapy for primary hypertension. *Cochrane Database Syst Rev* 11: CD007450, 2014.